

UC San Diego

UC San Diego Electronic Theses and Dissertations

Title

Synthesis and applications of side chain-functionalized polylactic acid-based polymers and studies toward a chemical method to degrade Alzheimer's disease-related beta-amyloid peptides

Permalink

<https://escholarship.org/uc/item/5w04w6z3>

Author

Rubinshtein, Mark

Publication Date

2011

Peer reviewed|Thesis/dissertation

UNIVERSITY OF CALIFORNIA, SAN DIEGO

Synthesis and Applications of Side Chain-Functionalized Polylactic Acid-based Polymers
and Studies Toward a Chemical Method to Degrade Alzheimer's Disease-Related
beta-Amyloid Peptides.

A Dissertation submitted in partial satisfaction of the Requirements for the degree Doctor
of Philosophy

in

Chemistry

by

Mark Rubinshtein

Committee in charge:

Professor Jerry Yang, Chair
Professor Edward Koo
Professor Joseph O'Connor
Professor Kimberly Prather
Professor James Whitesell

2011

Copyright

Mark Rubinshtein, 2011

All rights reserved.

The Dissertation of Mark Rubinshtein is approved, and it is acceptable in quality and form for publication on microfilm and electronically:

Chair

University of California, San Diego

2011

EPIGRAPH

“Those who have an excessive faith in their theories or in their ideas are not only poorly disposed to make discoveries, but they also make very poor observations.”

Claude Bernard

TABLE OF CONTENTS

Signature page.....	iii
Epigraph.....	iv
Table of Contents.....	v
List of Abbreviations.....	viii
List of Figures.....	x
List of Schemes.....	xvi
List of Tables.....	xvii
Acknowledgements.....	xviii
Vita.....	xxiv
Abstract of the Dissertation.....	xxvi
Part I: Synthesis and Applications of Side Chain-Functionalized Polylactic Acid-based Polymers.....	1
Chapter 1 Polylactic acid and its derivatives.....	2
1.1 Biodegradable polymers.....	2
1.2 Synthesis and properties of polylactic acid.....	4
1.3 Incorporating functionalization into PLA.....	7
1.4 Goals of the dissertation research.....	10
Chapter 2 Development of facile methods to synthesize biodegradable materials from side chain-functionalized polylactic acid based polymers.....	11
2.1 Introduction.....	11
2.2 The Ugi and Passerini reactions in organic synthesis.....	12
2.3 Passerini-type condensations for generating α -hydroxy- <i>N</i> -acylindoles precursors to functionalized lactide monomers.....	15

2.4 Incorporation of functionalized hemilactides into PLA copolymers.....	19
2.5 Attempting direct polymerization of α -hydroxy- <i>N</i> -Acylindoles.....	22
2.6 Preparatory scale production of an alkyne-functionalized polylactic acid copolymer.....	26
2.7 Preparation of polymeric nanoparticles from alkyne-functionalized PLAs.....	27
2.8 Encapsulation of small molecules inside of functionalized PLA nanoparticles.....	29
2.9 Future directions for side-chain functionalized PLA-based polymers.....	31
2.10 Chapter summary.....	32
2.11 Experimental methods.....	33
Part II: Studies Toward a Chemical Method to Degrade Alzheimer’s Disease-Related beta-Amyloid Peptides.....	47
Chapter 3 Alzheimer’s Disease: Causes, Mortality and Treatment Options.....	48
3.1 Alzheimer’s disease: an emerging health crisis.....	48
3.2 Alzheimer’s disease and the amyloid cascade hypothesis.....	50
3.3 Current state of Alzheimer’s disease therapeutics.....	52
3.4 Small-molecule based strategies and targets for AD therapy.....	54
3.5 Degradation of A β as a therapeutic strategy.....	54
3.6 Goal of the dissertation research.....	56
Chapter 4 An Ene-ene-Based Target-Directed Chemical Method to Degrade Alzheimer’s-Related β -Amyloid.....	57
4.1 Introduction.....	57
4.2 A target-directed strategy toward selective peptide degradation.....	58

4.3 Ene-diyne as potent chemical warheads.....	59
4.4 Preparation of the BTA binding moiety.....	64
4.5 Synthesis and binding affinity of the BTA-ene-diyne conjugate.....	66
4.6 Effect of the BTA-ene-diyne conjugate on aggregated A β	67
4.7 Chapter summary.....	72
4.8 Experimental methods.....	73
Chapter 5 Efficient Synthesis and Applications of Oligoethylene glycol derivatives of Benzothiazole Anilines.....	85
5.1 Introduction.....	85
5.2 Microwave-assisted synthesis of BTA-EG ₄ and BTA-EG ₆	86
5.3 Further derivatization of BTA-EG ₆	88
5.4 Blocking HIV-1 transmission with BTA-EG ₆	89
5.5 Self-assembled cation-selective ion channels formed from BTA-EG ₄	94
5.6 Chapter summary.....	96
5.7 Experimental Methods.....	97
Appendix A.....	106
References.....	114

LIST OF ABBREVIATIONS

A β	β -amyloid
AChE	acetylcholinesterase
AD	Alzheimer's disease
APP	amyloid precursor protein
BTA	6-methylbenzothiazole aniline
CuAAC	Cu(I)-catalyzed azide-alkyne cycloaddition
DBU	1,8-diazabicyclo[5.4.0]undec-7-ene
DCM	dichloromethane
4-DMAP	4-dimethylaminopyridine
DMF	<i>N,N</i> -dimethylformamide
DMSO	dimethyl sulfoxide
EDC	1-ethyl-3-(3-dimethylaminopropyl)carbodiimide
ELISA	enzyme-linked immunosorbent assay
Et ₂ O	diethyl ether
HIV	human immunodeficiency virus
EtOAc	ethyl acetate
M _n	number average molecular weight
M _w	weight average molecular weight
MeOH	methanol
NFT	neurofibrillary tangle
NMDA	<i>N</i> -methy-D-aspartase
PDI	polydispersity index
PGA	polyglycolic acid
PLA	polylactic acid / polylactide
pS	picoSiemens
PTSA	<i>p</i> -toluenesulfonic acid
ROP	ring-opening polymerization
SDS-PAGE	sodium dodecyl sulfate-polyacrylamide gel electrophoresis

SEVI	semen-derived Enhancer of viral infection
Sn(Oct) ₂	stannous 2-ethylhexanoate or tin octoate
T_g	glass transition temperature
T_m	melting temperature
THF	tetrahydrofuran

LIST OF FIGURES

Figure 1.1: Example of a compostable food packaging made from biodegradable polymers. The bag of SunChips® is shown (A) prior to composting and (B) after 18 days of composting.....	2
Figure 1.2: Two examples of biodegradable polymers used for biomedical applications: (A) surgical bone screws manufactured by NP Pharm from the biodegradable polymer Lactel® and (B) A prototype of a fully absorbable, biodegradable stent produced by Abbott Vascular in conjunction with Biotronic and REVA Medical. Images obtained from NP Pharm and Advanced Medical Technologies.....	3
Figure 1.3: Current commercial preparation of polylactic acid (PLA). Direct polymerization of lactic acid (A) results in the formation of oligomeric material. Alternatively, dehydrative dimerization (B) leads to the formation of monomeric lactide that can then be polymerized via ring opening polymerization (C).....	5
Figure 1.4: Synthesis of a PLA derivative containing pendant protected carboxylic acid functional groups from a functionalized lactide precursor. The carboxylic acid is unmasked upon hydrogenation of the benzyl ester.....	9
Figure 1.5: Feijen's preparation of various polyesteramides via copolymerization of DL-lactide with substituted morpholine-2,5-diones prepared from protected L-aspartic acid, L-lysine and L-cysteine.....	9
Figure 1.6: Synthesis (A) and polymerization (B) of an alkyne-functionalized lactide.....	10
Figure 2.1: The mechanism of the multicomponent Ugi Reaction between an aldehyde or ketone (black), amine (blue) isocyanide (green) and carboxylic acid (red) to generate a bis-amide.....	13
Figure 2.2: Proposed concerted (A) or stepwise (B) mechanisms for the multicomponent Passerini reaction. Both proposed mechanisms proceed via an alkylimidic anhydride intermediate that rapidly rearranges to form an esteramide.....	13
Figure 2.3: Formation of pyroglutamic acids using a convertible isocyanide. The bis-amide formed via the Ugi reaction is readily converted to the <i>N</i> -acylindole upon treatment with PTSA. The <i>N</i> -acylindole is subsequently hydrolyzed to give pyroglutamic acid and indole.....	14

Figure 2.4: Proposed stepwise mechanism of the Passerini-like reaction for the generation of α -hydroxy- <i>N</i> -acylindoles. This variant of the Passerini replaces the carboxylic acid component with water a catalytic amount of PTSA. The catalytic acid initiates the reaction and also affects the transformation of the esteramide intermediate to the α -hydroxy- <i>N</i> -acylindole. In principle, the generation of the esteramide may also proceed by concerted mechanism similar to that described in Figure 2.2.....	15
Figure 2.5: Proposed route toward generating PLAs. The <i>N</i> -acylindoles formed during the Passerini-type reaction may be further converted to sidechain functionalized hemilactides and incorporated into poly(α -hydroxy acid) copolymers.....	17
Figure 2.6: Modification of copolymers 6b-d using CuAAC click reactions. (A-D) Size exclusion chromatographic traces of crude samples containing CuSO ₄ and sodium ascorbate with: (A) PLA 6a and dansyl azide 7 , (B) alkyne-functionalized polymer 6b and dansyl azide 7 , (C) azide-functionalized polymer 6c and dansyl alkyne 8 , or (D) azide-functionalized polymer 6d and dansyl alkyne 8 . The chromatograms of crude polymer-containing solutions were monitored by differential refractive index (dRI, black) and UV absorbance (red). The UV was monitored at $\lambda = 365$ nm to indicate species containing a dansyl group.....	22
Figure 2.7: One possible pathway of α -hydroxy- <i>N</i> -acylindole decomposition upon treatment with a thiol. Initial attack of the α -hydroxy- <i>N</i> -acylindole by the highly nucleophilic thiol may lead to the formation of an α -hydroxythioester, which can subsequently undergo self-condensation to form dimeric, trimeric and ultimately multimeric products.....	23
Figure 2.8: ESI-MS analysis of attempted polymerization of α -hydroxy- <i>N</i> -acylindole 3a using Cs ₂ CO ₃ as an initiator. Peaks at $m/z = 644, 716, 788, 860$ and 932 have differences of 72 , corresponding to the mass of a monomeric unit of PLA.	24
Figure 2.9: ESI-MS analysis of attempted polymerization of α -hydroxy- <i>N</i> -acylindole 3b initiated with DBU in DCM. Peaks at $m/z = 701, 811, 921, 1031, 1141, 1251, 1361, 1471, 1581,$ and 1691 have differences of 110 , corresponding to the mass of a monomeric unit of poly(2-hydroxy-5-hexynoic acid).....	25
Figure 2.10: Structures of the anticancer drugs camptothecin and doxorubicin and the Thioflavin T analogue BTA-EG ₄	30

Figure 2.11: Alkyne-functionalized PLA provides a means for covalently linking small molecule-based drugs onto the polymer scaffold. Drugs may be attached (A) directly to the scaffold using an azide-functionalized drug, or (B) indirectly by exploiting a bifunctional acid-cleavable linker.....	32
Figure 3.1: A portion of the amyloid precursor protein sequence (APP) represented by one-letter codes, with the sequence of A β ₁₋₄₂ shown in bold. α -Secretase cleaves APP between the Lys16 and Leu17 residues within the A β sequence, resulting in non-amyloidogenic peptide fragments. However, APP cleaved successively by β -secretase and γ -secretase produces A β peptides of varying length, depending on the specific cleavage site of γ -secretase.....	51
Figure 3.2: Structure of the β -secretase inhibitor GRL-8234.....	54
Figure 3.3: Examples of several γ -secretase modulators.....	55
Figure 4.1. Bergman cycloaromatization of (A) a linear enediyne and (B) a cyclic enediyne in a 10-membered ring system to a reactive <i>p</i> -benzyne diradical intermediate.....	59
Figure 4.2: Cartoon depicting the target-directed approach of A β degradation. A cyclic enediyne warhead bearing a suitable binding group is predicted to associate with A β peptides, delivering the enediyne moiety to the target peptide. Subsequent cyclization to the <i>p</i> -benzyne diradical may provide the reactive species necessary to degrade A β	61
Figure 4.3: Possible mechanisms of peptides degradation by the reactive <i>p</i> -benzyne diradical. Abstraction of an α -hydrogen from the peptide backbone leads to peroxide formation and ultimately peptide scission to give an amide and α -oxo ketone (or aldehyde). Alternatively, the highly reactive diradical may abstract an α -hydrogen from the peptide backbone (or a hydrogen atom from an amino acid side chain) to give other degradation products.....	62
Figure 4.4: Structures of the A β binding molecules Thioflavin T (ThT) and Pittsburgh compound B (PiB) containing the benzothiazole moiety.....	64

Figure 4.5: Briefly, the design of this ELISA-based competition assay entails the evaluation of molecules that inhibit the interaction of A β fibrils (here, formed from A β ₁₋₄₀) with a monoclonal anti-A β IgG raised against residues 3-8 of AD-related A β peptide (clone 6E10). This assay is based on the hypothesis that molecules that can effectively and efficiently coat A β fibrils will be able to inhibit the binding of this anti-A β IgG to A β fibrils. The relative inhibition of IgG-A β fibril interactions by small molecules is quantified using a standard ELISA protocol. Inhibition (Inh.) of anti-A β IgG (clone 6E10)-A β interactions with compound: a) **21**, 55% Maximal Inh., IC₅₀ = 220 μ M; b) **22**, No Inhibition; and c) **20**, 51% Maximal Inh., IC₅₀ = 100 μ M. Error bars represent \pm SEM..... 67

Figure 4.6: A Circular dichroism spectrum of a 100 μ M aqueous solution of A β after incubation at 37°C for 4 days..... 68

Figure 4.7: Chromatographic and electrophoretic analyses of the degradation of A β peptides using a targeted enediyne. (A) RP-HPLC analysis of A β ₁₋₄₀ peptides after incubation with 1 molar equivalent of **21** at 37°C after 0 days (top) and 7 days (middle), or 10 equivalents of **21** after 7 days (bottom). (B) SDS-PAGE analysis of A β ₁₋₄₀ peptides after incubation with 1 molar equivalent of **21** or 5 molar equivalents of **22** or **20** at 37°C for 7 days. Lane 1: Mark12™ standard. Lane 2: A β ₁₋₄₀ alone. Lane 3: A β ₁₋₄₀ + 1 molar equivalent **21** incubated for 7 days. Lane 4: A β ₁₋₄₀ + 5 molar equivalent **22** incubated for 7 days. Lane 5: A β ₁₋₄₀ + 5 molar equivalent **20** incubated for 7 days. SDS-PAGE gels were run using a 16% tricine gel and visualized via silver staining..... 69

Figure 4.8: SDS-PAGE analysis of ubiquitin (8.6 kDa) alone and after incubation with 1 molar equivalent of **21** at 37 °C for 7 days. Lane 1: Mark12™ standard. Lane 2: ubiquitin (90%, from Sigma-Aldrich, used without further purification). Lane 3: ubiquitin + 1 molar equivalent **21** incubated for 7 days. SDS-PAGE gels were performed using a 16% tricine gel and visualized via silver staining..... 70

Figure 4.9: Relative cell viability of SH-SY5Y human neuroblastoma cells in the presence of aggregated A β peptides with or without incubation with molecule **21**. Cells incubated with **21** alone were treated with a solution of **21** that was incubated for 7 days in sterile water prior to exposure to cells. A β samples were prepared by incubation in sterile water for 4 days and: 1) incubated further for 7 days prior to exposure to cells, 2) incubated further for 7 days, mixed with **21**, and immediately exposed to cells (labeled as 0 days), or 3) incubated with **21** for 7 days prior to exposure to cells (labeled as 7 days). The data are expressed as mean values + standard deviations. The viability of cells exposed to A β incubated with molecule **21** for 7 days was significantly different than the viability of cells exposed to A β alone (P < 0.001)..... 72

Figure 5.1: Structures of BTA-EG₄ (**23**) and BTA-EG₆ (**24**). BTA-EG₄ is synthesized using tetraethylene glycol as a starting material, while BTA-EG₆ is prepared from hexaethylene glycol..... 86

Figure 5.2: Schematic representation of the putative role of aggregated PAP248-286 peptides (also called SEVI peptides) in HIV-1 infection. a) Primary sequence and helical representation of PAP248-286 peptides; these abundant peptides have been reported to spontaneously form aggregated amyloid fibrils in semen. b) Illustration of the SEVI amyloid-mediated infection of a T cell (pink/red) with HIV-1 (blue/purple). Also depicted is the proposed method to attenuate SEVI-mediated infection by forming bio-resistive coatings on aggregated amyloids derived from PAP248-286..... 90

Figure 5.3: Binding of BTA-EG₆ to SEVI fibrils as determined by a previously reported centrifugation assay. Briefly, various concentrations of BTA-EG₆ in PBS were incubated overnight at room temperature in the presence or absence of SEVI fibrils. After equilibration, each solution was centrifuged, and the supernatants were separated from the pelleted fibrils. The fluorescence of BTA-EG₆ was determined from the resuspended pellets in PBS solution. *Error bars* represent S.D. of duplicate measurements. The K_d was determined by fitting the data to a one-site specific binding algorithm: $Y = B_{\max}[X/(K_d+X)]$, where X is the concentration of BTA-EG₆, Y is the specific binding fluorescence intensity, and B_{\max} corresponds to the apparent maximal observable fluorescence upon binding of BTA-EG₆ to SEVI fibrils. *RFI*, relative fluorescence intensity..... 91

Figure 5.4: (A) HIV-1 IIIB virions were preincubated with increasing concentrations of BTA-EG₆ (**24**) (0, 5.5, 11, and 22.5 µg/ml) and with or without SEVI (15 µg/ml) as indicated. The samples were then added to CEM-M7 cells. Cells were washed at 2 h, and infection was assayed at 48 h by measuring Tat-driven luciferase expression. Results shown are average values ± S.D. of triplicate measurements from one of four independent experiments that yielded equivalent results. * indicates $p < 0.05$ when compared with control cells exposed to HIV-IIIB + SEVI alone by ANOVA with Tukey's post test. RLU, relative luciferase units; Uninf, uninfected. (B) B, zoom in of panel A to show data for cells treated with HIV-IIIB virions with and without increasing concentrations of BTA-EG₆, in the absence of SEVI. BTA-EG₆ had no effect on the infectivity of HIV alone; concentrations of BTA-EG₆ are noted above for panel A..... 92

Figure 5.5: HIV-1IIIIB virions were preincubated with 50% pooled human semen, with or without increasing concentrations of BTA-EG₆ (5.5, 11, and 22.5 μg/ml). After 10 min, these stocks were diluted 15-fold into CEM-M7 cells. Cells were washed after 1 h, and luciferase expression was measured at 48 h to quantify the extent of infection. Results shown are average values ± S.D. of triplicate measurements from one of three independent experiments that yielded equivalent results. * indicates $p < 0.05$ when compared with control cells exposed to HIV-1IIIIB + semen alone, by ANOVA with Tukey's post test. RLU, relative luciferase units.....

93

Figure 5.6: The cervical endothelial cell lines A2En (endocervical), 3EC1(ectocervical), and SiHa were treated for 12 h with BTA-EG₆ at concentrations up to 10 times greater than the IC₅₀. Control cultures were treated with nonoxynol-9 (non-9) at 0.1% final concentration as a positive control for induction of cell death (33). At 12 h, viability was measured by resazurin cytotoxicity assay (alamarBlue™ assay). Representative results from A2En cells are shown; results from 3EC1 and SiHa cells were very similar (not shown).....

93

Figure 5.7: (A) Original current versus time trace from single ion channel recording through self-assembled pores from BTA-EG₄ in a planar lipid bilayer composed of 1,2-diphytanoyl-*sn*-glycero-3-phosphatidylcholine (DiphyPC) lipids. Histogram of current amplitudes reflects their number of occurrence in the corresponding current trace. (B) Normalized survival plot of the open channel lifetime determined from 174 single channel opening events under the same experimental conditions as in A). The average lifetime, τ , for BTA-EG₄ pores was determined from a fit of the histogram to the equation, $N(t)/N(0) = \exp(-t/\tau)$, where $N(t)$ represents the number of channels with lifetimes longer than the time t , and $N(0)$ represents the total number of channels with observable single conductance. BTA-EG₄ was added at a final concentration of 20 μM to both bilayer compartments, the applied voltage was +50 mV, and the electrolyte contained 1.0 M CsCl with 10 mM HEPES buffer, pH 7.4.....

95

Figure 5.8: (A) Inhibitory effect of BTA-EG₄ **23** on the growth of *Bacillus subtilis* bacteria 22 h after exposure to LB media containing various concentrations of BTA-EG₄. Growth was quantified by the optical density at a wavelength of 600 nm relative to untreated control cells. The concentration of BTA-EG₄ molecules that inhibited growth by 50% (IC₅₀ values) was 50 μM. Each point represents the mean of 2 experiments with 3 replicates in each experiment; error bars represent the standard error of the mean. (B) Cytotoxicity of BTA-EG₄ on human neuroblastoma (SH-SY5Y) cells 24 h after exposure. Each point represents the mean of 2 or 3 experiments with 6 replicates in each experiment. Error bars reflect the standard error of the mean. The IC₅₀ value was 65 μM.....

96

LIST OF SCHEMES

Scheme 2.1: Scheme for the facile two-step conversion of α -hydroxy- <i>N</i> -acylindoles to the corresponding hemilactides.....	19
Scheme 2.2: Synthesis of poly(DL-lactide)-co-(3-(but-3-yn-1-yl)-6-methyl-1,4-dioxane-2,5-dione) (9).....	26
Scheme 4.1: Synthesis of the substituted cyclic enediyne bearing a terminal carboxylic acid pendant functional group 14 from linear dibromide 10	63
Scheme 4.2: Synthesis of BTA-EG ₅ amine 20	65
Scheme 4.3: Formation of the enediyne-BTA conjugate 21 and a related control molecule 22 containing the enediyne warhead but lacking an A β -binding group.....	66
Scheme 5.1: Synthesis of BTA-EG ₄ 23 and BTA-EG ₆ 24 from tetraethylene glycol 25 and hexaethylene glycol 28 , respectively.....	87
Scheme 5.2: Tosylation of BTA-EG ₆ 24 under different conditions. Treatment of BTA-EG ₆ with TsCl in pyridine/DCM (A) affords the <i>N,O</i> -ditosylated product 31 , while using triethylamine/4-DMAP in DCM gives toluenesulfonyl ester 33 as the major product. Subsequent substitution of 31 and 33 with sodium azide affords the organoazide BTA derivatives 32 and 34 , respectively.....	89

LIST OF TABLES

Table 1.1: Common biodegradable polyesters and their uses.....	4
Table 1.2: Physical properties of polylactic acids.....	7
Table 2.1: Isolated yields of <i>N</i> -acylindoles from the Passerini-type condensation reaction.....	18
Table 2.2: Incorporation of functionalized hemilactides into PLA-based polymers.....	22
Table 2.3: Preparation of nanoparticles from commercial PLA and alkyne-functionalized PLA.....	29
Table 2.4: Preparation of nanoparticles containing encapsulated small molecule drugs.....	31
Table 3.1: Percentage change in selected causes of death in the United States between 2000 and 2006.....	50
Table 3.2: Current FDA-approved small molecule treatments for Alzheimer's Disease.....	54

ACKNOWLEDGEMENTS

I would like to thank everyone with whom I have had the pleasure to work with at UCSD over the last several years. Although I only had the opportunity to work with Petra Inbar and Enrico Bellomo for a short period of time, they were very helpful in getting me established in the lab when I first arrived at UCSD. I must also take this opportunity to thank Dr. Matt Alexander, who constantly answered many of my synthesis and purification-related questions during my first year, even though he didn't even work in our lab. I would like to thank my first labmates in 6117, and also the first graduates from the Yang lab: Steven Blake and Lani Bautista. I am fortunate to have had the opportunity to work with both of you—thank you for paving the way and demonstrating that there is a light at the end of the tunnel. Much of my time in 6117 was spent with Mike Macrae (before he started doing all of those ion channel measurements). I enjoyed sharing lab space with him for several years. He was often there to offer encouraging words as I attempted different syntheses, and offered company during the sometime long days of poring over the literature. I will certainly not forget the good times we have shared. I would like to thank my labmates from next door and across the hall: Alice Luong, Christina Capule, Lila Habib and Yuchen Cao. Thank you for answering all of my questions about biological and biochemical techniques and for tolerating my insanity when I would drift over from 6117. Your presence during my time in graduate school has made it a much more pleasant experience.

I would also like to thank several visiting scholars who have come through the lab: Barbara Breitenbucher, Eva Siedler and Jun Miyamoto. Although sometimes my

clean glassware would mysteriously disappear, I still very much enjoyed the opportunity to work with all of you. All of you have taught me in some way, and have enriched my experience as a graduate student.

The work presented in this dissertation would not have been possible without the expertise of Dr. Yongxuan Su of the Mass Spectrometry Facility, who ran countless samples for me over the years and always made time to analyze many of my most sensitive compounds. I would also like to thank Dr. Anthony Mrse of the NMR facility for his assistance with NMR experiments and for the many baseball-related conversations we have had during my time at UCSD.

I would like to acknowledge several people from my days at Columbia who were very influential in my decision to pursue a Ph.D. I would like to thank my undergraduate advisor, Professor Gerard Parkin, for giving me the opportunity to work in his lab for two years and gain valuable research experience. I would also like to thank Dr. David Churchill, with whom I worked side by side during my entire time in the Parkin Lab, for helping me first develop laboratory skills. I would like to extend a very special thanks to my mentor and friend, Professor Luis Avila. He has been a source of constant encouragement over the years and I cannot thank him enough for his support.

I would like to thank Professor Joseph O'Connor for his input on enediyne-related matters, especially during the initial stages of my project. Additionally I would like to thank Betsy Rodgers, formerly of the O'Connor group, who was instrumental in showing me the proper techniques for synthesizing the temperamental and volatile enediyne compounds discussed in the second half of this dissertation.

The PLA-related work presented in this thesis would not be possible without the efforts of Professor Nathan Gianneschi, Carrie James and Jennifer Young. I would like to thank them for all of their hard work in getting the PLA project off the ground. In addition, I owe a debt of gratitude to Dr. Matt Thompson, who trained me on the SEC and helped me set up my initial experiments related to the PLA project.

My graduate experience was greatly enhanced by Professor Charles Perrin. I learned very much from his very pointed observations and questions during group meetings. I am very grateful to him for making me feel welcome whenever I would come downstairs and knock on his office door to talk chemistry. Discussing science with him was an absolute pleasure and his input about life after graduate school has been invaluable.

I would like to thank my thesis committee—Professors Edward Koo, Kimberly Prather, Joseph O’Connor and James Whitesell—for the time and energy they have spent on my committee for my second year exam, third year exam, and now my defense. Of course, I would like to thank my advisor and committee chair, Professor Jerry Yang, who provided me with not only bench space and chemicals for the last five and a half years, but has taught me the value of guidance, support and the importance of doing thorough science. The lessons I have learned from him I will not soon forget.

Teaching during my undergraduate years at Columbia and graduate studies at UCSD has been immensely enjoyable and has helped me develop as both a scientist and educator. I would like to thank all of the people that I have had the opportunity to work with while a teaching assistant at Columbia: Joan Raitano, Rani Lopez, Al Mercado and especially Tauqir Fillebeen, Kim Lee-Granger, Walter Arnold and Luis Avila. I cannot

think of a better group of people with whom to work. In addition, I would like to thank all of the faculty members at UCSD with whom I had the opportunity to work as a teaching assistant. My time as a TA for my advisor, Professor Jerry Yang, and for Professor Patricia Jennings was particularly enjoyable and has prepared me well for any future teaching positions I may have. Of course, I would also like to extend my gratitude to all the students in the laboratory and lecture courses I have had the privilege to teach over the years.

I would like to take this opportunity to thank great friends who have been instrumental in my keeping a part of the sanity with which I started the Ph.D. program. My classmate and closest friend in the graduate program, Agnes Flach, has been a constant source of support throughout our entire time at UCSD. Our frequent lunches and beverage walks helped keep me from going off the deep end when things were at their toughest. My closest friend from back in New York, Wayne Pezzella, has known me for well over half my life and has offered me constant encouragement not only during my doctoral studies, but in every other aspect of my life. I am very lucky to have him as a friend.

I would like to give a very special thanks to my wife, Jessica, who has been there with me from the very first step on the road to the Ph.D. I could not have done this without her love and unending support. I frequently had to draw upon her strength to make it through the program and I cannot thank her enough for standing by me, loving me and putting up with me. She has earned this degree as much as I have.

Finally, I would like to thank all of my family for their support during the Ph.D. process. My parents, Yuri and Marina Rubinshtein, gave me life, raised me, and worked

tirelessly to provide me with an education and a desire to constantly pursue knowledge and better myself. I will be forever in their debt. In addition I would like to thank my grandmother, Sonya, my sister and brother-in law, Irene and Eddie, my nieces and nephews, Bella, Alec, Stephanie and David, and my in-laws Frank and Marilyn Kretzer for their encouragement during my graduate studies. All of you were a big part of helping me get through the program and I do not even know how to begin to express my gratitude for all of your love and support.

Notes about the chapters

Chapter 2, in part, is based on material which appears in "Facile Procedure for Generating Side Chain Functionalized Poly (alpha-hydroxy acid) Copolymers from Aldehydes via a Versatile Passerini-Type Condensation" Rubinshtein, M.; James, C. R.; Young, J. L.; Ma, Y. J.; Kobayashi, Y.; Gianneschi, N. C.; Jerry Yang, J. *Organic Letters*, **2010**, *12*, 3560-3563. I am the primary author of this paper. In addition, Chapter 2 contains material currently being prepared for submission for publication: "Direct synthesis of side chain functionalized alpha-hydroxy acid oligomers from alpha-hydroxy-*N*-acylindole precursors." Rubinshtein, M.; James, C. R.; Young, J. L.; Gianneschi, N. C.; Yang, J. I am the primary author of this manuscript.

Chapter 4 is based on material currently being prepared for submission for publication: Mark Rubinshtein, Lila K. Habib, Mahealani R. Bautista, and Jerry Yang "Chemical Degradation of Alzheimer's-Related beta-Amyloid Peptides Using a Targeted Ene-diyne." I am the primary author of this manuscript.

Chapter 5 contains material that appears in "Amyloid binding small molecules efficiently block SEVI (semen-derived enhancer of infection) and semen mediated enhancement of HIV-1 infection." Olsen, J. S.; Brown, C.; Capule, C. C.; Rubinshtein, M.; Doran, T. M.; Srivastava, R. K.; Feng, C.; Nilsson, B. L.; Yang, J.; Dewhurst, S. J. *Biol. Chem.* **2010**, 285, 35488-35496. I am a co-author on this paper. Additionally, Chapter 5 contains material as it may appear in a paper recently submitted for publication: "Self-assembled, cation-selective ion channels from oligo(ethylene glycol) derivatives of benzothiazole aniline." Prangkio, P.; Rao, D.; Lance, K.; Rubinshtein, M.; Yang, J.; Mayer, M. I am a co-author of this paper.

VITA

- 2001 Bachelor of Arts in Chemistry, *magna cum laude*, Columbia College, Columbia University, New York, NY.
- 2003 Master of Science in Chemical Engineering, Fu Foundation School of Engineering and Applied Science, Columbia University, New York, NY.
- 2011 Doctor of Philosophy in Chemistry, University of California, San Diego, La Jolla, CA.

PUBLICATIONS

7. **Rubinshtein, M.**; James, C. R.; Young, J. L.; Gianneschi, N. C.; Yang, J. "Direct synthesis of side chain functionalized alpha-hydroxy acid oligomers from alpha-hydroxy-*N*-acylindole precursors" *Manuscript in Preparation*.
6. **Rubinshtein, M.**; Habib, L. K.; Bautista, M. R.; Yang, J.; "Chemical Degradation of Alzheimer's-Related beta-Amyloid Peptides Using a Targeted Ene-diyne." *Manuscript in Preparation*.
5. Song, J. M.; Spitzer, M. H.; Megill, A.; **Rubinshtein, M.**; Habib, L. K.; Capule, C. C.; Xie, Y. Keenoy, K. E.; Mayer, M.; Turner, R. S.; Yang, J.; Pak, D. T. S.; Lee, H-K.; Hoe, H-S. "Pharmacological targeting of beta-amyloid enhances dendritic spine density and memory." *Submitted*.
4. Prangkio, P.; Lance, K.; Rao, D.; **Rubinshtein, M.**; Yang, J.; Mayer, M. "Self-assembled, cation-selective ion channels from oligo(ethylene glycol) derivatives of benzothiazole aniline." *Submitted*.
3. Olsen, J. S.; Brown, C.; Capule, C. C.; **Rubinshtein, M.**; Doran, T. M.; Srivastava, R. K.; Feng, C.; Nilsson, B. L.; Yang, J.; Dewhurst, S. "Amyloid binding small molecules efficiently block SEVI (semen-derived enhancer of infection) and semen mediated enhancement of HIV-1 infection." *J. Biol. Chem.* **2010**, 285, 35488-35496.
2. **Rubinshtein, M.**; James, C. R.; Young, J. L.; Ma, Y. J.; Kobayashi, Y.; Gianneschi, N. C.; Yang, J. "Facile procedure for generating side chain functionalized poly(α -hydroxy acid) copolymers from aldehydes via a versatile Passerini-Type condensation." *Org. Lett.* **2010**, 12, 3560-3563.

1. Ghosh, P., Churchill, D. G.; **Rubinshtein, M.**; Parkin, G. Synthesis and Molecular Structure of bis(pyrazolyl)(3,5-di-tert-butylpyrazolyl)hydroborato thallium: a hetero-tris(pyrazolyl)-hydroborato ligand derived from two different pyrazoles *New J. Chem.* **1999**, 23, 961-963.

ABSTRACTS AND POSTERS

Olsen, J. T.; Brown, C.; **Rubinshtein, M.**; Yang, J.; Dewhurst, S. "SEVI, a Natural Enhancer of HIV Infection, as a Novel Target to Prevent HIV Transmission." American Physician Scientists Association 6th Annual Meeting, Chicago, IL, 2010.

James, C. R.; **Rubinshtein, M.**; Yang, J.; Gianneschi, N. C. "Facile synthetic route to polylactic acid and other functionalized polymers" 239th ACS National Meeting, San Francisco, CA, United States, March 21-25, 2010.

Rubinshtein, M.; Habib, L. K.; Bautista, M. R.; Lee, M.; Yang, J. "Chemical degradation of Alzheimer's-related β -amyloid peptides" 237th ACS National Meeting, Salt Lake City, UT, United States, March 22-26, 2009.

Inbar, P.; **Rubinshtein, M.**; Habib, L.; Prangkio, P. Capone, Ricardo; Bautista, M. R.; Lee, M.; Li, C.; Takayama, S.; Mayer, M. "Neutralizing the toxicity of Alzheimer's-related beta-amyloid fibrils using small molecules" 235th ACS National Meeting, New Orleans, LA, United States, April 6-10, 2008.

Parkin, G.; **Rubinshtein, M.**; Bridgewater, B. M.; Churchill, D. G. "Ansa effects in permethylmolybdenocene and permethyltungstenocene chemistry," 222nd ACS National Meeting, Chicago, IL, United States, August 26-30, 2001.

ABSTRACT OF THE DISSERTATION

Synthesis and Applications of Side Chain-Functionalized Polylactic Acid-based Polymers and Studies Toward a Chemical Method to Degrade Alzheimer's Disease-Related beta-Amyloid Peptides.

by

Mark Rubinshtein

Doctor of Philosophy in Chemistry

University of California, San Diego, 2011

Professor Jerry Yang, Chair

The first part of this dissertation focuses on new methodology to prepare functionalizable derivatives of polylactic acid (PLA), an important biodegradable and biocompatible polymer often used for drug-delivery applications. Chapter 1 provides a brief background covering the uses and properties of biodegradable polymers and outlines previous strategies to synthesize functionalized PLA. Chapter 2 presents a novel synthetic route to functionalized lactide monomers via a Passerini-type condensation reaction. This methodology provides access to a variety of functionalized PLA molecules, including those with derivatizable alkyne and azide pendant groups. In addition, the chapter explores the preparation of polymeric nanoparticles from these functionalized PLAs for potential use in drug delivery applications.

The second part of this dissertation focuses on studies toward the development of a small molecule capable of chemically degrading the Alzheimer's related β -amyloid (A β) peptide. Chapter 3 provides a brief introduction to Alzheimer's disease (AD) and

its potential impact on global health. The chapter discusses the amyloid cascade hypothesis (which implicates A β as a causative factor in developing AD) as well as the current drugs and therapeutic strategies used to stop or reverse the progression of this disease. Chapter 4 introduces target-directed degradation of A β with a small molecule as a potential approach for the treatment of AD. The chapter presents the design and synthesis of a small molecule comprised of a cyclic enediyne chemical “warhead” moiety and a benzothiazole aniline (BTA) A β binding group. This designed BTA-enediyne conjugate reduces the toxicity of A β , presumably by degrading the amyloid to lower molecular weight fragments that are less harmful than full-length A β . Chapter 5 describes the development of a methodology leading to an improved synthesis of oligoethylene glycol derivatives of BTA and the collaborations made possible because of the increased availability of these molecules. These compounds exhibit many interesting, biomedically relevant properties including the ability to inhibit SEVI and semen-mediated infectivity of HIV-1 and form ion channels in lipid bilayers.

**Part I: Synthesis and Applications of Side Chain-
Functionalized Polylactic Acid-based Polymers**

Chapter 1

Polylactic Acid and its Derivatives

1.1 Biodegradable polymers

Biodegradable polymers have attracted significant attention for their wide range of potential applications. Scores of commercial products such as disposable plastics and compostable food packaging have been manufactured from these extraordinary macromolecules.¹⁻³ The agricultural sector has also employed these materials for uses such as controlled release of fertilizers and pesticides.^{4, 5} Most recently, however, investigation of the synthesis and properties of biodegradable polymers has stemmed from the desire to exploit their highly favorable properties for biocompatible applications including surgical sutures^{6, 7} and materials for tissue engineering.⁸⁻¹¹



Figure 1.1: Example of a compostable food packaging made from biodegradable polymers.¹² The bag of SunChips® is shown (A) prior to composting and (B) after 18 days of composting.

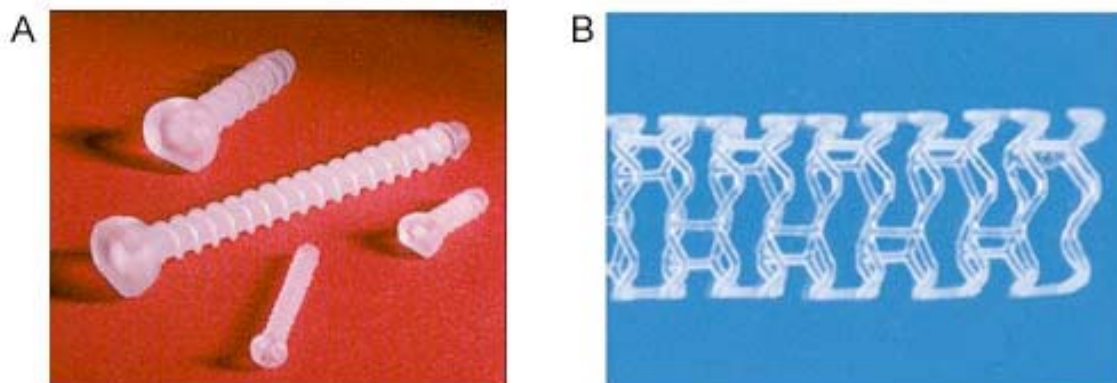


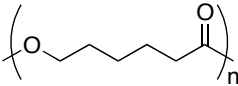
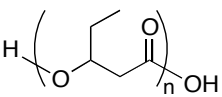
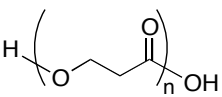
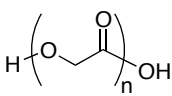
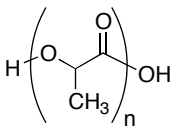
Figure 1.2: Two examples of biodegradable polymers used for biomedical applications: (A) surgical bone screws manufactured by NP Pharm from the biodegradable polymer Lactel® and (B) A prototype of a fully absorbable, biodegradable stent produced by Abbott Vascular in conjunction with Biotronic and REVA Medical. Images obtained from NP Pharm¹² and Advanced Medical Technologies.¹³

Polyesters are among the most exhaustively studied and widely used biodegradable polymeric materials. Polycaprolactone and the poly(hydroxyalkanoate)s, which include poly-3-hydroxyvalerate (PHV) and poly-4-hydroxybutyrate (P4HB), are produced in large quantities and have been explored for their potential commercial and biomedical applications. However, it is the poly(α -ester)s polyglycolic acid (PGA) and polylactic acid (PLA) that have garnered tremendous interest over the past several decades due to the low toxicity of the polymers and their biodegradation products. PGA, PLA and their copolymers have been chosen for biologically compatible applications since the 1960's. The commercially available suture materials Vicryl® and Dexcon®, for example, are made from PGA and PLA/PGA copolymers.

Because of the low toxicity of PLA and its biodegradation products, PLA and PLA copolymers are used in numerous applications including biodegradable bone screws,^{14, 15} surgical stents¹⁶⁻¹⁹ and controlled-release drug delivery systems.^{8, 19, 20} PLA's

status as an FDA-approved material²¹⁻²³ and its predictable properties make it an ideal material to explore in order to expand its possible applications in the biomedical sciences.

Table 1.1: Common biodegradable polyesters and their uses.

Type of polyester	structure	uses
Polycaprolactone (PCL)		Specialty polyurethane production, drug encapsulation.
Poly-3-hydroxyvalerate (PHV)		Drug delivery systems (often in co-polymers with P4HB).
Poly-4-hydroxybutyrate (P4HB)		Heart valves, sutures and medical textile products.
polyglycolic acid (PGA)		Surgical sutures, drug delivery devices, skin care products.
polylactic acid (PLA)		Compostible food packaging, surgical bone screws, drug delivery systems.

1.2 Synthesis and properties of polylactic acid

Commercial production of polylactic acid begins with bacterial fermentation of natural sources such as cornstarch and cane sugar to produce lactic acid.²⁴ Attempts at direct polymerization of lactic acid, however, results in the formation of oligomeric species that are not useful for commercial applications (Figure 1.3A). The water produced during direct polymerization acts to hydrolyze the growing polymer chain,

resulting in the formation of low molecular weight oligomers. In order to circumvent this problem, lactic acid is first dimerized to give lactide while the water generated is removed to drive the reaction (Figure 1.3B). The resulting lactide is then converted into commercially useful polymer via ring-opening polymerization (ROP) by heating it in the presence of a suitable catalyst (Figure 1.3C). Industrial production of PLA utilizes tin(II)bis-2-ethylhexanoate (tin octoate) as the catalyst due to its good solubility in molten lactide, high catalytic activity, and low rate of racemization of the polymer chain.^{25, 26} Other inorganic²⁷ and organic²⁸ catalysts have been explored, however, tin octoate remains the catalyst of choice for large-scale production of PLA.

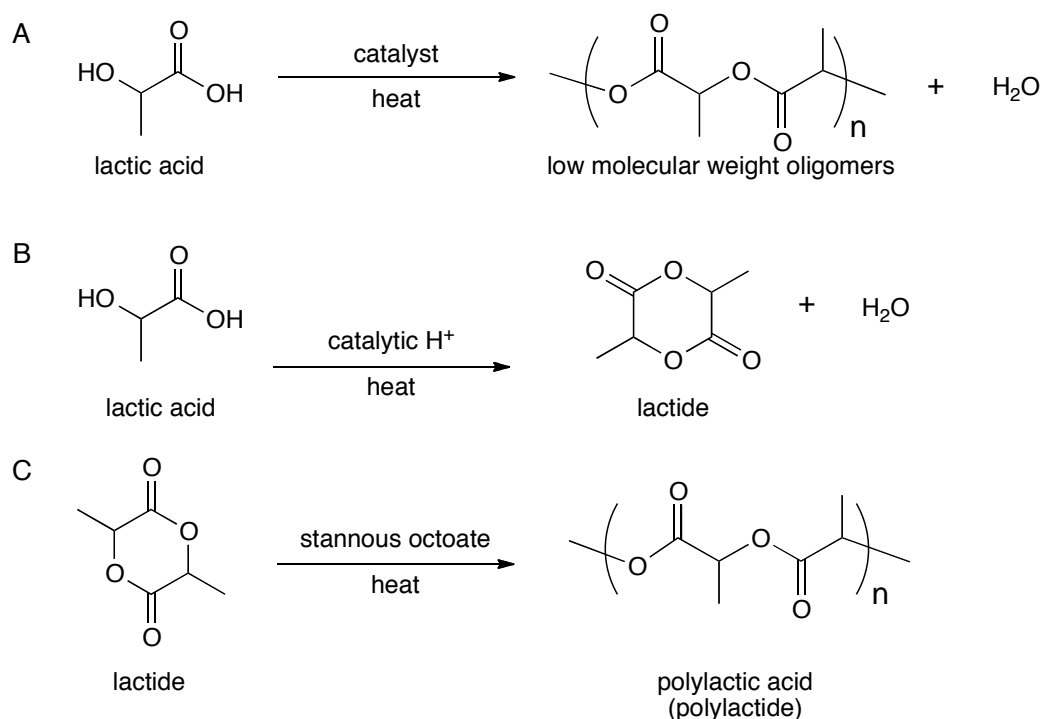


Figure 1.3: Current commercial preparation of polylactic acid (PLA). Direct polymerization of lactic acid (A) results in the formation of oligomeric material. Alternatively dehydrative dimerization (B) leads to the formation of monomeric lactide that can then be polymerized via ring opening polymerization (C).

The chiral nature of lactic acid leads to the formation of several different PLA products. Dimerization of the naturally occurring L-lactic acid gives L-lactide and subsequent polymerization leads to the formation of poly(L-lactic acid) (PLLA). Similarly, D-lactic acid leads to poly(D-lactic acid). Both PLLA and PDLA are semicrystalline polymers with a melting point (T_m) of about 180°C and a glass transition temperature (T_g) of 60-65°C.^{15, 29} Physical blends of PLLA and PDLA result in materials with higher crystallinity (and therefore a higher T_m) that are more suitable for applications requiring increased stiffness or resistance to high temperature.³⁰ Polymerization of either racemic or *meso* lactide generally produces amorphous material that still has wide application as films, membranes and coatings;³¹ however, using stereoselective catalysts in polymerization can lead to the formation of semicrystalline polymers from either the racemic^{32, 33} or *meso*³⁴ lactide.

Degradation of poly(α -hydroxy acid)s such as PGA and PLA occurs primarily via an ester hydrolysis mechanism first proposed by Chu.³⁵ Under physiological conditions (pH 7.4, 37°C), PLA is first hydrolyzed into smaller oligomers and ultimately broken down into its constituent lactic acid units,³⁶ with degradation rates dependent on parameters such as molecular weight and degree of crystallinity of the particular polymer.³⁷ In the case of PLA-based implantable devices used in humans, the lactic acid that is generated can be enzymatically oxidized to pyruvate by lactate dehydrogenase and further processed by various physiological mechanisms such as the Krebs (citric acid) cycle.³⁸ Accordingly, PLA-based materials particularly attractive for use in biomedical applications as they break down to byproducts of low toxicity that are effectively processed by the human body.

Table 1.2: Physical properties of polylactic acids.

compound	Crystallinity	T_m (°C)	T_g (°C)
Poly(L-lactide) (PLLA)	semicrystalline	173-178	60-65
Poly(D-lactide) (PDLA)	semicrystalline	173-178	60-65
50:50 PLLA:PDLA	semicrystalline	230	n/a
<i>meso</i> -Poly(DL-lactide) ^a	amorphous	130-135	44-48
<i>rac</i> -Poly(DL-lactide) ^a	amorphous	n/a	38-42
<i>meso</i> -Poly(DL-lactide) ^b	semicrystalline	152	34
<i>rac</i> -Poly(DL-lactide) ^b	semicrystalline	191	55

^a Prepared using standard polymerization techniques using a non-stereospecific catalyst. ^b Prepared using a stereospecific catalyst.

1.3 Incorporating functionalization into PLA

Although PLA is a commercially useful material, its utility is limited by its insolubility in aqueous media and lack of functionalizable side chains. Ouchi and Fujino have demonstrated the synthesis of a PLA derivative containing pendant benzyl ester functional groups, which may be easily converted to the free acid by hydrogenation (Figure 1.4).³⁹ The catalytic effect of the acid groups, however, can lead to the accelerated hydrolysis of the PLA backbone.

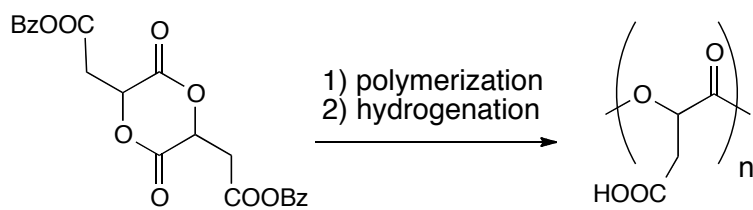


Figure 1.4: Synthesis of a PLA derivative containing pendant protected carboxylic acid functional groups from a functionalized lactide precursor. The carboxylic acid is unmasked upon hydrogenation of the benzyl ester.

Other groups have tried copolymerizing lactide with monomers to introduce useful functional pendant groups. In particular, Feijen and coworkers have produced polyesteramides by copolymerizing DL-lactide with various substituted morpholine-2,5-diones (Figure 1.5).⁴⁰ The morpholine-2,5-diones were readily synthesized from protected amino acids L-aspartic acid L-lysine and L-cysteine to ultimately provide PLA functionalized with acid, amine, and thiol groups, respectively. This methodology generates a viable synthetic route to functionalizable polymers using a variety of α -amino acids as starting materials, and was successfully employed by Langer to make the amine-substituted polyesteramide poly(lactic acid-co-lysine) that was further modified with RGD peptide and evaluated for tissue engineering applications.^{41, 42} This approach has several limitations: morpholine-2,5-diones are less reactive than their lactide counterparts, which results in a lower percent conversion for the morpholine-2,5-dione monomer as compared to DL-lactide. Therefore, the morpholine-2,5-diones are not as easily incorporated into the growing polymer chain.⁴⁰ Practical considerations also limit the scope of the morpholinedione methodology. Although many α -amino acids can, in principle, be used as starting materials for the morpholinedione monomer, only those

obtained at reasonable cost can be used to make this a commercially viable process. For example, incorporating the highly desirable terminal alkyne function group via the unnatural amino acid propargylglycine is prohibitively expensive for large-scale production: DL-propargylglycine costs over \$130 per gram and the price of the enantiomerically pure L-propargylglycine is over \$500 per gram—over 200 times the cost of L-lysine.

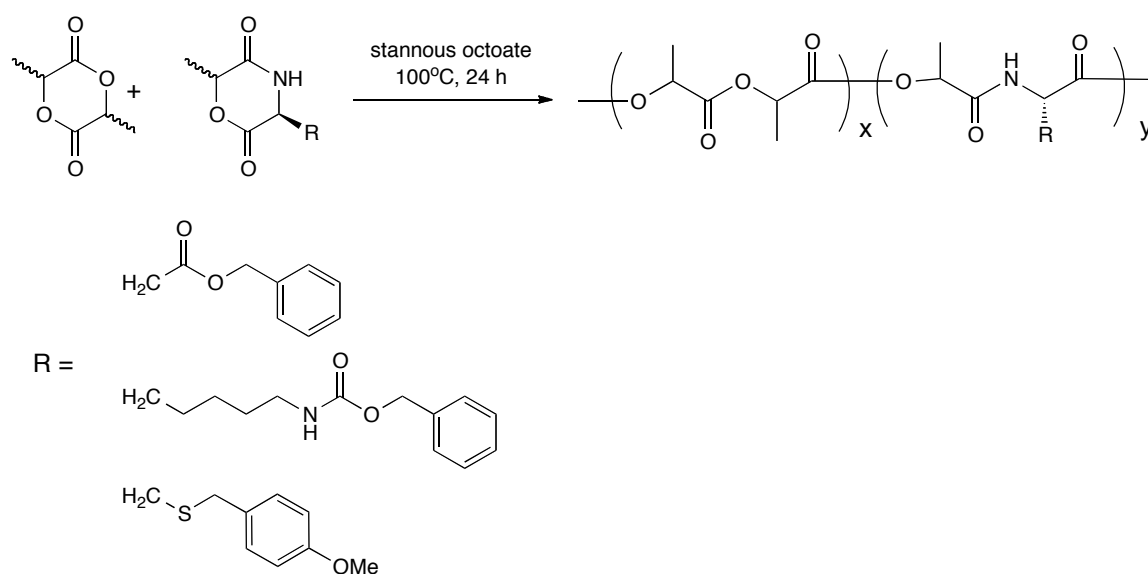


Figure 1.5: Feijen’s preparation of various polyesteramides via copolymerization of DL-lactide with substituted morpholine-2,5-diones prepared from protected L-aspartic acid, L-lysine and L-cysteine.

Baker and coworkers developed a method for the synthesis of terminal alkyne-functionalized PLA from the alkyne-bearing lactide (Figure 1.6).⁴³ The substituted lactide is prepared in three steps. First propargyl bromide is treated with zinc metal to generate the corresponding organozinc reagent and reacted with ethyl glyoxylate to give the α -hydroxy acid ethyl ester, which is then readily hydrolyzed to give the free acid in good

yield. Dimerization of the acid in the presence of *p*-toluenesulfonic acid (PTSA) with simultaneous azeotropic removal of water gives the desired lactide, but in a modest 34% yield. Although this methodology permits synthesis of the alkyne-substituted lactide on a multi-gram scale at relatively low cost, the approach is not general enough to produce lactide products with a variety of derivatizable pendant groups.

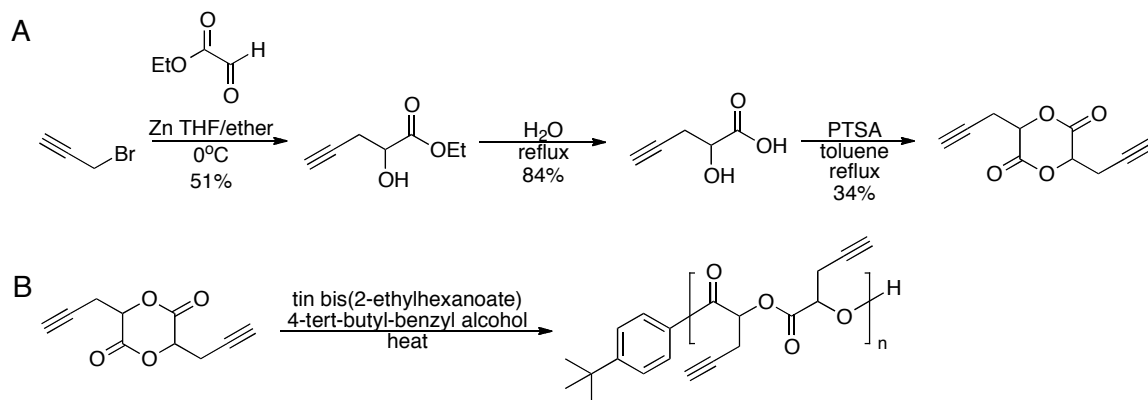


Figure 1.6: Synthesis (A) and polymerization (B) of an alkyne-functionalized lactide.

1.4 Goals of the dissertation research

PLA and its derivatives have many demonstrated uses, particularly in FDA-approved biomedical application, and its biodegradability and biocompatibility make this material ideally suited to further exploration. This portion of the dissertation will focus on developing a general method for introducing a wide range of useful pendant groups to PLA and demonstrating potential applications of these polymeric materials. The successful synthesis of a variety of derivatized PLAs may provide access to PLA-based materials with interesting new functionality while retaining the physical properties that make them particularly useful for current commercial and biomedical applications.

Chapter 2

Development of a facile procedure for generating sidechain functionalized poly(α -hydroxy acid) copolymers from aldehydes via a versatile Passerini-type condensation

2.1 Introduction

Poly(lactic acid (PLA), one of the most well-known members of the poly(α -ester) class of polymers, has attracted significant interest for its potential uses in biodegradable and biocompatible material; however PLA has inherent limitations due to its insolubility in aqueous media and lack of functionalizable sidechains. Simple, general, and scalable methods to incorporate functionality in PLA-based polymers may enable new applications of these materials for biomedical and commercial uses. Although previous reports describe the preparation of PLA-based copolymers containing functionalized sidechains,^{43, 44} these methodologies are often laborious or require specialized reagents to obtain a specific, desired functional group in the polymer. The research presented in this chapter describes a method to produce high molecular weight PLAs with functionalized side chains via a multi-component, Passerini-type condensation reaction. This methodology has led to the synthesis of PLAs and PLA precursors functionalized with terminal alkyne, azide, oligoethylene glycol and phthalimide groups, which will allow further derivatization of these polymers. These functionalized PLAs provide an entry

into the synthesis of biologically compatible polymeric compounds with potentially useful properties for various biomedical applications.

2.2 The Ugi and Passerini reactions in organic synthesis

The Ugi⁴⁵ and Passerini⁴⁶ reactions are related multicomponent condensations that employ isocyanides to generate bis-amides and esteramides, respectively. A powerful tool for convergent synthesis, the Ugi reaction generates a complex product in high yield via the one-pot reaction of an aldehyde (or ketone), an amine, an isocyanide and a carboxylic acid (Figure 2.1).⁴⁵ The reaction proceeds initially by forming an imine *in situ* from the aldehyde or ketone and amine components. Protonation of the resulting imine generates the highly electrophilic iminium ion, which is readily attacked by the isocyanide to generate a nitrilium species. Subsequent reaction with the carboxylate forms an alkylimidic anhydride that is rapidly converted to the stable bis-amide product via Mumm rearrangement,⁴⁷ which provides the driving force for the Ugi reaction.

The closely related Passerini reaction does not have an amine component and therefore proceeds by direct attack of the aldehyde or ketone by the isocyanide; however, other aspects of the reaction are similar to the Ugi. It has been proposed that the Passerini reaction may proceed via stepwise (ionic) or concerted mechanisms depending on the polarity of the solvent used. Both variations are illustrated in Figure 2.2 and account for the formation the esteramide product via an alkylimidic anhydride intermediate.

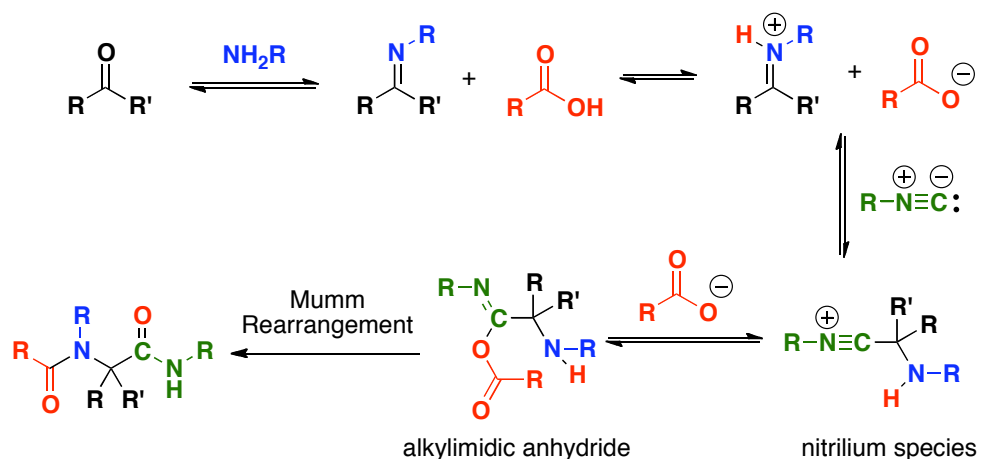


Figure 2.1: The mechanism of the multicomponent Ugi Reaction between an aldehyde or ketone (black), amine (blue) isocyanide (green) and carboxylic acid (red) to generate a bis-amide.

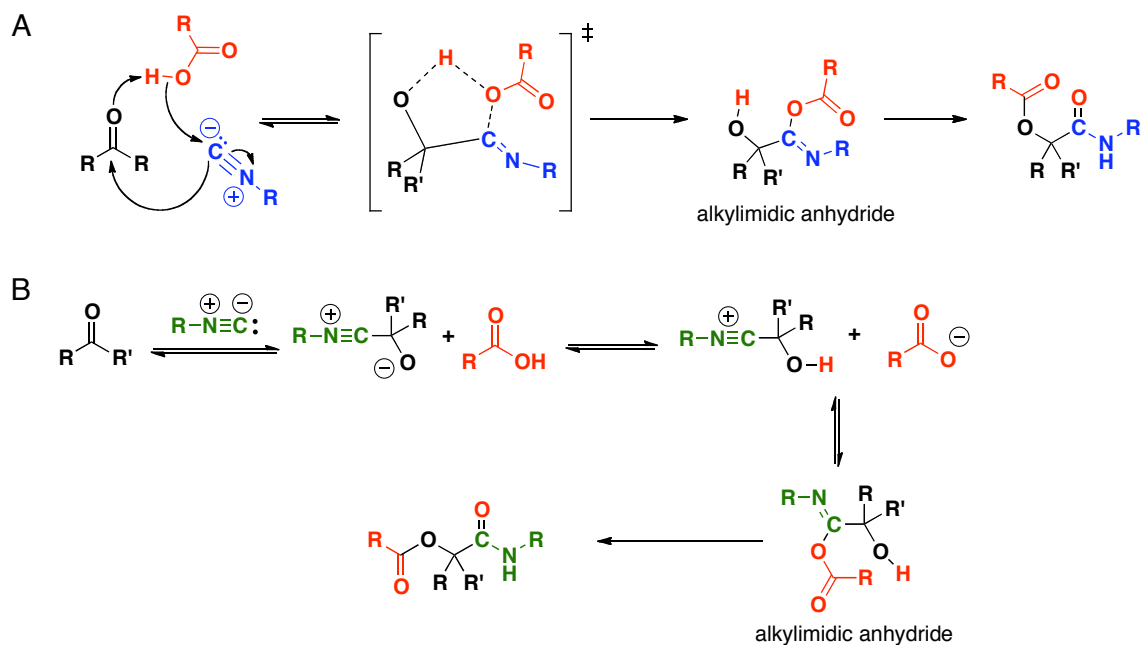


Figure 2.2: Proposed concerted (A) or stepwise (B) mechanisms for the multicomponent Passerini reaction. Both proposed mechanisms proceed via an alkyimidic anhydride intermediate that rapidly rearranges to form an esteramide.

Recently, Kobayashi and co-workers reported successful syntheses of various pyroglutamic acids via the Ugi reaction by employing a convertible isocyanide (**1**) (Figure 2.2).⁴⁸ The reaction proceeds as expected to give the bis-amide product in high yield; however, the functionality introduced by the convertible isocyanide allows further reactivity that is centrally important to this synthesis. Treating the bis-amide with an acid such as *p*-toluenesulfonic acid (PTSA) leads to collapse of the acetal and subsequent cyclization to form the readily hydrolyzable *N*-acylindole product.

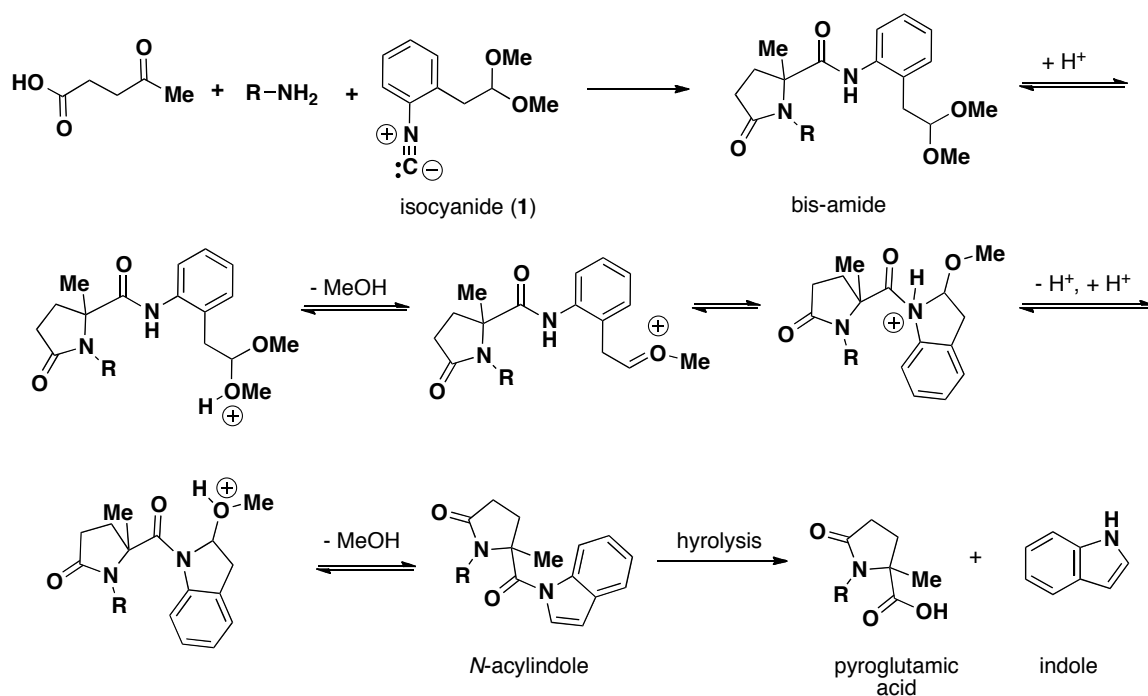


Figure 2.3: Formation of pyroglutamic acids using a convertible isocyanide. The bis-amide formed via the Ugi reaction is readily converted to the *N*-acylindole upon treatment with PTSA. The *N*-acylindole is subsequently hydrolyzed to give pyroglutamic acid and indole.

2.3 Passerini-type condensations for generating α -hydroxy-*N*-acylindoles precursors to functionalized lactide monomers

Motivated by Kobayashi's success in utilizing Ugi chemistry for the synthesis of pyrroglutamic acid, we explored the possibility of using convertible isocyanide **1** in a Passerini-type condensation reaction to develop a general method for generating α -hydroxy-*N*-acylindoles containing a variety of side chain functionality. We proposed a variation of the Passerini where the normally present carboxylic acid is replaced by water and a catalytic amount of a sulfonic acid such as PTSA. Catalytic PTSA serves two

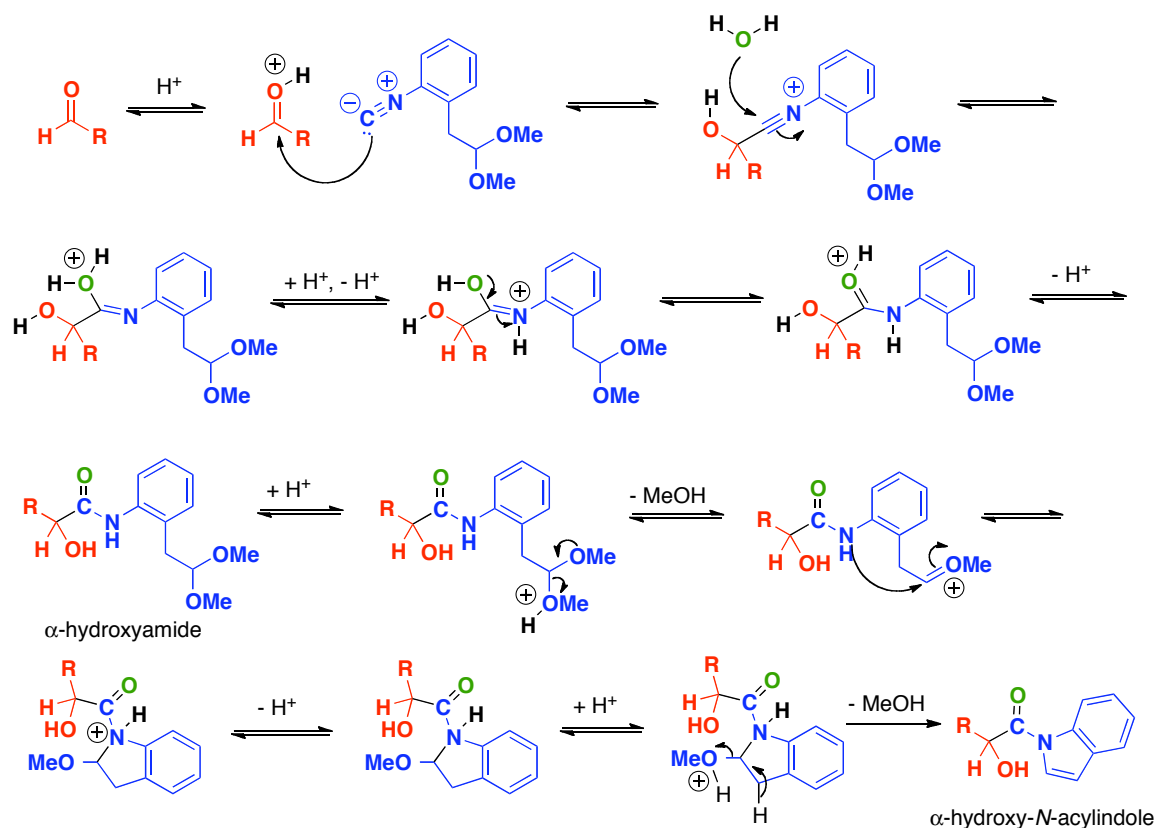


Figure 2.4: Proposed stepwise mechanism of the Passerini-like reaction for the generation of α -hydroxy-*N*-acylindoles. This variant of the Passerini replaces the carboxylic acid component with water a catalytic amount of PTSA. The catalytic acid initiates the reaction and also affects the transformation of the esteramide intermediate to the α -hydroxy-*N*-acylindole. In principle, the generation of the esteramide may also proceed by concerted mechanism similar to that described in Figure 2.2.

purposes: 1) it initiates the reaction by protonating the aldehyde, and 2) it provides the necessary acid to affect the cyclization of the esteramide to the α -hydroxy *N*-acylindole. Other aspects of this reaction, however, presumably remain the same (Figure 2.4). Because of the dual role of the catalytic acid, we speculated that this reaction may be used to generate the α -hydroxy *N*-acylindole in a one-pot process. Once formed, we hypothesized that these functionalized α -hydroxy *N*-acylindoles could be readily hydrolyzed to the corresponding acids and further converted to hemilactides for subsequent incorporation into PLA-based copolymers (Figure 2.5). A significant advantage of this synthetic approach is its versatility, since this common strategy can potentially generate a large and diverse set of tailored polymers from simple, commercial or readily prepared aldehydes.

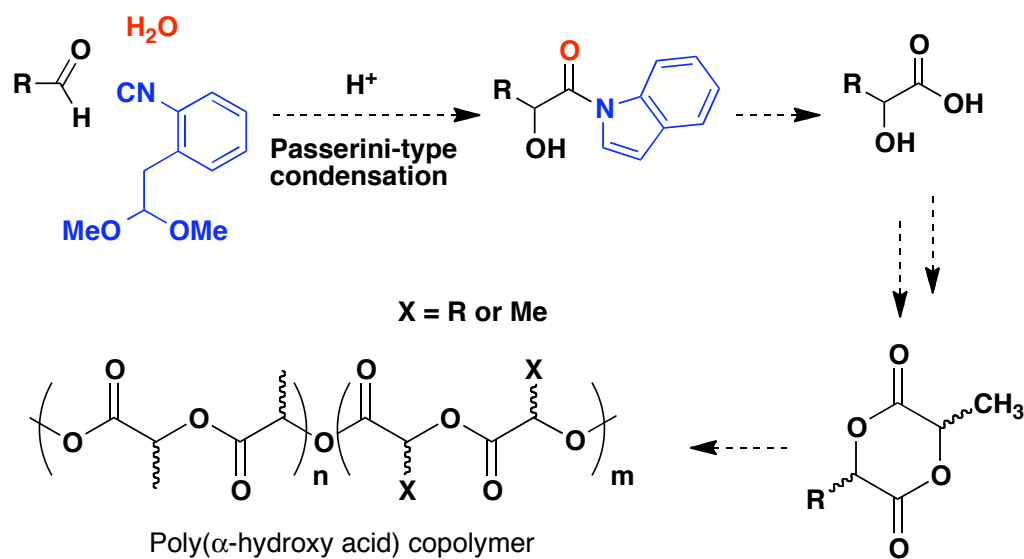


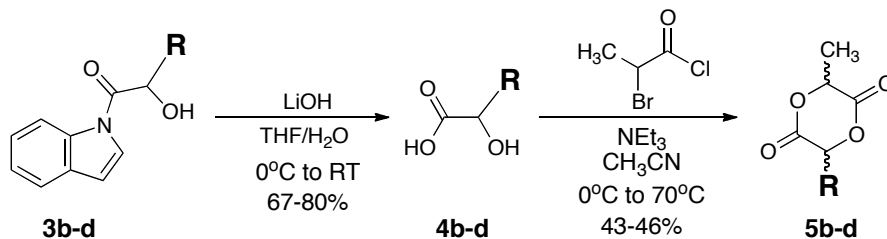
Figure 2.5: Proposed route toward generating PLAs. The *N*-acylindoles formed during the Passerini-type reaction may be further converted to sidechain functionalized hemilactides and incorporated into poly(α -hydroxy acid) copolymers.

We demonstrated that reaction of convertible isocyanide **1**, acetaldehyde **2a** and water afforded the *N*-acylindole of lactic acid **3a** in good yield (Table 2.1). To investigate the general utility of these condensation conditions, we tested several aldehydes for the ability to generate sidechain functionalized *N*-acylindoles. The results indicate that we can introduce a range of chemical properties in good yield using this method—that is, functionality with azide-reactive (**2b**), alkyne-reactive (**2c** and **2d**), hydrophilic (**2d**), or sterically bulky (**2e**) properties. We chose to incorporate sidechains from aldehydes **2b-2e**, which are easily prepared from commercially available compounds, in the condensation reaction in order to provide chemical handles for post-polymerization modification or to introduce other potentially useful chemical or physical properties into the polymer. Functional groups provided by aldehydes **2b-d**, for instance, would lead to PLA-based copolymers that could be modified by utilizing a Cu(I)-catalyzed azide-alkyne cycloaddition (CuAAC) reaction.⁴⁹⁻⁵¹ Compound **2d**, in addition to providing a handle for CuAAC, may also impart a degree of water solubility to a polymer that is otherwise insoluble in aqueous solution. Aldehyde **2e** may also afford access to a PLA-based copolymer containing sidechains with amine handles upon deprotection of the phthalimide group.^{52, 53} To illustrate another potential advantage of this Passerini-type condensation for generating large-scale quantities of *N*-acylindoles, we prepared multiple grams of **3b** from 4-pentynal from a single condensation reaction.

Table 2.1: Isolated yields of *N*-acylindoles from the Passerini-type condensation reaction.

compound	aldehyde	yield (%)
3a		74
3b		67
3c		69
3d		65
3e		69

In order to demonstrate the utility of *N*-acylindoles as functionalized polymeric precursors, we converted compounds **3b-d** to the corresponding hemilactides **5b-d**. The *N*-acylindoles were readily hydrolyzed using LiOH in THF/H₂O to give the corresponding α -hydroxy acids **4b-d** in 67-80% isolated yields; these α -hydroxy acids required minimal purification and were isolated as pure products after solution phase extraction. Subsequent reaction of α -hydroxy acids with 2-bromopropionyl chloride afforded hemilactides **5b-d** in moderate yield as mixtures of stereoisomers (Scheme 2.1).



Scheme 2.1: Scheme for the facile two-step conversion of α -hydroxy *N*-acylindoles to the corresponding hemilactides.

2.4 Incorporation of functionalized hemilactides into PLA copolymers

To show these novel hemilactides **5b-d** could be incorporated into PLA-based copolymers, we reacted 15 mol % of **5b-d** with commercial D,L-lactide and catalytic amounts of stannous octoate (as a polymerization catalyst) and 4-*tert*-butylbenzyl alcohol (as a co-initiator) at 130 °C under an inert atmosphere for 2 h. We analyzed the resulting polymers **6b-d** by NMR and size-exclusion chromatography (SEC) to estimate the percent conversion of lactide or hemilactide to polymer, the number-average molecular weight (M_n), and the polydispersity (PDIs) of the copolymers. As a control, we compared these parameters of copolymers **6b-d** to pure PLA polymer **6a** that was synthesized under the same polymerization conditions. Lactide and hemilactide were efficiently converted to copolymer under these reaction conditions (Table 2.2). SEC analysis of **6b-d** indicated that these polymerization conditions resulted in polymers with a molecular weight range of 22-32 kDa and PDIs in the range of 1.1-1.2, which were similar in size and dispersity as pure PLA polymer **6a** that was synthesized in the absence of a hemilactide as a dopant. The SEC traces may be found in Appendix A.

We next wanted to verify that copolymers **6b-d** were amenable to post-polymerization modification, therefore, we subjected **6a-d** to CuAAC conditions in the

presence of an excess of a dansyl derivative containing either an azide (**7**) or a terminal alkyne (**8**) group. The UV-active dansyl group incorporated into all three copolymers **6b-d** under these reaction conditions (Figure 2.6), whereas pure PLA polymer **6a** remained unmodified. These results strongly support that hemilactides **5b-d** were indeed incorporated into polymers **6b-d** and that the functionalized sidechains retained their specific reactive properties.

We estimated the percent conversion of the polymerization reactions of hemilactides into polymer **6b-d** by analysis of crude reaction samples by $^1\text{H-NMR}$ (Appendix A). Percent conversion was estimated by integrating the methine protons in the monomeric species (M) and the methine protons in the polymeric compound (P). The percent conversion was estimated to be $1 - [\text{M}/(\text{M}+\text{P})]$. The data from $^1\text{H-NMR}$ and $^{13}\text{C-NMR}$ of crude samples of polymers **6b-d** (Appendix A) also provided evidence that hemilactides **5b-d** incorporated into polymers **6b-d**. The degree of incorporation of hemilactide appeared to be nearly quantitative from comparison of the integration of methyl Hs and methine Hs within the polymers by $^1\text{H-NMR}$ (within the inherent error limits of $^1\text{H-NMR}$). Additionally, we saw evidence that **5b-5d** had been incorporated into the polymers by examining key regions in the $^{13}\text{C-NMR}$. For **6b**, for instance, the $^{13}\text{C-NMR}$ resonance at $\delta = 14.2$ ppm (which represents the propargylic carbon in hemilactide **5b**) was absent and a new broad peak was observed at around 14.4 ppm, suggesting that the alkyne functionality is present on the polymeric species rather than the monomeric hemilactide form. For **6c-6d**, a broadening of the $^{13}\text{C-NMR}$ peak is observed at the resonances near $\delta = 51$ ppm (which represents the carbon atom bearing

the azide functionality), suggesting that the azide functionality is present in the polymeric species rather than in the monomeric hemilactide form.

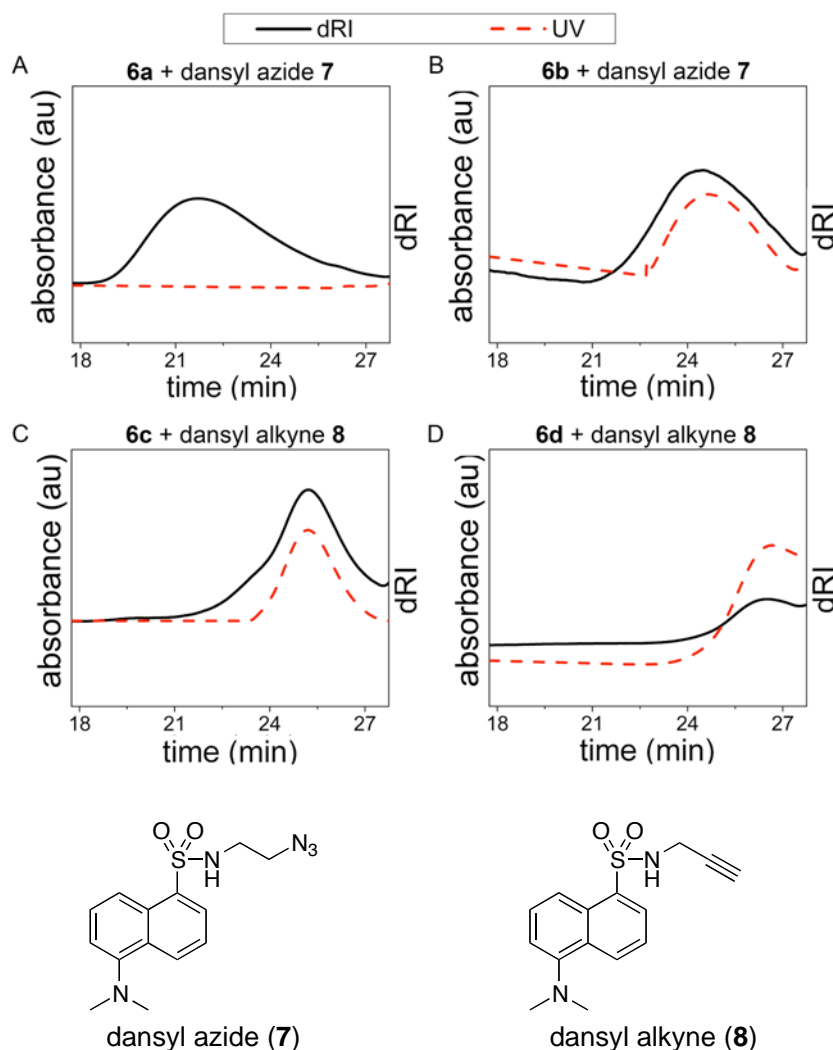
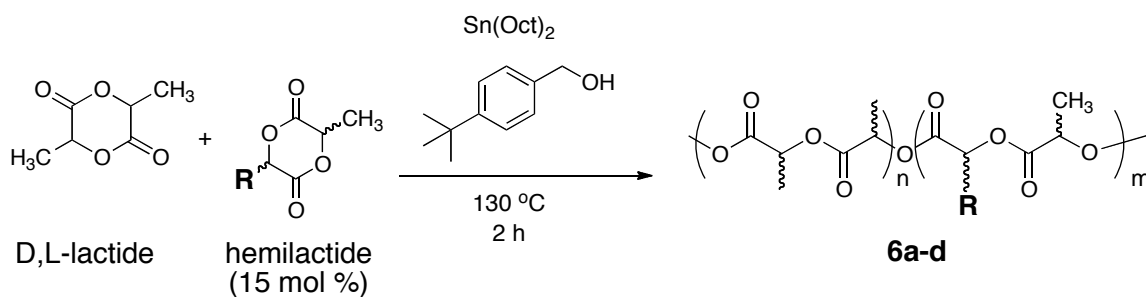


Figure 2.6: Modification of copolymers **6b-d** using CuAAC click reactions. (A-D) Size exclusion chromatographic traces of crude samples containing CuSO_4 and sodium ascorbate with: (A) PLA **6a** and dansyl azide **7**, (B) alkyne-functionalized polymer **6b** and dansyl azide **7**, (C) azide-functionalized polymer **6c** and dansyl alkyne **8**, or (D) azide-functionalized polymer **6d** and dansyl alkyne **8**. The chromatograms of crude polymer-containing solutions were monitored by differential refractive index (dRI, black) and UV absorbance (red). The UV was monitored at $\lambda = 365$ nm to indicate species containing a dansyl group.

Table 2.2: Incorporation of functionalized hemilactides into PLA-based polymers.

hemilactide	conversion (%)	$10^{-3} \cdot M_n$ (g/mol)	PDI (M_w/M_n)
none	91	27.4	1.19
	94	22.6	1.11
	77	34.5	1.12
	71	23.1	1.17

2.5 Attempting direct polymerization of α -hydroxy-*N*-acylindoles

The curious behavior of the α -hydroxy-*N*-acylindoles led us to investigate the possibility of using these compounds as the monomeric starting material for direct polymerization to form PLA derivatives. α -Hydroxy-*N*-acylindoles are easily hydrolyzed to form carboxylic acids and readily form esters and amides upon treatment with alcohols and amides, respectively. However, attempts to generate thioesters by treating α -hydroxy-*N*-acylindoles with thiols led to decomposition products—likely oligomeric and polymeric species—that formed via the rapid intermolecular self-condensation reaction

of the short-lived α -hydroxythioester intermediate (Figure 2.7). Accordingly, we speculated that treating α -hydroxy-*N*-acylindoles with a suitable base could remove the proton from the α -hydroxy group, generating enough nucleophilic alkoxide to initiate polymerization of the α -hydroxy-*N*-acylindole to directly produce a poly(α -hydroxy acid) and indole without the need to first prepare lactide-based monomers.

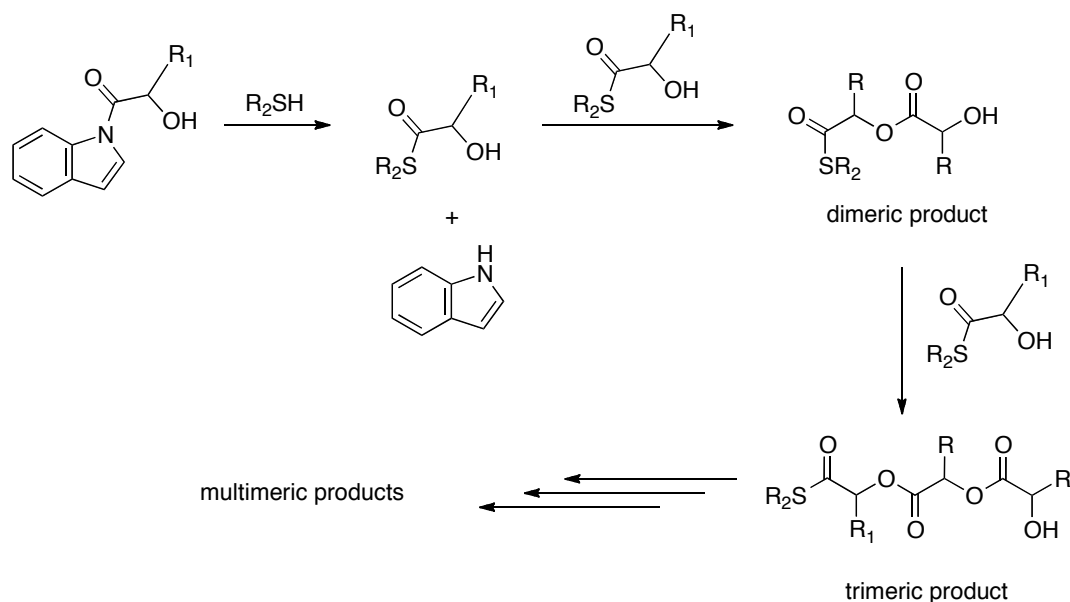


Figure 2.7: One possible pathway of α -hydroxy-*N*-acylindole decomposition upon treatment with a thiol. Initial attack of the α -hydroxy-*N*-acylindole by the highly nucleophilic thiol may lead to the formation of an α -hydroxythioester, which can subsequently undergo self-condensation to form dimeric, trimeric and ultimately multimeric products.

We attempted to directly polymerize acylindole **3b** using 1 molar equivalent of triethylamine as the base with anhydrous THF as the solvent. Only starting material was observed after a day of stirring at room temperature. Adding 0.1 molar equivalents of anhydrous Cs_2CO_3 , however, resulted in complete disappearance of starting material after

several hours. Analysis of the reaction mixture by SEC showed that no high molecular weight polymer was produced. Electrospray Ionization Mass Spectrometry (ESI-MS) analysis of the reaction mixture, however, revealed a series of molecular ion peaks separated by $m/z = 72$, corresponding to the mass of a monomeric lactic acid unit (Figure 2.7). Thus, the SEC and ESI-MS evidence together suggest that only low molecular weight oligomers are formed during the reaction. Attempts to initiate polymerization of functionalized α -hydroxy-*N*-acylindole **3b** using Cs_2CO_3 in THF led to oligomer formation as well. We suspected that the low molecular weight could be attributed to residual water in THF, therefore we attempted to initiate polymerization of **3b** in dry dichloromethane with the strong organic base 1,8-diazabicyclo[5.4.0]undec-7-ene (DBU)

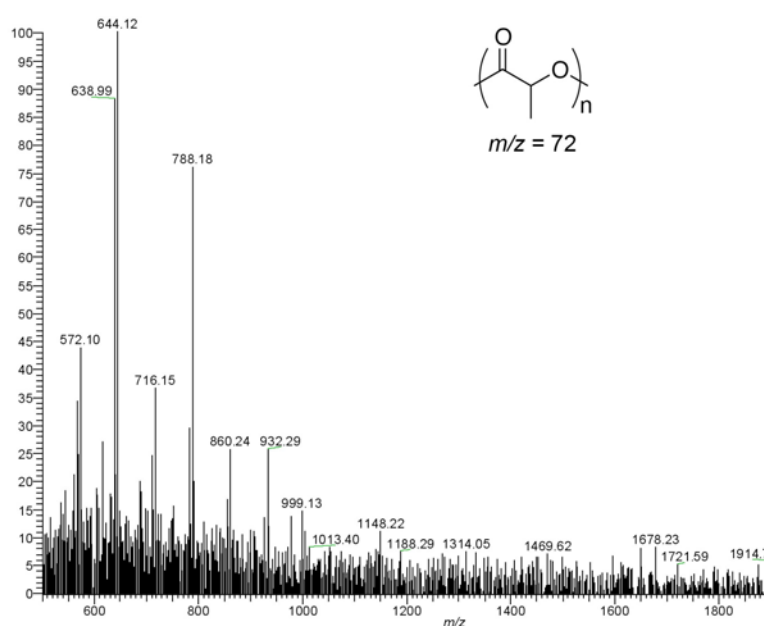


Figure 2.8: ESI-MS analysis of attempted polymerization of α -hydroxy-*N*-acylindole **3a** using Cs_2CO_3 as an initiator. Peaks at $m/z = 644, 716, 788, 860$ and 932 have differences of 72 , corresponding to the mass of a monomeric unit of PLA.

under the assumption that it would be easier to keep the reaction moisture-free; however, these conditions also generated oligomeric products and the expected pattern of molecular ion peaks (differences of $m/z = 110$) were observed (Figure 2.8).

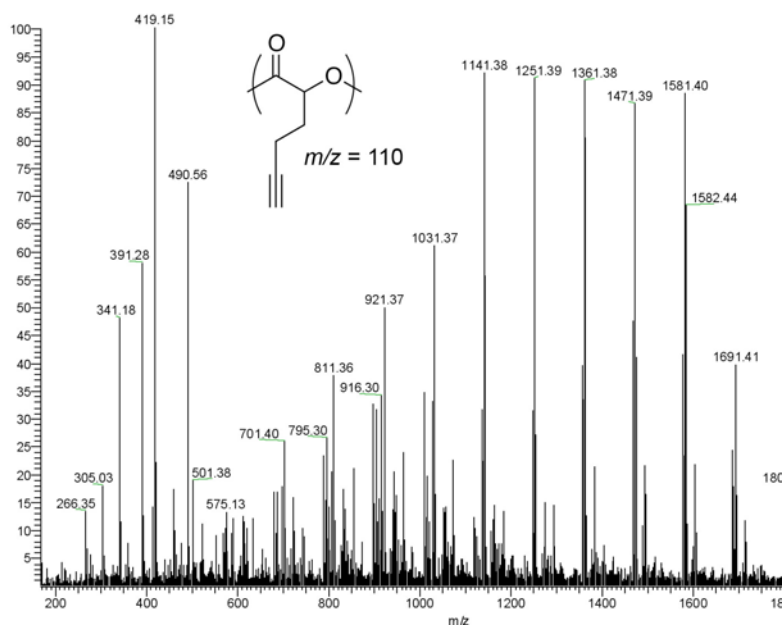


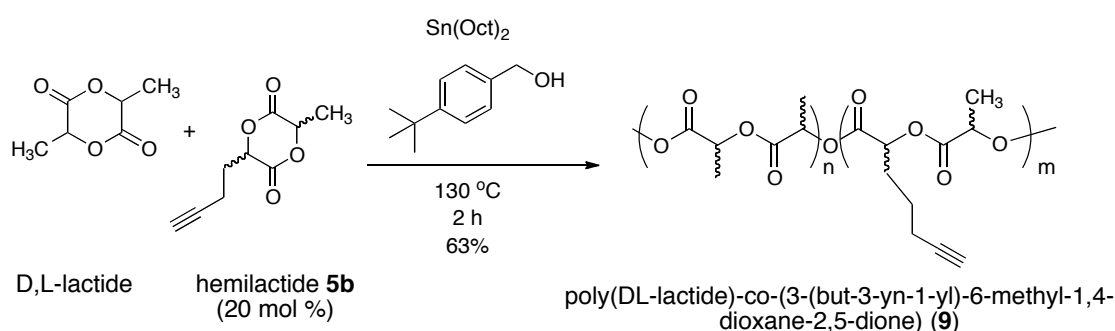
Figure 2.9: ESI-MS analysis of attempted polymerization of α -hydroxy-*N*-acylindole **3b** initiated with DBU in DCM. Peaks at $m/z = 701, 811, 921, 1031, 1141, 1251, 1361, 1471, 1581,$ and 1691 have differences of 110, corresponding to the mass of a monomeric unit of poly(2-hydroxy-5-hexynoic acid).

Unfortunately, attempts to vary base concentrations and solvents did not yield products of high molecular weight. The formation of the electron rich indole side product may react with electrophilic intermediates generated during polymerization and lead to side products that limit multimer size and yields. Additionally, as this process is a living polymerization,⁵⁴ chain-transfer kinetics may limit the size of multimer formed. The thermodynamics of the reaction may be improved by using α -hydroxy-*N*-acylindoles

that have more electron-withdrawing groups on the indole ring to improve its ability as a leaving group. However, this avenue has yet to be explored.

2.6 Preparatory scale production of an alkyne-functionalized polylactic acid copolymer.

In order to demonstrate the utility of this methodology for practical applications, we synthesized polymer **9**, a copolymer of DL-lactide and the alkyne-functionalized hemilactide, on the gram scale (Scheme 2.2). Commercially available DL-lactide doped with 20 mol% of the alkyne-substituted hemilactide were copolymerized using stannous octoate and 4-*tert*-butylbenzyl alcohol as co-initiators, in a manner nearly identical to the preparation of polymer **6b**. The alkyne-functionalized copolymer was recovered in 63% yield after repeated precipitation (made possible by the large scale of the reaction) to remove monomer, low molecular weight polymer and the tin catalyst. Size-exclusion chromatography of the copolymer revealed a PDI of 1.26 and a M_n of 46.9 kDa. In addition, analysis of the copolymer via ^1H and ^{13}C NMR spectroscopy displayed the peak



Scheme 2.2: Synthesis of poly(DL-lactide)-co-(3-(but-3-yn-1-yl)-6-methyl-1,4-dioxane-2,5-dione) (**9**)

broadening expected for polymeric species. The degree of incorporation of alkyne hemilactide **5b** appeared to be nearly quantitative from comparison of the integration of methyl Hs and methine Hs within the polymers by $^1\text{H-NMR}$. Accordingly, this scaled-up synthesis demonstrates a viable methodology for the preparation of useful quantities of alkyne (and possibly other) functionalized PLA-based copolymers.

2.7 Preparation of polymeric nanoparticles from alkyne-functionalized PLAs

PLA and its copolymers have captured the interest of the biomedical community for their potential applications in drug delivery. Polymeric nanoparticles made from PLA and its derivatives have been successfully used as drug delivery systems that encapsulate and predictably release small molecule-based therapeutics.^{55, 56} Proof-of principle studies by Görner and coworkers have shown that PLA-based nanoparticles can encapsulate the hydrophobic anesthetic lidocaine and release it over a period of about 24 hours.^{57, 58} Others have shown that a variety of small molecules including pentamidine,⁵⁹ haloperidol,^{60, 61} 9-nitrocamptothecin⁶² and others⁶³ can be encapsulated in PLA and PLGA nanoparticle drug delivery systems. These demonstrated success have inspired investigation into the feasibility of making nanoparticles from PLA derivatives such as the alkyne-functionalized copolymer **9** previously described in this dissertation.

Many different methodologies are available for the preparation of polymeric nanoparticles.⁶⁴ Among the most widely used techniques is the oil/water emulsion method, in which a polymeric species dissolved in a water-immiscible solvent such as DCM is emulsified in an aqueous solution containing a stabilizer (usually polyvinyl alcohol). Subsequent evaporation of the organic solvent gives the desired

nanoparticles.⁶⁵ A somewhat more involved variation of this procedure includes the double emulsion method, in which a prepared oil/water emulsion is added to an aqueous phase containing a stabilizer, has been used by Faisant and coworkers to prepare polymeric nanoparticles loaded with the anticancer drug 5-fluorouracil.⁶⁶ Alternatively, PLA nanoparticles may be prepared via nanoprecipitation. This particularly facile method of producing nanoparticles first developed by Fessi and coworkers involves the addition of a solution of PLA (and drug if desired) dissolved in a water-soluble organic solvent (acetone or acetonitrile) to an aqueous solution containing a stabilizer followed by evaporation of the organic solvent.⁶⁷ The nanoprecipitation procedure is useful for encapsulating hydrophobic drug molecules while not very effective for trapping hydrophilic reagents, as they readily leak into the aqueous phase during the process. In addition nanoprecipitation tends to produce smaller particles with a narrower size distribution than those made using emulsion-based methods.

Initially, we attempted to prepare nanoparticles from commercially available PLA using the oil/water emulsion method. The PLA was predissolved in DCM and emulsified with an aqueous phase containing 0.3% (w/v) polyvinyl alcohol as a stabilizer. Analysis by dynamic light scattering gave poor quality data and revealed that the particles formed using this procedure were over 400 nm in diameter and had a large polydispersity. (Table 2.3) The oil/water emulsion method was repeated several times, but the data obtained was neither high quality nor reproducible. As a result, we shifted our efforts to preparing particles using a nanoprecipitation protocol.

Table 2.3 summarizes the different conditions we used to make PLA-based nanoparticles. Acetone and acetonitrile were chosen as the organic solvents due to their

volatility, miscibility with water, and ability to dissolve both PLA and small hydrophobic molecules. Although particle size varied slightly based on the concentration of PLA and the nature of the organic solvent, nanoprecipitation of PLA produced consistently small particles with a narrow PDI. Functionalized PLA particles were produced with somewhat higher PDI, which may be the result of larger molecular weight distribution of the functionalized PLA compared to commercially available PLA. Interestingly, nanoparticles formed from the alkyne-functionalized PLA derivative were considerably smaller, possibly due to the increased hydrophobic effect from the longer alkyl chains.

Table 2.3: Preparation of nanoparticles from commercial PLA and alkyne-functionalized PLA.

polymer	organic solvent	polymer concentration (mg/mL)	method	diameter (nm)	PDI
PLA	DCM	20	o/w emulsion	425	0.779
PLA	acetone	10	nanoprecipitation	163	0.078
PLA	acetone	2.0	nanoprecipitation	111	0.034
PLA	acetone	1.0	nanoprecipitation	119	0.026
9	CH ₃ CN	2.0	nanoprecipitation	66	0.215
9	acetone	2.0	nanoprecipitation	76	0.242

Solvent for precipitation was a 0.3% w/v aqueous solution of poly(vinyl alcohol).

2.8 Encapsulation of small molecules inside of functionalized PLA nanoparticles

In order to exploit the possibility of using our polymeric nanoparticles as vehicles for controlled release of small molecules, we attempted to prepare nanoparticles

containing encapsulated small molecules via nanoprecipitation. We chose several small molecules with both known and potential therapeutic properties to encapsulate in the alkyne-functionalized nanoparticles: the FDA-approved chemotherapeutic agent doxorubicin,⁶⁸ the topoisomerase I inhibitor camptothecin,⁶⁹ and the Thioflavin T analogue BTA-EG₄ (Figure 2.10).

As our initial trial, we attempted to encapsulate doxorubicin (which we purchased as the HCl salt) in commercial PLA. Although nanoparticles were successfully made, the doxorubicin proved to be too water-soluble and did not appear to be encapsulated in the particles. Due to its hydrophobicity, we anticipated that camptothecin would be a more ideal choice for encapsulation. Indeed, it appeared that camptothecin was encapsulated in both commercial PLA and alkyne-functionalized PLA nanoparticles (Table 2.4).

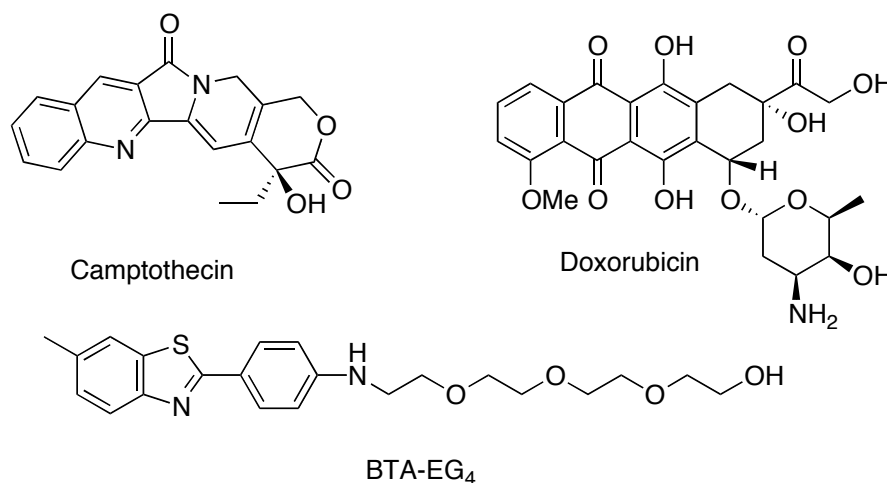


Figure 2.10: Structures of the anticancer drugs camptothecin and doxorubicin and the ThioflavinT analogue BTA-EG₄.

BTA-EG₄ has demonstrated many interesting amyloid-binding and ion channel-forming properties (discussed in chapter 5 of this dissertation); however, its extremely poor water solubility may limit its efficacy as a drug. Accordingly, encapsulating this

molecule within a polymeric nanoparticle may improve its therapeutic properties. We attempted encapsulation of BTA-EG₄ in PLA-based polymeric nanoparticles derived from both commercial PLA and **9** and obtained nanoparticle suspensions that was highly fluorescent even after purification using a size-exclusion column and passage through a 0.45 μm syringe filter. On the contrary, aqueous suspensions of BTA-EG₄ did not exhibit any fluorescence after being similarly treated. It must be noted, however, that the fluorescence observed could also be attributed to small molecules that may be adsorbed to the surface of the nanoparticles, both in the case of BTA-EG₄ and camptothecin.

Table 2.4: Preparation of nanoparticles containing encapsulated small molecule drugs.

polymer	organic solvent	polymer concentration (mg/mL)	Encapsulated drug	method	diameter (nm)	PDI
PLA	acetone	1.0	doxorubicin	nanoprecipitation	167	0.060
PLA	acetone/ methanol	1.0	doxorubicin	nanoprecipitation	215	0.176
PLA	CH ₃ CN	1.0	camptothecin	nanoprecipitation	122	0.030
9	CH ₃ CN	1.0	camptothecin	nanoprecipitation	62	0.130
PLA	acetone	2.0	BTA-EG ₄	nanoprecipitation	133	0.048
PLA	CH ₃ CN	1.0	BTA-EG ₄	nanoprecipitation	146	0.064
9	acetone	2.0	BTA-EG ₄	nanoprecipitation	85	0.234

2.9 Future Directions for side-chain functionalized PLA-based polymers

The introduction of a derivatizable functional group to PLA has opened the door to many future areas of investigation. Alkyne-functionalized PLA nanoparticles can not

only encapsulate small molecule drugs, but also have their properties modified to affect drug loading and drug release. The presence of alkyne functionality on the PLA provides for a means of making nanoparticle-based drug delivery systems by covalently linking small molecule drugs or targeting groups either directly onto the polymeric scaffold or via a pH cleavable linker such as *N*-ethoxybenzimidazole (NEBI) (Figure 2.11).^{70, 71} We anticipate that these alkyne-functionalized polymers will increase their applicability in the area of polymeric nanoparticle-based drug delivery systems and expand their already important role in other biomedical applications.

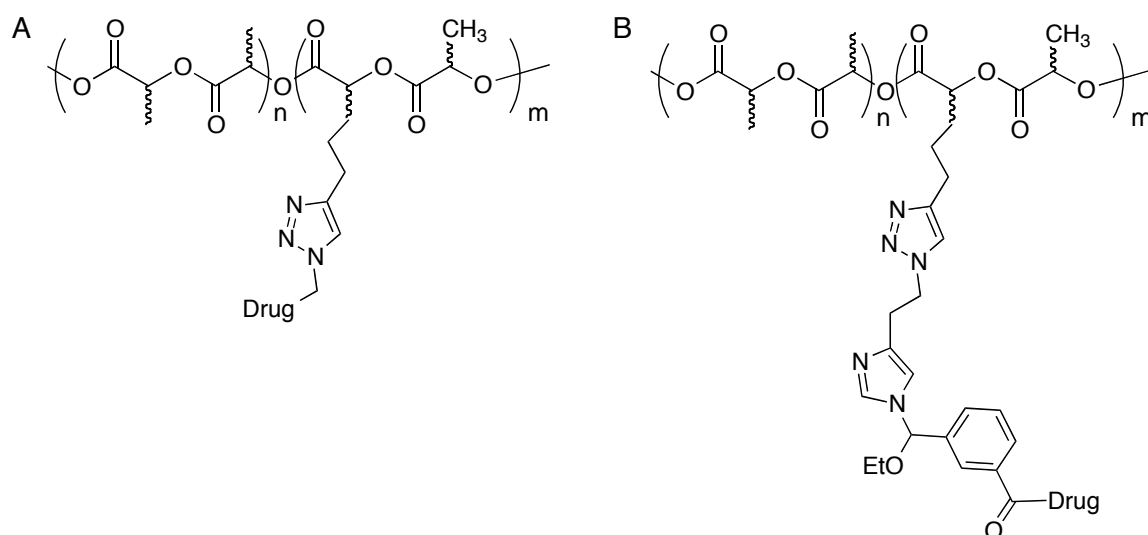


Figure 2.11: Alkyne-functionalized PLA provides a means for covalently linking small molecule-based drugs onto the polymer scaffold. Drugs may be attached (A) directly to the scaffold using an azide-functionalized drug, or (B) indirectly by exploiting a bifunctional acid-cleavable linker.

2.10 Chapter summary

In summary, this chapter presents an efficient and versatile Passerini-type condensation reaction to generate α -hydroxy acid derivatives that can be readily

incorporated into sidechain functionalized PLA-based copolymers. A particularly attractive feature of this method is the capability of incorporating a range of tailored sidechain functionality into the polymers from a variety of commercially available or readily prepared aldehydes. Furthermore, the procedure outlined in this work affords access to copolymers at potentially practical scales and makes it possible to incorporate functionality for further modification of the polymer. This new methodology, therefore, represents a significant step towards accessing biodegradable and biocompatible materials with improved functional and potentially tunable properties that may find utility in a variety of applications including polymeric nanoparticle drug delivery systems.

2.11 Experimental methods

All synthetic reagents were purchased from Aldrich, Fisher Scientific, Alfa Aesar, Fluka or TCI. DL-lactide was recrystallized twice from toluene before use. Poly(D,L-lactide) (specific viscosity: 0.55-0.75, $M_n = 75,000-125,000$), poly(vinyl alcohol) ($M_n = 13,000-23,000$, 87-89% hydrolyzed). Doxorubicin (purchased as the hydrochloride salt), and camptothecin were used without purification. BTA-EG₄ was prepared according to methods described in chapter 5 of this dissertation. All solvents used for reactions were obtained from Fisher scientific and dried on Alumina columns prior to use. Solvents used for polymer purification were ACS technical grade and used without further purification. Solvents used for nanoparticle formation were HPLC grade and used without further purification. Water (18.2 $\mu\Omega/\text{cm}$) was filtered through a NANOPure DiamondTM (Barnstead) water purification system before use.

All NMR spectra of the monomeric lactides and small molecule precursors were

recorded on a Varian Mercury Plus 400 MHz NMR spectrometer in CDCl_3 . ^1H and ^{13}C NMR spectra of polymerized products **6b-6d** were obtained on a Varian VNMRS NMR spectrometer equipped with a 500MHz XSens Cold Probe in CDCl_3 . Low resolution MS analysis was performed on a ThermoFinnigan LCQdeca mass spectrometer with an atmospheric pressure electrospray ionization (APCI) source or an electrospray ionization (ESI) source. High resolution MS analysis was performed on a Thermo Scientific LTQ Orbitrap XL mass spectrometer with an electrospray ionization source.

Polymer polydispersities and molecular weights were determined by size-exclusion chromatography (Phenomenex Phenogel 5u **10**, 1K-75K, 300 x 7.80 mm in series with a Phenomex Phenogel 5u **10**, 10K-1000K, 300 x 7.80 mm (0.05 M LiBr in DMF, 0.75 mL/min 60°C)) using a Hitachi-Elite LaChrom L-2130 pump equipped with a UV detector (Hitachi- Elite LaChrom L-2420), a multi-angle light scattering detector (DAWN-HELIOS: Wyatt Technology) and a refractive index detector (Hitachi L-2490). Data analysis was performed using the ASTRA software package.

Particle size determination by dynamic light scattering was performed on a Malvern Zetasizer Nano 3690 instrument using Malvern microvolume disposable polystyrene cuvettes. All samples were passes through 0.45 μm syringe filters prior to taking measurements. Data analysis was performed using Nanosizer software (Southborough, MA). All data values were based on a minimum of six average runs.

Synthesis of aldehydes 2b-2e

4-pentynal (2b)

To a stirred solution of oxalyl chloride (3.40 g, 26.8.6 mmol, 2.54 mL) in 50 mL dichloromethane (DCM) under argon at -78°C was added dimethyl sulfoxide (4.40 g, 56.3 mmol, 4.0 mL) in 10 mL DCM dropwise over 10 minutes. The mixture was then stirred under argon at -78°C for 30 minutes, at which time a solution of 4-pentyn-1-ol (1.99 g, 23.6 mmol, 2.2 mL) in 20 mL DCM was added dropwise over 10 minutes. When addition was complete, the reaction mixture was stirred for a further 1h. Triethylamine (18.5 mL) was added and the reaction mixture was stirred for 1.5h at -78°C followed by 1h at RT. The reaction mixture was diluted with 100 mL DCM, washed with 5% HCl, (2 x 30 mL), DI H₂O (1 x 30 mL), saturated NaCl (1 x 30 mL), dried over anhydrous sodium sulfate, filtered and concentrated *in vacuo*. The residue was purified by Kugelrohr distillation (600 mtorr, 40 °C) giving the aldehyde as a colorless oil (1.34 g, 69%). ¹H-NMR (400 MHz, CDCl₃); δ 9.79 (t, 1.2 Hz, 1H), 2.73-2.67 (tt, 9.6 Hz, 1.2 Hz, 2H), 2.53-2.47 (m, 2H), 1.99 (t, 4.8 Hz, 1H), 1.64 (s, 5H). ¹³C-NMR (100 MHz, CDCl₃): δ = 200.34, 82.49, 69.49, 42.54, 11.84.

5-azidopentanal (2c)

To a 100 mL round bottom flask equipped with a stirbar, 5-bromo-1-pentanol (2.64 g, 15.8 mmol) and NaN₃ (3.08 mg, 47.4 mmol) were dissolved in 35 mL of DMF. The reaction flask was stirred at 90 °C for 12 h. The reaction flask was allowed to cool to room temperature upon which the solvent was removed *in vacuo* to yield a yellow

residue. The residue was diluted to 150 mL with ethyl acetate (EtOAc), washed with DI H₂O (4 x 20 mL), saturated NaCl (2 x 20 mL), dried over anhydrous sodium sulfate, filtered and concentrated *in vacuo* to give 1.74 g of crude 5-azido-1-pentanol as a pale yellow oil which was used immediately without further purification.

To a stirred solution of oxalyl chloride (3.42, 26.9 mmol, 2.31 mL) in 120 mL DCM under argon at -78°C was added dimethyl sulfoxide (4.21 g, 53.8 mmol, 2.31 mL) dropwise over 15 minutes. The mixture was then stirred under argon at -78°C for 30 minutes, at which time a solution of crude 5-azido-1-ol (1.74 g, 13.5 mmol) in 30 mL DCM was added dropwise over 10 minutes. When addition was complete, the reaction mixture was stirred for a further 1h. Triethylamine (11.5 mL) was added and the reaction mixture was stirred for 1h at -78°C followed by 1h at 0°C. The reaction mixture was diluted with 50 mL DCM, washed with saturated NH₄Cl, (2 x 30 mL), DI H₂O (1 x 30 mL), saturated NaCl (1 x 30 mL), dried over anhydrous sodium sulfate, filtered and concentrated *in vacuo*. The residue was purified by column chromatography (90:10 hexanes:ethyl acetate) giving the aldehyde as a pale yellow oil (912 mg, 45% over two steps). ¹H-NMR (400 MHz, CDCl₃); δ 9.78 (t, 1.6 Hz, 1H), 3.31 (t, 6.8 Hz, 2H), 2.50 (dt, 6.8 Hz, 1.6 Hz, 2H), 1.76-1.59 (m, 4H). ¹³C-NMR (100 MHz, CDCl₃): δ = 201.92, 51.31, 43.44, 28.50, 19.44.

5-phthalimidopentanal (2d)

To a 50 mL round bottom flask equipped with a stirbar, 5-amino-1-pentanol (2.06 g, 20.0 mmol) and phthalic anhydride (2.96 g 20.0 mmol) were dissolved in 60 mL of toluene. The reaction flask was heated to reflux under Dean-Stark conditions for 3h. The

reaction flask was allowed to cool to room temperature upon which the solvent was removed *in vacuo* to yield a yellow residue. The residue was purified by column chromatography (100% CHCl₃) to give 5-phthalimido-1-pentanol as a white-yellow solid (3.34 g, 72%). ¹H-NMR (400 MHz, CDCl₃); δ = 7.83 (m, 2H), 7.71 (m, 2H), 3.70, (t, 7.2 Hz, 2H), 3.64 (t, 6.4 Hz, 1H), 1.75-1.58 (m, 4H), 1.46-1.40 (m, 2H). ¹³C-NMR (100 MHz, CDCl₃): δ = 168.72 (2C), 134.12 (2C), 132.33 (2C), 123.41 (2C), 62.90, 38.05 32.41, 28.59, 23.23. ESI-MS (*m/z*) calcd for C₁₃H₁₅NO₃ [M]⁺ 233.1052; found [M+H]⁺ 234.07, [M+NH₄]⁺ 250.90 and [M+Na]⁺ 256.05.

To a stirred solution of oxalyl chloride (1.45 g, 11.4 mmol, 1.08 mL) in 60 mL DCM under argon at -78°C was added dimethyl sulfoxide (1.78 g, 22.8 mmol, 1.62 mL) dropwise over 10 minutes. The mixture was then stirred under argon at -78°C for 30 minutes, at which time a solution of 5-phthalimido-1-pentanol (1.33 g, 5.71 mmol) in 12 mL DCM was added dropwise over 10 minutes. When addition was complete, the reaction mixture was stirred for a further 1h. Triethylamine (5 mL) was added and the reaction mixture was stirred for 1h at -78°C followed by 1h at 0°C. The reaction was quenched with 10 mL DI H₂O and diluted with 350 mL diethyl ether. The organic layer was separated, washed with DI H₂O (2 x 50 mL), and saturated NaCl (2 x 50 mL), dried over anhydrous sodium sulfate, and concentrated *in vacuo*. The residue was purified by column chromatography (70:30 hexanes:ethyl acetate) giving the aldehyde as a pale yellow oil (1.00 g, 76%). ¹H-NMR (400 MHz, CDCl₃); δ 9.76 (t, 1.2 Hz, 1H), 7.84 (m, 2H), 7.72 (m, 2H), 3.71 (t, 6.8 Hz, 2H), 2.51 (dt, 6.8 Hz, 1.2 Hz, 2H), 1.77-1.63 (m, 4H). ¹³C-NMR (100 MHz, CDCl₃): δ = 173.72, 83.01, 35.39 28.23, 22.48. ESI-MS (*m/z*)

calcd for $C_{13}H_{13}NO_3$ $[M]^+$ 231.0895; found $[M+H]^+$ 232.11, $[M+NH_4]^+$ 248.91 and $[M+Na]^+$ 254.06.

2-(2-(2-(azidoethoxy)ethoxy)ethoxy)acetaldehyde (2e)

Tetraethylene glycol (10.0 g, 51.5 mmol) was dissolved in 500mL dry DCM and stirred at room temperature. To the reaction flask were successively added KI (1.71 g, 10.3 mmol), Ag_2O (17.9 g, 77.2 mmol), and tosyl chloride (10.8 g, 56.6 mmol) and then was stirred vigorously at room temperature for 2h. The reaction mixture was filtered through a glass frit to remove the solids and concentrated *in vacuo*. The residue was purified via silica column chromatography (using a gradient from 100% EtOAc to 98:2 EtOAc:MeOH as eluent) giving 2-(2-(2-(2-azidoethoxy)ethoxy)ethoxy)ethanol a colorless oil (13.2 g, 74%). 1H -NMR (400 MHz, $CDCl_3$): δ = 7.74 (d, 8.0 Hz, 2H), 7.30 (d, 8.0 Hz, 2H), 4.11 (t, 4.8 Hz, 2H), 3.66-3.53 (m, 12H), 2.79 (s, 1H), 2.39 (s, 3H). ^{13}C -NMR (100 MHz, $CDCl_3$): δ = 145.04, 133.17, 130.10 (2C), 128.19 (2C), 70.95, 70.79, 70.70, 69.49, 68.88, 21.87. ESI-MS (m/z) calcd for $C_{15}H_{24}O_7S$ $[M]^+$ 348.1243; found $[M+H]^+$ 348.96, $[M+NH_4]^+$ 365.94 and $[M+Na]^+$ 371.08.

To a 50 mL round bottom flask equipped with a stirbar, 2-(2-(2-(2-hydroxyethoxy)ethoxy)ethoxy)ethyl toluenesulfonate (2.0 g, 5.74 mmol) and NaN_3 (186 mg, 17.2 mmol) were dissolved in 15 mL of DMF. The reaction flask was stirred at 90 °C for 12 h. The reaction flask was allowed to cool to room temperature upon which the solvent was removed *in vacuo* to yield a yellow residue. The residue was diluted with 150 mL of ethyl acetate, washed with DI H_2O (4 x 20 mL), saturated NaCl (2 x 20 mL), dried over anhydrous sodium sulfate, filtered and concentrated *in vacuo* to give 763 mg

of crude 2-((2-(2-azidoethoxy)ethoxy)ethoxy)ethanol as a yellow oil which was used immediately without further purification.

To a stirred solution of oxalyl chloride (883 mg, 6.96 mmol, 0.597 mL) in 30 mL DCM under argon at -78°C was added dimethyl sulfoxide (1.09 g, 13.9 mmol, 0.989 mL) dropwise over 10 minutes. The mixture was then stirred under argon at -78°C for 30 minutes, at which time a solution of crude 2-((2-(2-azidoethoxy)ethoxy)ethoxy)ethanol (763 mg) in 5 mL DCM was added dropwise over 10 minutes. When addition was complete, the reaction mixture was stirred for a further 1h. Triethylamine (3 mL) was added and the reaction mixture was stirred for 1h at -78°C followed by 1h at 0°C . The reaction mixture was diluted with 100 mL DCM, washed with saturated NH_4Cl , (2 x 25 mL), DI H_2O (1 x 25 mL), saturated NaCl (1 x 25 mL), dried over anhydrous sodium sulfate, filtered and concentrated *in vacuo*. The residue was purified by column chromatography (100% ethyl acetate) giving the aldehyde as a pale yellow oil (334 mg, 27% over two steps). $^1\text{H-NMR}$ (400 MHz, CDCl_3); δ 9.73 (t, $J = 0.8$ Hz, 1H), 4.16 (d, 0.8 Hz, 2H), 3.75-3.65 (m, 10H), 3.39 (t, 5.2 Hz, 2H). $^{13}\text{C-NMR}$ (100 MHz, CDCl_3): $\delta = 201.16, 77.06, 71.46, 71.04-70.81$ (4C), 70.27, 50.88. HR-MS (m/z) calcd for $\text{C}_{22}\text{H}_{20}\text{N}_2\text{O}_4\text{Na}$ $[\text{M} + \text{Na}]^+$ 240.0955; found $[\text{M} + \text{Na}]^+$ 240.0957.

2-hydroxy-1-(1H-indol-1-yl)hex-5-yn-1-one (3a)

1-(2,2-dimethoxyethyl)-2-isocyanobenzene (192 mg, 1.0 mmol), 4-pentynal (98.5 mg, 1.2 mmol) and water (36 mg, 36 μL) were dissolved in 5 mL dry DCM and allowed to stir in a scintillation vial at room temperature. After 5 minutes, DL-camphorsulfonic acid (46.5 mg, 0.2 mmol) was added to the vial. The reaction was allowed to stir at room

temperature for 4h, concentrated *in vacuo* and immediately purified by column chromatography (85:15 hexanes:EtOAc) giving the title *N*-acylindole **3a** as a colorless oil (150 mg, 67%). ¹H-NMR (400 MHz, CDCl₃): 8.46 (d, 8.0 Hz, 1H), 7.58 (d, 7.2 1H), 7.47-7.30 (m, 3H) 6.72 (d, 4 Hz, 1H), 5.07 (m, 1H), 3.47 (d, 7.6 Hz, 1H), 2.65-2.57 (m, 1H), 2.49-2.41 (m, 1H), 2.15-2.07 (m, 2H), 1.89-1.80 (m, 1H). ¹³C-NMR (100 MHz, CDCl₃); δ = 173.49, 135.92, 130.47, 125.82, 124.69, 123.72, 121.31, 116.91, 111.11, 83.01, 70.11, 68.98, 35.02, 15.05. HR-MS (*m/z*) calcd for C₁₄H₁₃NO₂Na [M + Na]⁺ 250.0838; found [M + Na]⁺ 250.0841.

6-azido-2-hydroxy-1-(1*H*-indol-1-yl)hexan-1-one (3b)

1-(2,2-dimethoxyethyl)-2-isocyanobenzene (192 mg, 1.0 mmol), 5-azidopentanal (154 mg, 1.2 mmol) and water (36 mg, 36 μL) were dissolved in 5 mL dry DCM and allowed to stir in a scintillation vial at room temperature. After 5 minutes, DL-camphorsulfonic acid (46.5 mg, 0.2 mmol) was added to the vial. The reaction was allowed to stir at room temperature for 4h, concentrated *in vacuo* and immediately purified by column chromatography (80:20 hexanes:EtOAc) giving the title *N*-acylindole **3b** as a colorless oil (190 mg, 69%). ¹H-NMR (400 MHz, CDCl₃): 8.46 (d, 8.0 Hz, 1H), 7.58 (d, 7.2 1H), 7.47-7.30 (m, 3H) 6.72 (d, 4 Hz, 1H), 4.85 (dt, 1H, Hz), 3.49 (d, 7.2 Hz, 1H), 3.28 (t, 6.4 Hz, 2H), 1.96-1.93 (m, 1H), 1.79-1.58 (m, 5H). ¹³C-NMR (100 MHz, CDCl₃); δ = 173.61, 135.92, 130.45, 125.92, 124.67, 123.59, 121.32, 116.86, 111.02, 70.38, 51.43, 37.59, 28.79, 22.55. HR-MS (*m/z*) calcd for C₁₄H₁₆N₄O₂Na [M + Na]⁺ 295.1165; found [M + Na]⁺ 295.1161.

2-(5-hydroxy-6-(1*H*-indol-1-yl)-6-oxohexyl)phthalimide (3c)

1-(2,2-dimethoxyethyl)-2-isocyanobenzene (192 mg, 1.0 mmol), 5-phthalimido-1-pentanol (278 mg, 1.2 mmol) and water (36 mg, 36 μ L) were dissolved in 5 mL dry DCM and allowed to stir in a scintillation vial at room temperature. After 5 minutes, DL-camphorsulfonic acid (46.5 mg, 0.2 mmol) was added to the vial. The reaction was allowed to stir at room temperature for 4h, concentrated *in vacuo* and immediately purified by column chromatography (70:30 hexanes:EtOAc) giving the title acyl indole as a pale yellow oil (261 mg, 69%). $^1\text{H-NMR}$ (400 MHz, CDCl_3); 8.46 (d, 8.4 Hz, 1H), 7.82-7.80 (m, 2H), 7.71-7.68 (m, 2H), 7.57 (d, 8 Hz, 1H), 7.42-7.28 (m, 3H), 6.72 (d, 4 Hz, 1H), 4.85 (dt, 8 Hz, 3.2 Hz, 1H), 3.70 (t, 6.8 Hz, 2H), 3.44 (d, 7.6 Hz, 1H), 2.01-1.95 (m, 1H), 1.77-1.57 (m, 5H). $^{13}\text{C-NMR}$ (100 MHz, CDCl_3): δ = 173.72, 168.63, 135.94, 134.13, 132.29, 130.48, 125.81, 124.57, 123.43, 121.25, 116.87, 110.91, 83.01, 70.11, 70.40, 37.59, 35.39, 28.23, 22.48. HR-MS (*m/z*) calcd for $\text{C}_{22}\text{H}_{20}\text{N}_2\text{O}_4\text{Na}$ [$\text{M} + \text{Na}$] $^+$ 399.1315; found [$\text{M} + \text{Na}$] $^+$ 399.1310.

3-(2-(2-(2-azidoethoxy)ethoxy)ethoxy)-2-hydroxy-1-(1*H*-indol-1-yl)propan-1-one (3d)

1-(2,2-dimethoxyethyl)-2-isocyanobenzene (192 mg, 1.0 mmol), 2-(2-(2-(azidoethoxy)ethoxy)ethoxy)acetaldehyde (261 mg, 1.2 mmol) and water (36 mg, 36 μ L) were dissolved in 5 mL dry DCM and allowed to stir in a scintillation vial at room temperature. After 5 minutes, DL-camphorsulfonic acid (46.5 mg, 0.2 mmol) was added to the vial. The reaction was allowed to stir at room temperature for 4h, concentrated *in vacuo* and immediately purified by column chromatography (50:50 hexanes:EtOAc)

giving the title acyl indole as a pale yellow oil (237 mg, 65%). $^1\text{H-NMR}$ (400 MHz, CDCl_3): δ = 8.46 (d, 8.0 Hz, 1H), 7.58-7.28 (m, 4H), 6.72 (d, 7.6 Hz, 1H), 5.01 (d, 5.2 Hz, 1H), 3.90 (t, 4.4 Hz, 2H), 3.69-3.54 (m, 11H), 3.34 (t, 5.2 Hz, 2H). $^{13}\text{C-NMR}$ (100 MHz, CDCl_3): δ = 171.16, 136.00, 130.53, 125.62, 124.81, 124.54, 121.14, 116.94, 110.30, 73.74, 71.58, 70.93-70.79 (4C), 70.19, 68.98, 50.84. HR-MS (m/z) calcd for $\text{C}_{17}\text{H}_{22}\text{N}_4\text{O}_5\text{Na}$ $[\text{M} + \text{Na}]^+$ 385.1482; found $[\text{M} + \text{Na}]^+$ 385.1476.

General procedure for polymerization 6b-6d

All polymerizations were carried out with tin(II) 2-ethylhexanoate (stannous octoate, $\text{Sn}(\text{Oct})_2$) (purchased from Alfa Aesar) and 4-*tert*-butylbenzyl alcohol (purchased from Acros) without further purification. The polymerization method is similar to that described by Baker and coworkers.⁴³ Freshly prepared 0.01 M solutions of $\text{Sn}(\text{Oct})_2$ and 4-*tert*-butylbenzyl alcohol in anhydrous toluene were used for all polymerizations. $\text{Sn}(\text{Oct})_2$ (0.01 M in anhydrous toluene, 796 μL) and 4-*tert*-butylbenzyl alcohol (0.01 M in anhydrous toluene, 796 μL) were added to a small glass vial and the solution was concentrated *in vacuo*. The sides of the vial were washed with small portions of additional anhydrous toluene and concentrated *in vacuo* to concentrate the initiators and the bottom of the vial. To the vial was then added D,L-lactide (144 mg, 1.0 mmol) and either more D,L-lactide or substituted hemilactide (0.15 mmol). The vial was then placed under vacuum. After 20 minutes, the vial was equipped with a small stirbar, flushed with N_2 gas, tightly sealed and heated at 130°C in a silicone oil bath for 2 h. After the reaction was completed the vials were cooled on an icebath, dissolved in CDCl_3 and the crude was analyzed by ^1H and ^{13}C NMR. A small aliquot of the CDCl_3

solution was concentrated *in vacuo*, redissolved in DMF, filtered through a Whatman Anontop 10 0.2 μm filter and analyzed by Gel Permeation Chromatography.

General procedure for CuAAC functionalization of polymers 6a-6d.

An aliquot containing ~5 mg of polymer **5a-5d** in CDCl_3 was withdrawn, concentrated *in vacuo* and redissolved in 0.2 mL DMF. To the polymer sample was added an excess of either dansyl azide **7** or dansyl alkyne **8** dissolved in DMF (0.5 mL of a 2.0 mg/mL solution), an excess of sodium ascorbate (1 mg) and finally ~0.3 mL of a 1 mg/mL solution of $\text{CuSO}_4 \cdot 5\text{H}_2\text{O}$ in DMF. The vials were allowed to stand for 2 h at room temperature with occasional shaking. The solutions were then filtered through a Whatman Anontop 10 0.2 μm filter and analyzed by size exclusion chromatography.

Attempted polymerization of α -hydroxy-*N*-acylindole **3a**

In a dry 20 mL scintillation vial equipped with a small stirbar, acylindole **3a** (19 mg, 0.1 mmol) was dissolved in 5 mL of dry THF and allowed to stir at room temperature. Anhydrous Cs_2CO_3 (33 mg, 0.1 mmol) was added to the reaction vial. The reaction was stirred for 24 h at room temperature, and directly analyzed by ESI-MS. In addition, a small aliquot of the reaction mixture was removed from the vial, redissolved in DMF and analyzed by size exclusion chromatography.

Attempted polymerization of **3b**

In a dry 20 mL scintillation vial equipped with a small stirbar, acylindole **3b** (22 mg, 0.1 mmol) was dissolved in 5 mL of dry DCM and allowed to stir at room temperature. A solution of DBU in anhydrous DCM (13.8 mg/mL, 100 μ L, 0.010 mmol) was added to the reaction vial. The reaction was stirred for 24 h at room temperature, and directly analyzed by ESI-MS. In addition, a small aliquot of the reaction mixture was removed from the vial, redissolved in DMF and analyzed by size exclusion chromatography.

Synthesis of the copolymer poly(DL-lactide)-co-(3-(but-3-yn-1-yl)-6-methyl-1,4-dioxane-2,5-dione) (**9**)

Freshly prepared 0.01 M solutions of Sn(Oct)₂ and 4-*tert*-butylbenzyl alcohol in anhydrous toluene were used for the copolymerization. Sn(Oct)₂ (1.0 mM in anhydrous toluene, 694 μ L, 69.4 μ mol) and 4-*tert*-butylbenzyl alcohol (1.0 mM in anhydrous toluene, 694 μ L, 69.4 μ mol) were added to a small glass vial and the solution was concentrated *in vacuo*. The sides of the vial were washed with small portions of additional anhydrous toluene and concentrated *in vacuo* to concentrate the initiators and the bottom of the vial. To the vial was then added D,L-lactide (800 mg, 5.55 mmol) and the alkyne substituted hemilactide (253 mg, 1.39 mmol). The vial was then placed under vacuum. After 20 minutes, the vial was equipped with a small stirbar, flushed with N₂ gas, tightly sealed and heated at 130°C in a silicone oil bath. After 2 h, the reaction vial was cooled on an icebath and the vial contents were dissolved in approximately 5 mL of

chloroform. The chloroform solution was slowly added to 75 mL of methanol and the resulting cloudy suspension was separated into four centrifuge tubes and spun at 10,000 rpm for 30 minutes. The supernatant was decanted from each tube, combined, concentrated in vacuo and the precipitation repeated with the supernatant discarded. The viscous material concentrated at the bottom of each tube was washed several times with methanol to remove remaining low molecular weight oligomers and tin catalyst, dissolved in a small volume of toluene and added dropwise to heptane to precipitate a white solid, which was collected by filtration. The recovered solid was redissolved in toluene and precipitated in heptane to give the alkyne-substituted polymer as a white solid (660 mg, 63 % yield, $M_n = 46.9$ kDa, PDI = 1.26). ^1H and ^{13}C NMR were virtually identical to that of polymer **6b**.

General Procedure for nanoprecipitation:

20 mg of polymeric material (either PLA or PLA-co-PLA-alkyne) is dissolved in 20 mL of the organic solvent acetone or acetonitrile) to make a 1.0 mg/mL solution. If encapsulation of a drug is desired, the drug of choice was added to the organic polymer solution. The solution is transferred to an addition funnel and added dropwise slowly to 40 mL of a rapidly stirring 0.3% w/v aqueous polyvinyl alcohol solution. An opalescent suspension is observed after addition of the organic phase is complete. After addition, 20 mL of DI H₂O was added to the opalescent suspension while stirring. To prepare nanoparticles using more concentrated solutions, a volume of polymer solution in organic volume is added to twice the volume of aqueous phase containing stabilizer. When addition of the organic phase is complete, enough DI water is added to the opalescent

suspension such that the organic solvent constitutes 25% of the total volume.. After 5 minutes, the suspension is placed under reduced pressure for 30 minutes to remove the organic solvent. The aqueous nanoparticle suspension was then passed through a 0.45 μm syringe filter and further purified on a Sephadex NAP-25 size exclusion column (Amersham Biosciences) to remove traces of small molecules.

Notes about this chapter

Chapter 2, in part, is based on material which appears in "Facile Procedure for Generating Side Chain Functionalized Poly (alpha-hydroxy acid) Copolymers from Aldehydes via a Versatile Passerini-Type Condensation" Rubinshtein, M.; James, C. R.; Young, J. L; Ma, Y. J.; Kobayashi, Y.; Gianneschi, N. C.; Jerry Yang, J. *Organic Letters*, **2010**, *12*, 3560-3563. I am the primary author of this paper. In addition, Chapter 2 contains material currently being prepared for submission for publication: "Direct synthesis of side chain functionalized alpha-hydroxy acid oligomers from alpha-hydroxy-*N*-acylindole precursors." Rubinshtein, M.; James, C. R.; Young, J. L.; Gianneschi, N. C.; Yang, J. I am the primary author of this pending manuscript.

Part II: Studies Toward a Chemical Method to Degrade Alzheimer's Disease-Related beta-Amyloid Peptides.

Chapter 3

Alzheimer's Disease: Causes, Mortality and Treatment Options

3.1 Alzheimer's disease: An emerging health crisis

Alzheimer's disease (AD) is a progressive, neurodegenerative disorder and the most common form of dementia. AD begins with the mild decline of cognitive function and memory and progresses to rob the patient of his or her most human qualities, including the ability to recognize family members and friends and the capacity to care for oneself. Ultimately, AD results in the impairment of even the most basic bodily processes, resulting in patient death. Although significant research efforts are ongoing, there is currently no cure or disease-altering therapeutic for this debilitating condition.

The overwhelming majority of those afflicted with AD are elderly, and the biggest risk factor for developing AD is advanced age. One in eight people over 65 have AD, with this number increasing to over 40 percent for those 85 and older.⁷² With longer life expectancies and increasing healthcare standards around the world, the number of people with AD is expected to climb. Currently, AD is the sixth leading cause of death in the United States, with over 5 million Americans afflicted with the disease.⁷² This value is projected to reach 11-16 million by 2050.⁷² The incidence of AD is also increasing at an alarming rate relative to other top killers. Between 2000 and 2006, AD related-death has increased nearly 50 percent, while mortality from heart disease, stroke, breast cancer

and prostate cancer have declined (Table 3.1),⁷³ further illustrating AD's role as a growing health concern. In addition to its human toll, AD also has a profound economic impact: direct and indirect costs associated with AD currently top \$180 billion annually in the United States and are expected to rise to over \$1 trillion (in 2011 dollars) by 2050.⁷²

Table 3.1: Percentage change in selected causes of death in the United States between 2000 and 2006.⁷³

Cause of Death	Percentage change
Alzheimer's Disease	+46.1
Stroke	-18.2
Heart Disease	-11.1
Breast Cancer	-2.6
Prostate Cancer	-8.7
HIV/AIDS	-16.3

The problem of AD is not confined to the United States; worldwide cases of AD are expected to balloon, particularly in China, India and other developing Asian and Pacific Rim nations.⁷⁴ Projections estimate that by 2050, 115 million people worldwide will have AD and other dementias.⁷⁵ The increasing worldwide numbers of those with AD may precipitate a global health crisis and reinforces the importance of developing new strategies for combating this disease.

3.2 Alzheimer's disease and the amyloid cascade hypothesis

One of the major characteristics of AD is the prevalence of extracellular amyloid plaques and intracellular neurofibrillary tangles (NFT) in post-mortem analysis of brain tissue. The plaques are comprised mostly of aggregated β -amyloid peptide ($A\beta$), whereas the NFTs contain misfolded hyperphosphorylated tau protein. While NFTs are associated with a variety of tauopathies such as Pick's Disease⁷⁶ or ganglioglioma,⁷⁷ aggregated $A\beta$ plaques are uniquely present in the brain tissue of AD patients.

The $A\beta$ peptide is a 39-43 amino acid peptide, with $A\beta_{1-40}$ and $A\beta_{1-42}$ being two most abundant isoforms.⁷⁸ The N-terminus region of $A\beta$ is rich in hydrophilic residues while the C-terminal region is highly hydrophobic (Figure 3.1). The $A\beta$ peptide, particularly the $A\beta_{1-42}$ isoform, is highly prone to aggregation and can assemble into dimeric and oligomeric species in solution as well as form insoluble fibrils that are deposited extracellularly as amyloid plaques.⁷⁹

The $A\beta$ peptide is generated from the amyloid precursor protein (APP), an integral membrane protein found in high concentrations in the synapses of neurons.⁸⁰ APP is normally processed by the non-amyloidogenic α -secretase pathway, resulting in APP cleavage between the Lys16 and Leu17 residues in the transmembrane domain.⁸¹ Alternatively, APP may be cleaved successively by β -secretase and γ -secretase to generate $A\beta$. Initial enzymatic hydrolysis of APP by β -secretase gives a membrane-anchored, carboxy-terminated stub ($sAPP_{\beta}$) that is further cleaved within the transmembrane domain by γ -secretase to give $A\beta$.⁸¹ Because the cleavage site of γ -

secretase is not precise, this cleavage mechanism results in A β peptides of varying length.⁸²

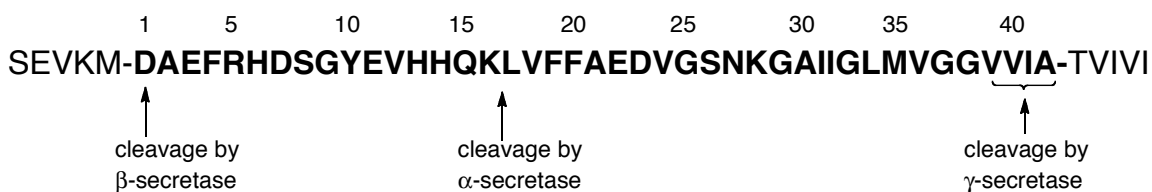


Figure 3.1: A portion of the amyloid precursor protein sequence (APP) represented by one-letter codes, with the sequence of A β_{1-42} shown in bold. α -Secretase cleaves APP between the Lys16 and Leu17 residues within the A β sequence, resulting in non-amyloidogenic peptide fragments. However, APP cleaved successively by β -secretase and γ -secretase produces A β peptides of varying length, depending on the specific cleavage site of γ -secretase.

Strong evidence suggests that A β is an important factor in the development of AD. For instance, A β is toxic to neuronal cells,⁸³ and mutations in the APP gene, located on chromosome 21, has been linked to early onset AD.⁸⁴ Furthermore, those with Down Syndrome (trisomy 21) overproduce APP and A β , develop AD by the time they are in their forties.⁸⁵ The causative role of A β in AD is the cornerstone of the amyloid cascade hypothesis.⁸⁶⁻⁸⁹ First proposed by Hardy and Selkoe in early 1990s and refined over the last 20 years, the amyloid cascade hypothesis proposes that AD is caused by an imbalance between A β production and clearance by natural cellular mechanisms.⁹⁰⁻⁹² Accumulation of A β leads to the formation of various aggregated forms such as soluble oligomers and the insoluble fibrils that deposit extracellularly as plaques. The toxic aggregates (particularly the soluble oligomers) cause an inflammatory response that

triggers oxidative stress in neuronal cells leading to decline in neuronal function and ultimately cell death.

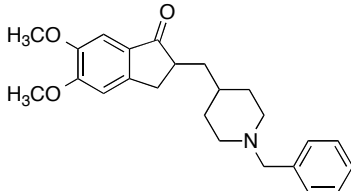
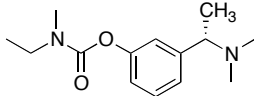
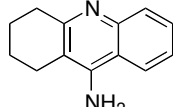
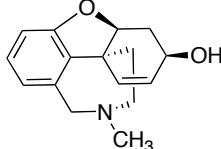
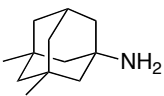
Although the exact mechanisms of A β toxicity are unknown, it has been proposed that A β induces oxidative stress in the AD brain. A β can generate reactive oxygen species in the presence of metal ions such Cu²⁺ that result in cellular damage.^{93, 94} Oxidative stress can also be manifested via interaction of A β with other cellular components. Recent work by Habib et al showed that inhibiting the A β -catalase interaction protects cells from the toxic effects of A β -induced oxidative stress, presumably by restoring catalase function to permit H₂O₂ dismutation.⁹⁵ Another potentially detrimental interaction occurs when A β binds to the enzyme amyloid-beta binding alcohol dehydrogenase (ABAD) and modifies its function, which promotes the production of reactive oxygen species and increased oxidative stress to cells.^{94, 96, 97} It has also been suggested that another possible mechanism of A β toxicity involves the formation of pores in cell membranes and subsequent alteration of membrane permeability.⁹⁸

3.3 Current state of Alzheimer's disease therapeutics

Several small molecule-based drugs that are currently FDA-approved for use in the treatment of AD disease are listed in Table 3.1; however, none of these compounds are disease-altering therapeutics.⁹⁹ Rather, these drugs treat the symptoms of AD and begin to lose their potency after a short time, sometimes accelerating the cognitive decline of patients after their initial period of efficacy.¹⁰⁰⁻¹⁰² The majority of available

drugs are a class of molecules known as acetylcholinesterase (AChE) inhibitors, which combat the decrease in the levels of the acetylcholine, a neurotransmitter that facilitates synapse function, observed in AD patients.¹⁰³ The only non-AChE inhibitor currently approved for AD treatment is memantine, an *N*-methyl-D-aspartase (NMDA) antagonist. Memantine works by binding to NMDA receptors to restrict cellular influx of Ca^{2+} ions, which can overstimulate and damage neuronal cells.¹⁰⁴⁻¹⁰⁶ Ultimately, however, there are no current AD treatments that alter the causative factors of this debilitating condition.

Table 3.2: Current FDA-approved small molecule treatments for Alzheimer's Disease.

Drug	Structure	Drug Type
Dopenizil		AChE Inhibitor
Risvastigmine		AChE Inhibitor
Tacrine		AChE Inhibitor
Galantamine		AChE Inhibitor
Memantine		NMDA antagonist

3.4 Small-molecule based strategies and targets for AD therapy

Since A β is believed to be a causative factor in AD, one research strategy has focused on blocking the production of A β by inhibiting the function of β -secretase and γ -secretase. Ghosh and coworkers have successfully prepared GRL-8234 a peptidomimetic compound that shows tremendous potential as a clinically useful β -secretase inhibitor (Figure 3.2); GRL-8234 was found to be a potent β -secretase inhibitor with a $K_i = 1.8$ nM and significantly reduces the production A β in transgenic mice by up to 65 %.^{107, 108}

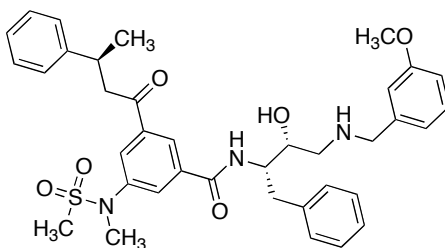


Figure 3.2: Structure of the β -secretase inhibitor GRL-8234.

Several compounds have been identified that inhibit γ -secretase *in vitro*;¹⁰⁹ however, developing safe γ -secretase inhibitors remains an obstacle due to its additional cellular functions, particularly cleavage of the Notch signaling protein.¹¹⁰ Instead, γ -secretase modulation has been explored as an alternative strategy. γ -Secretase modulators selectively lower the production of A β_{1-42} in favor of the shorter A β isoforms that are less prone to aggregation. Several non-steroidal anti-inflammatory drugs (NSAIDs) have been identified as γ -secretase modulators including ibuprofen and

sulindac.¹¹¹⁻¹¹⁵ One NSAID, (*R*)-Flurbiprofen, showed initial promise as an AD therapeutic; however it was ultimately discontinued in 2008 after poor results during Phase III clinical trials.¹¹⁶

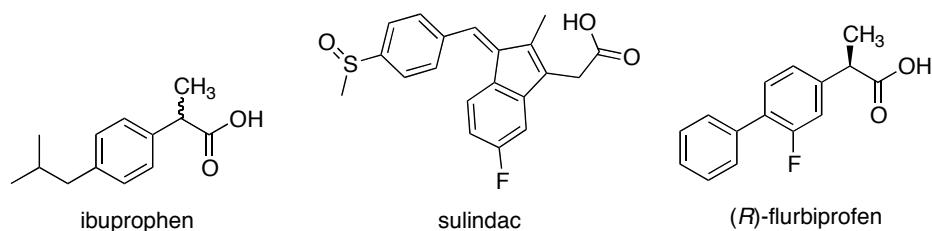


Figure 3.3: Examples of several γ -secretase modulators.

Other attempts to modify the pathology of AD involve small molecules that directly target $A\beta$. Gestwicki illustrates a strategy that utilizes small molecules that recruit molecular chaperones in order to inhibit $A\beta$ fibril formation and reduce $A\beta$ toxicity.¹¹⁷ Cole and coworkers demonstrate the efficacy of curcumin, found in the spice turmeric, can inhibit $A\beta$ formation as well as effect disaggregation of multimeric assemblies of the peptide.¹¹⁸ Additionally, Yang and coworker have designed a class of molecules that generate surface coatings on $A\beta$ to prevent harmful amyloid interactions with cellular components.^{119, 120} This was recently shown to be an effective strategy in reducing $A\beta$ toxicity by using surface coatings to inhibit the detrimental $A\beta$ -catalase interaction.⁹⁵

3.5 Degradation of $A\beta$ as a therapeutic strategy

Since aggregated $A\beta$ peptides are largely resistant to normal degradation mechanisms in cells,^{90-92, 121} the development of chemical methods to selectively cleave

A β peptides under physiological conditions could lead to an effective strategy to permanently eradicate these toxic biomolecules from the brain. Selective cleavage of A β using a Co(III)-cyclen complex tethered to an A β -binding was demonstrated by Suh and coworkers in 2007,¹²² and a very similar strategy was employed using a Cu(II)-cyclen complex as the active species by Wu et al.¹²³ However, there are no other examples of small-molecule promoted A β cleavage in literature and currently there are no metal-free methods that effect A β degradation.

3.6 Goal of the dissertation research

The goal of this dissertation research is to develop a method for the selective degradation of A β using small molecules. Chapter 4 explores a strategy to degrade A β peptides in aqueous solutions at physiological temperatures with a metal-free small molecule system that utilizes a cyclic enediyne as the chemical warhead. A major challenge that was encountered was the tendency of A β to aggregate and be generally uncooperative, appropriately earning it the nickname “the peptide from hell.”¹²⁴ During the course of this research, an improved synthesis of a class of A β -binding was developed and led to several collaborations due to the increased availability of these compounds. Chapter 5 presents the improved synthesis of these A β -binding molecules, as well as several investigations into the uses and properties of these molecules ranging from inhibition of HIV transmission to formation of ion-channels in lipid bilayers.

Chapter 4

Studies Toward an Ene-yne-Based Target-Directed Chemical Method to Degrade Alzheimer's-Related β -Amyloid Peptides

4.1 Introduction

This chapter describes a chemical approach to degrade Alzheimer's-related A β peptides at physiological temperature in neutral aqueous solution. Since substantial evidence suggests that A β peptides play a pathological role in the development of AD,^{88, 125} many recent therapeutic strategies have focused on neutralizing the toxicity of this peptide. Examples of strategies currently being explored to directly modify the pathology of AD using A β -targeting synthetic molecules include: 1) the binding of A β peptides and soluble A β oligomers in order to prevent or retard the growth of A β fibrils;¹²⁶⁻¹²⁸ 2) the binding of A β fibrils or protofibrils in order to effect disaggregation of the peptide;^{118, 129, 130} and 3) the generation of protein resistive surface coatings on aggregated A β peptides in order to ameliorate harmful protein-amyloid interactions.^{119, 120, 131} Although all of these therapeutic strategies show promise for disfavoring the formation or deactivating the function of toxic forms of A β , they all rely on natural, biological degradation pathways for eventual clearance of these pathogenic peptides. Since aggregated A β peptides are largely resistant to normal degradation mechanisms in cells,^{132, 133} the development of chemical methods to selectively cleave A β peptides under

physiological conditions could lead to an effective strategy to permanently eradicate these toxic biomolecules from the brain.

4.2 A target-directed strategy toward selective peptide degradation

Proteins are most often degraded by living systems via enzymatic hydrolysis; however, researchers have long been interested using small, synthetically accessible molecules to affect peptide cleavage. One well-known chemical protease is cyanogen bromide, which demonstrates remarkable site-specific hydrolytic activity at the C-terminus side of methionine residues.¹³⁴ Several groups have successfully designed small protein-cleaving molecules that can target specific proteins. Notably, Schultz and coworkers demonstrated selective cleavage of streptavidin using a synthetic molecule comprised of a biotin moiety covalently linked to a metal-chelating ethylenediaminetetraacetic acid (EDTA) unit.¹³⁵ The extraordinarily high affinity of biotin for streptavidin¹³⁶ allows for non-covalent binding of the small molecule to the peptide, while the EDTA chelated and delivered the redox-active Fe^{3+} and Cu^{2+} cations responsible for degradation to the cleavage site. Schepartz exploited a similar strategy for site-specific degradation of the calcium receptor protein calmodulin using trifluoperazine, a synthetic molecule with a high affinity for the protein, tethered to a EDTA unit chelating a redox-active Fe^{2+} cation.^{137, 138} Inspired by this target-directed approach, we chose to design a small molecule bearing a chemical warhead covalently linked to a suitable binding group in an attempt to selectively degrade the Alzheimer's-related $\text{A}\beta$ peptide.

4.3 Ene-diyne as potent chemical warheads

The explosion of interest in enediyne-containing natural products began with the isolation and structural determination of the calicheamicin and esperamicin antibiotics. These classes of compounds, comprised of an unusual (*Z*)-cyclodeca-3-en-1,5-diyne (enediyne) moiety, were found to exhibit extraordinarily potent anticancer activity.¹³⁹ The toxicity of these molecules has been widely attributed to their ability to effect cleavage of DNA at the minor groove.^{139, 140}

Bergmann has previously shown that under appropriate conditions, enediynes undergo cycloaromatization to give a highly reactive *p*-benzyne diradical species that abstracts hydrogen from a suitable donor to give a benzene-containing product (Figure 4.1). The rate of cycloaromatization is highly dependent on the *cd* distance—the distance measured from the terminal *sp* carbon atoms in the enediyne moiety. Thermal cyclization of linear enediynes, which have *cd* distances on the order of 4 Å, requires temperatures in excess of 200°C; however, cyclic enediynes require considerably lower temperatures to

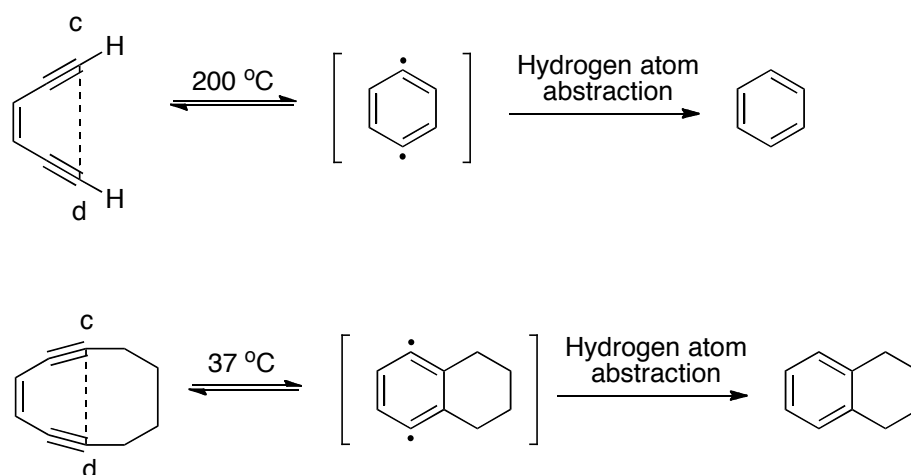


Figure 4.1. Bergman cycloaromatization of (A) a linear enediyne and (B) a cyclic enediyne in a 10-membered ring system to a reactive *p*-benzyne diradical intermediate.

effect cycloaromatization, presumably due to their increased strain energy. Cyclic enediynes in 10-membered ring systems, for example, have a cd distance of 3.25 Å and a cyclization half-life of about 18 hours at 37°C, while enediynes confined to 9-membered ring systems (cd < 3 Å), cyclize readily even at low temperatures and cannot be isolated.¹⁴¹

We chose to use a 10-membered cyclic enediyne ring moiety as a peptide degrading warhead for these studies because this class of enediynes has been previously reported to be capable of cleaving proteins¹⁴²⁻¹⁴⁴ and DNA^{145, 146} at physiological temperatures through reversible cyclization to a diradical species. Additionally, cyclic enediynes are synthetically accessible, do not require an external cofactor (such as a metal) for activation as a chemical cleaving agent and have been successfully implemented in an FDA-approved therapeutic agent.¹⁴⁷ We hypothesized that a small molecule comprised of a cyclic enediyne “warhead” moiety covalently linked to an Aβ-binding group can selectively cleave Aβ. The binding group is expected to deliver the enediyne warhead to the target peptide, where cyclization to the reactive diradical species at physiological temperature will promote degradation of the peptide backbone (Figure 4.2).

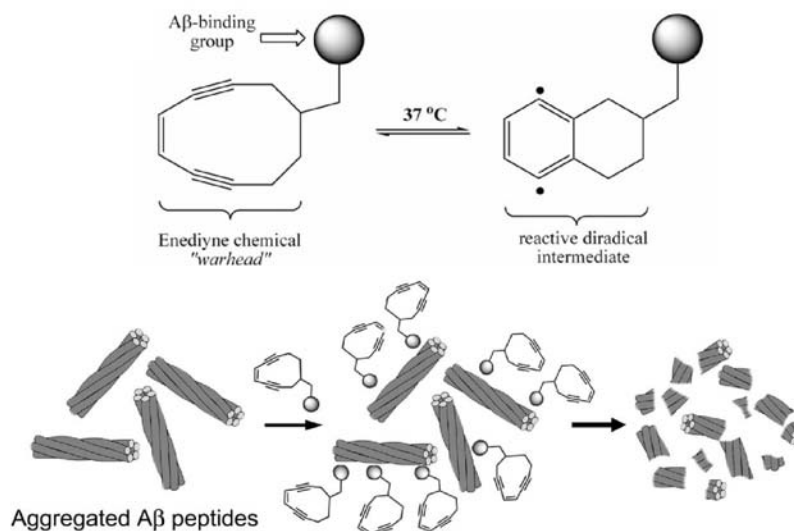


Figure 4.2: Cartoon depicting the target-directed approach of A β degradation. A cyclic enediyne warhead bearing a suitable binding group is predicted to associate with A β peptides, delivering the enediyne moiety to the target peptide. Subsequent cyclization to the *p*-benzyne diradical may provide the reactive species necessary to degrade A β .

The exact mechanism of enediyne-promoted peptide cleavage is unclear. One plausible mechanism of enediyne-induced scission of proteins under aerobic conditions has recently been proposed by Jones and coworkers, wherein the diradical intermediate generated from the enediyne abstracts a hydrogen atom α to the carbonyl in the peptide backbone.¹⁴⁸ The peptide radical formed from hydrogen abstraction proceeds to react with molecular oxygen to oxidatively cleave the polypeptide give a C-terminal amide and alpha-oxo ketone (or aldehyde in the case of glycine) fragments. Alternatively, degradation of the peptide could also occur through one or more radical abstractions of the hydrogen atoms from the amino acid side chains (Figure 4.3).¹⁴⁹

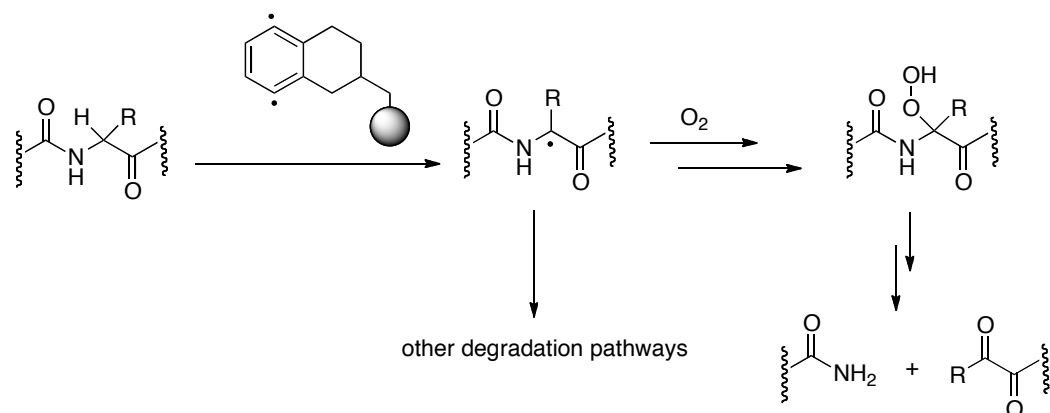
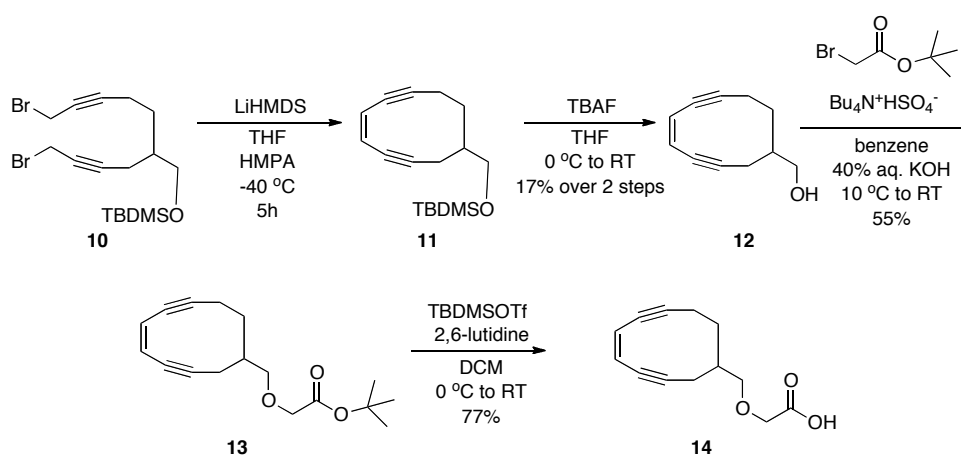


Figure 4.3: Possible mechanisms of peptides degradation by the reactive *p*-benzyne diradical. Abstraction of an α -hydrogen from the peptide backbone leads to peroxide formation and ultimately peptide scission to give an amide and α -oxo ketone (or aldehyde). Alternatively, the highly reactive diradical may abstract an α -hydrogen from the peptide backbone (or a hydrogen atom from an amino acid side chain) to give other degradation products.

We synthesized a 10-membered cyclic enediyne ring using a modified procedure as described by Jones and coworkers (Scheme 4.1).¹⁵⁰ Importantly, this molecule bears a pendant functional group that will ultimately permit covalent attachment of the enediyne warhead moiety onto a suitable A β targeting domain. The enediyne moiety was formed in one step from linear dibromide **10**, presumably via a carbenoid-coupling reaction, to give the desired TBDMS-protected macrocyclic product **11**. Jones and coworkers have reported yields of up to 95% for this cyclization; however, only poor yields were achieved using the published experimental protocol. Upon successful cyclization the TBDMS protecting group was removed with TBAF under standard conditions to afford enediyne alcohol **12**.

In order to make the enediyne more suitable for covalent linkage with an A β binding group, we chose to convert the alcohol pendant functionality of **12** to a terminal

carboxylic acid. The acid functionality would enable the formation of a very stable amide linkage between the enediyne and a binding group bearing a free amine. We explored several methods to oxidize the alcohol, however, direct oxidation proved to be too harsh for the cyclic enediyne moiety. Accordingly we decided to use milder methods to introduce a terminal carboxylic acid onto the warhead molecule. Reacting the enediyne alcohol **12** with *tert*-butyl bromoacetate under phase transfer conditions gave terminal ester **13** in moderate yield.^{151, 152} We assumed that ester **13** would be readily deprotected under standard conditions; however, both acid deprotection with trifluoroacetic acid and basic deprotection with potassium *tert*-butoxide resulted in immediate decomposition of the molecule. Ultimately we removed the *tert*-butyl group using a method described by Danishefsky.¹⁵³ Treating ester **13** with *tert*-butyl dimethylsilyl triflate and 2,6-lutidine provided enediyne free acid **14** in 77% yield, presumably by first forming the TBDMS ester which readily hydrolyzed during aqueous workup.



Scheme 4.1: Synthesis of the substituted cyclic enediyne bearing a terminal carboxylic acid pendant functional group **14** from linear dibromide **10**.

4.4 Preparation of the BTA binding moiety

In order to achieve targeted degradation of A β using small molecules, the designed synthetic molecule must bear a moiety known for binding effectively to A β . Several molecules are known to bind to A β with high affinity and have been exploited to aid in the visualization of these aggregates in brain tissue. Two such molecules include thioflavin T (ThT), commonly used to visualize A β plaques and a related analogue, Pittsburgh Compound B (PiB), often used in positron emission tomography (PET) imaging of amyloids (Figure 4.4). These molecules both contain a benzothiazole aniline (BTA) ring system and are thought to bind to the multiple repeated binding sites found on A β .¹⁵⁴

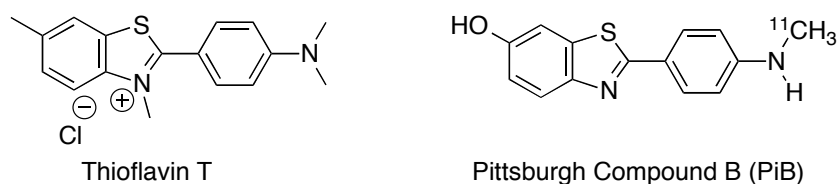
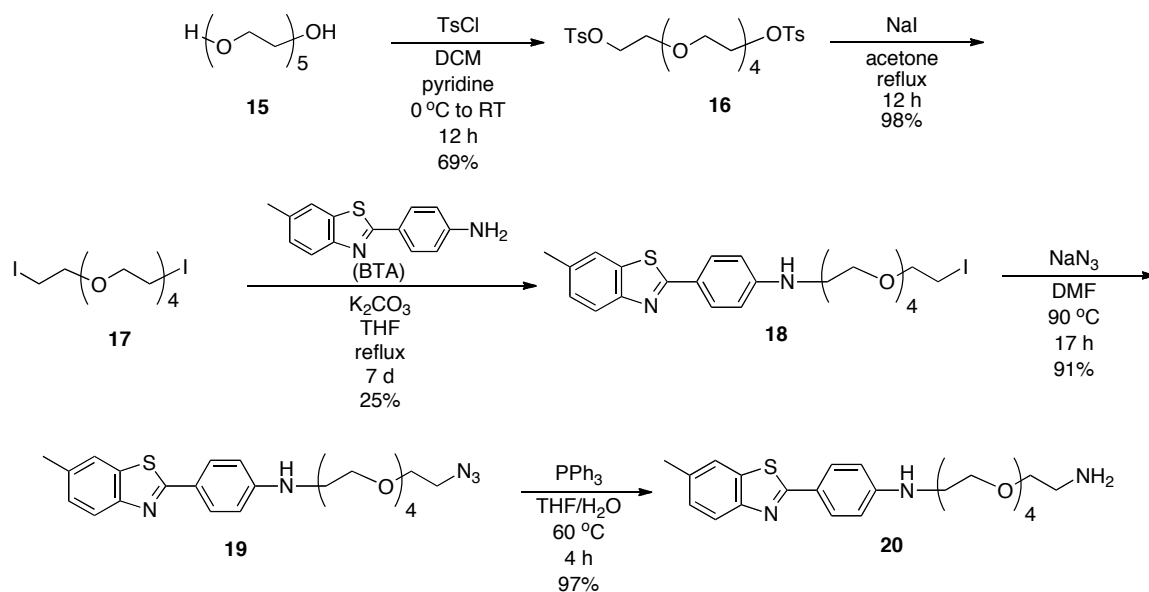


Figure 4.4: Structures of the A β binding molecules Thioflavin T (ThT) and Pittsburgh compound B (PiB) containing the benzothiazole moiety.

Yang and coworkers have previously shown that BTA analogues containing an oligoethylene glycol chain bind with high density to A β .¹¹⁹ Since the ethylene glycol group should also impart a degree of water solubility to the molecule, we chose to use BTA derivative prepared from pentaethylene glycol as the targeting group. The synthesis of BTA-EG₅ (**21**) is shown in Scheme 4.2. Di-tosylation of pentaethylene glycol (**15**) followed by reaction with excess sodium iodide readily afforded diiodide **16**. However,

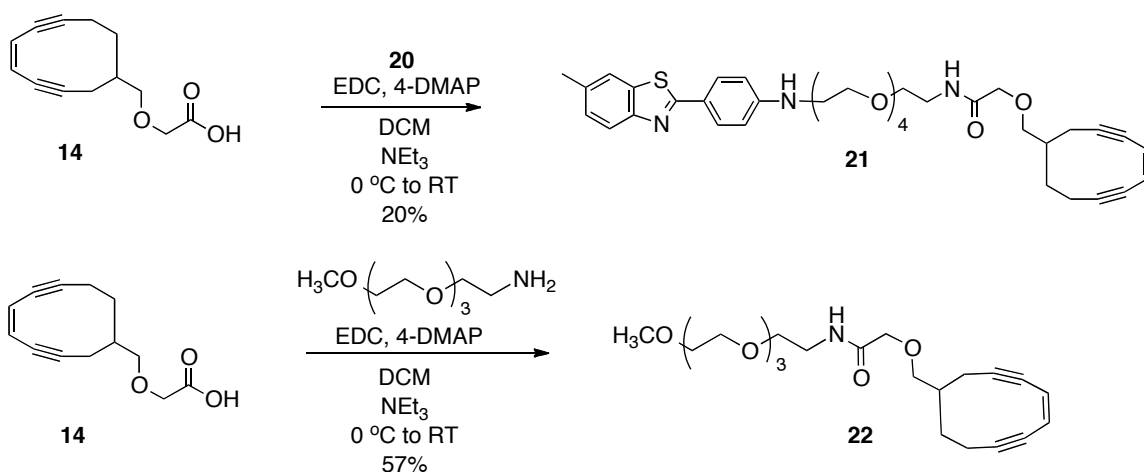
nucleophilic substitution of the BTA onto the oligoethylene glycol proved to be much less facile. The reaction of 6-methylbezothiazole aniline (BTA) with **17** afforded BTA-EG₅-monoiodide **18** in 25% after 3 days of refluxing in THF. Only a minute amount (< 1%) of dimeric BTA species was formed. The efficiency of this substitution reaction has recently been improved and is further discussed in chapter 5 of this thesis. Conversion of the BTA-EG₅-monoiodide to the free amine was accomplished by substitution with azide to provide **19**, followed by Staudinger reduction^{155, 156} to give BTA-EG₅-amine **20**. It is important to note that due to the cyclic enediyne's propensity to slowly cyclize, we took precautions to minimize deterioration: Accordingly, reaction times of enediyne-containing compounds at room temperature were minimized, workups were done as quickly as possible and cyclic enediyne intermediates were stored at -80°C.



Scheme 4.2: Synthesis of BTA-EG₅ amine **20**.

4.5 Synthesis and binding affinity of the BTA-enediyne conjugate

We covalently attached the cyclic enediynes to BTA-EG₅-amine via an amide coupling reaction promoted by 1-ethyl-3-(3-dimethylaminopropyl)carbodiimide (EDC) to afford the A β -targeting enediynes **21** (Scheme 4.3). In addition, we synthesized a similar control molecule **22** comprising a cyclic enediynes molecule that does not carry an A β -binding group. Our final control molecule was the BTA-EG₅-amine **20** as it contains an A β -binding group but lacks the enediynes warhead required for peptide degradation. We demonstrated, using a recently reported ELISA-based binding assay,¹³¹ that the BTA-containing molecules **20** and **21** associate with aggregated A β peptides, whereas molecule **22** does not appear to associate with A β (Figure 4.5).



Scheme 4.3: Formation of the enediynes-BTA conjugate **21** and a related control molecule **22** containing the enediynes warhead but lacking an A β -binding group.

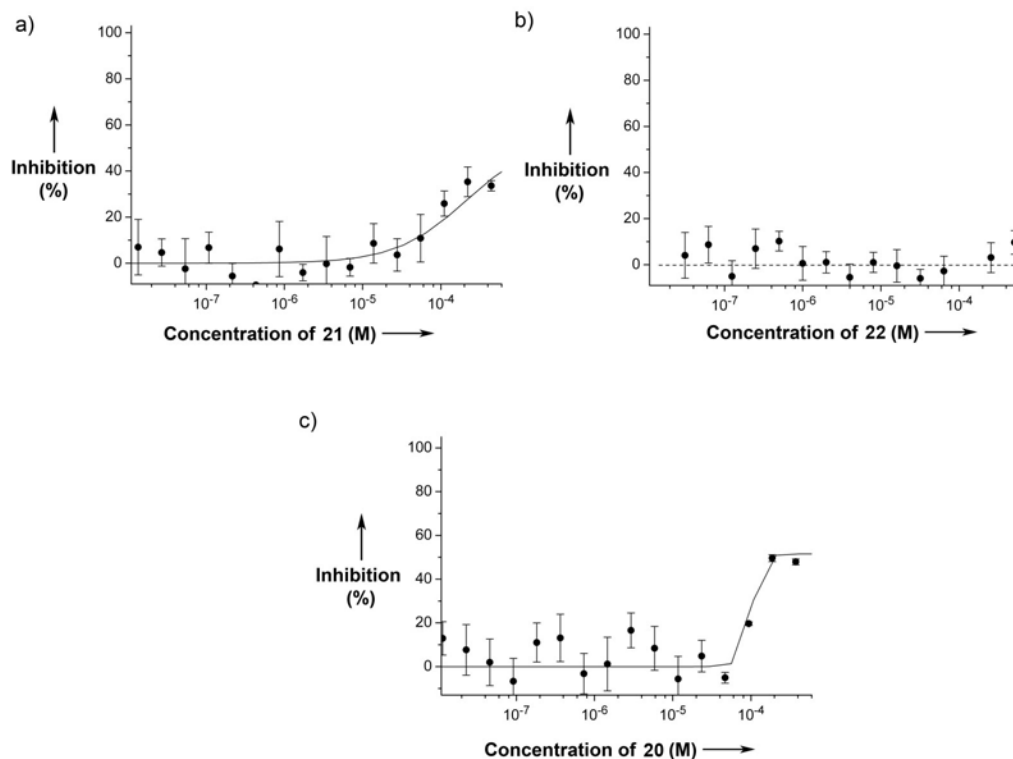


Figure 4.5: Briefly, the design of this ELISA-based competition assay entails the evaluation of molecules that inhibit the interaction of A β fibrils (here, formed from A β_{1-40}) with a monoclonal anti-A β IgG raised against residues 3-8 of AD-related A β peptide (clone 6E10). This assay is based on the hypothesis that molecules that can effectively and efficiently coat A β fibrils will be able to inhibit the binding of this anti-A β IgG to A β fibrils. The relative inhibition of IgG-A β fibril interactions by small molecules is quantified using a standard ELISA protocol. Inhibition (Inh.) of anti-A β IgG (clone 6E10)-A β interactions with compound: a) **21**, 55% Maximal Inh., $IC_{50} = 220$ μ M; b) **22**, No Inhibition; and c) **20**, 51% Maximal Inh., $IC_{50} = 100$ μ M. Error bars represent \pm SEM.

4.6 Effect of the BTA-enediye conjugate on aggregated A β

We prepared aggregated A β by incubating synthetic A β_{1-40} peptides for 4 days at 37 °C in deionized water. CD spectroscopy indicated that the solution of A β peptides contained significant β -sheet character (Figure 4.6), which is characteristic of aggregated A β peptides. Specifically, The CD spectrum shows a maximum at $\lambda = 197$ and a

minimum at $\lambda = 216$ nm, which confirmed the β -sheet character of A β and is consistent with experiments conducted by Gursky and Aleshkov.¹⁵⁷ Deconvolution software was used to analyze the β -sheet content and was determined to be 35% using the K2D software (available at <http://www.embl-heidelberg.de/~andrade/k2d>) and 40.2% using SOMCD software (available at <http://geneura.ugr.es/cgi-bin/somcd/index.cgi>).

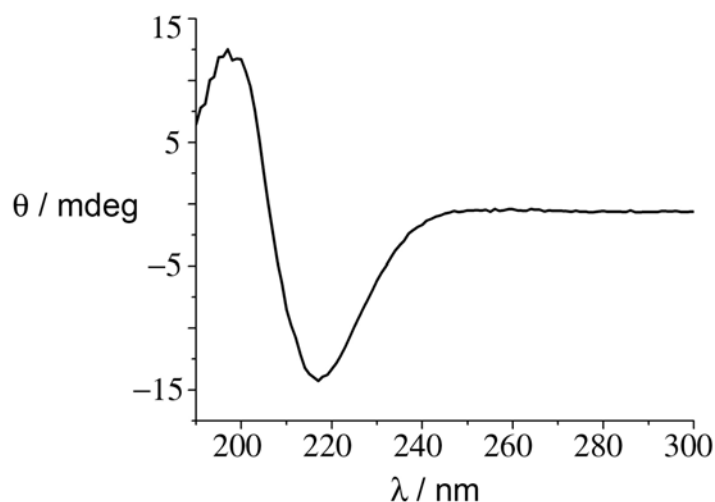


Figure 4.6: A Circular dichroism spectrum of a 100 μ M aqueous solution of A β after incubation at 37°C for 4 days.

We incubated A β peptides in deionized water with the BTA-enediyne conjugate **21** (at 37 °C) and analyzed the peptide solution by RP-HPLC and SDS-PAGE after 7 days (Figure 5.9A). We observed that the RP-HPLC peak at 12.1 minutes, corresponding to the A β peptide, decreased over the course of 7 days (with approximately 50% and 20% of the peak area of A β peptide remaining after incubation with 1 mole and 10 mole equiv. of **21**, respectively), while we also observed the appearance of several new peaks (Figure 4.7 A). The new HPLC peaks that appeared from incubating A β with **21** presumably

correspond to some of the major fragments from cleavage of A β peptides. Attempts to characterize these new fragments by LC-MS and LC-MS-MS were inconclusive, most likely due to the expected complicated mixture of products from reaction of the α and

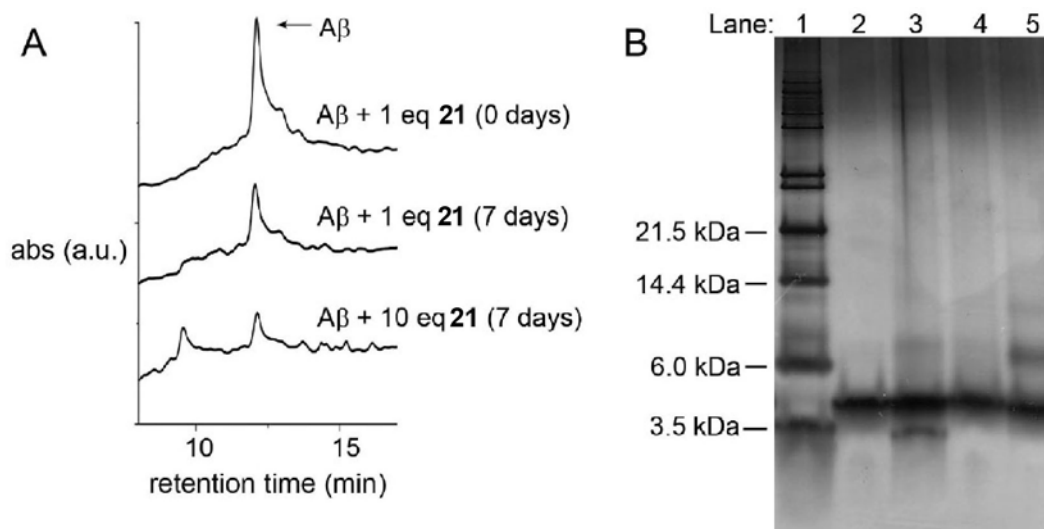


Figure 4.7: Chromatographic and electrophoretic analyses of the degradation of A β peptides using a targeted enediyne. (A) RP-HPLC analysis of A β_{1-40} peptides after incubation with 1 molar equivalent of **21** at 37°C after 0 days (top) and 7 days (middle), or 10 equivalents of **21** after 7 days (bottom). (B) SDS-PAGE analysis of A β_{1-40} peptides after incubation with 1 molar equivalent of **21** or 5 molar equivalents of **22** or **20** at 37°C for 7 days. Lane 1: Mark12TM standard. Lane 2: A β_{1-40} alone. Lane 3: A β_{1-40} + 1 molar equivalent **21** incubated for 7 days. Lane 4: A β_{1-40} + 5 molar equivalent **22** incubated for 7 days. Lane 5: A β_{1-40} + 5 molar equivalent **20** incubated for 7 days. SDS-PAGE gels were run using a 16% tricine gel and visualized via silver staining.

side-chain hydrogen atoms of the amino acids in A β under these radical conditions.¹⁴⁹

Although repeated reactions of A β with **21** consistently resulted in the same RP-HPLC peaks, the quantitative conversion of A β to peptide fragments varied between experiments presumably due to the well-known heterogeneity of aged solutions of A β .¹²⁴

SDS-PAGE analysis of A β (~ 4 kDa) incubated with 1 mole equivalent of **21** for 7 days supports partial degradation of A β_{1-40} to peptide fragments with a smaller mass than A β

(Figure 4.7B, lane 3). The new, lowest molecular weight band in lane 3 in Figure 4.7B presumably corresponds to a mixture of products from the degradation of A β peptides that could not be separated from each other under the SDS-PAGE conditions employed. We did not observe, however, any degradation of aggregated A β over 7 days when we incubated these aggregated peptides in the presence of 5 mole equivalents of enediyne **22** (i.e., lacking an A β -binding moiety, Figure 4.7B, lane 4), or in the presence of 5 mole equivalents of BTA derivative **20** (i.e., lacking the enediyne, Figure 4.7B, lane 5). As a further control, we incubated **21** with ubiquitin, an 8.6 kDa protein, and did not observe any degradation of this protein over the course of 7 days (Figure 4.8). These HPLC and SDS-PAGE studies collectively demonstrate that BTA-enediyne conjugate **21** may

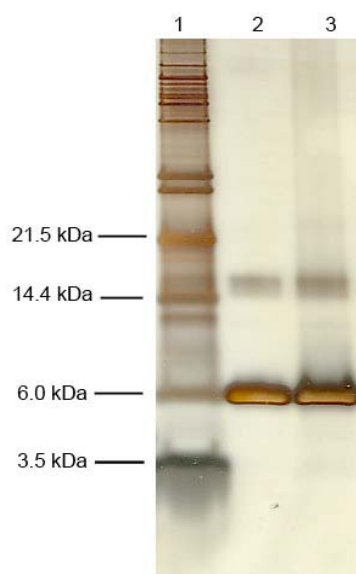


Figure 4.8: SDS-PAGE analysis of ubiquitin (8.6 kDa) alone and after incubation with 1 molar equivalent of **21** at 37 °C for 7 days. Lane 1: Mark12™ standard. Lane 2: ubiquitin (90%, from Sigma-Aldrich, used without further purification). Lane 3: ubiquitin + 1 molar equivalent **21** incubated for 7 days. SDS-PAGE gels were performed using a 16% tricine gel and visualized via silver staining.

selectively degrade A β peptides over other potential proteins in solution, and that the cleavage of A β by the enediyne moiety in **21** is directed by the A β -binding BTA group.

To assess whether the cleavage of A β_{1-40} by **21** had an effect on the toxicity of aggregated A β on cells, we exposed SH-SY5Y human neuroblastoma cells to aggregated A β_{1-40} peptides, or to aggregated A β peptides that were incubated with **21** for 0 or 7 days (Figure 4.9). Cell viability was estimated using a standard MTT assay as describe by Mosmann.¹⁵⁸ Incubation of 20 μ M A β peptides with 5 mole equivalents of **21** for 7 days resulted in a mixture of peptides and peptide fragments that was less toxic to these cells ($\sim 67 \pm 1\%$ retention of cell viability) compared to A β alone ($\sim 53 \pm 2\%$ retention of cell viability) or compared to when A β and **21** were mixed and immediately exposed to the cells ($\sim 42 \pm 6\%$ retention of cell viability). We did not perform these cytotoxicity studies using higher molar ratios of A β and **21** since **21** was significantly toxic to this cell line at concentrations above 100 μ M and we needed to use a 20 μ M solution of aggregated A β peptides to observe significant toxicity to these cells. These results indicate that **21** can, at least, partially protect cells from the toxicity of A β , presumably through its ability to degrade A β into less toxic species.

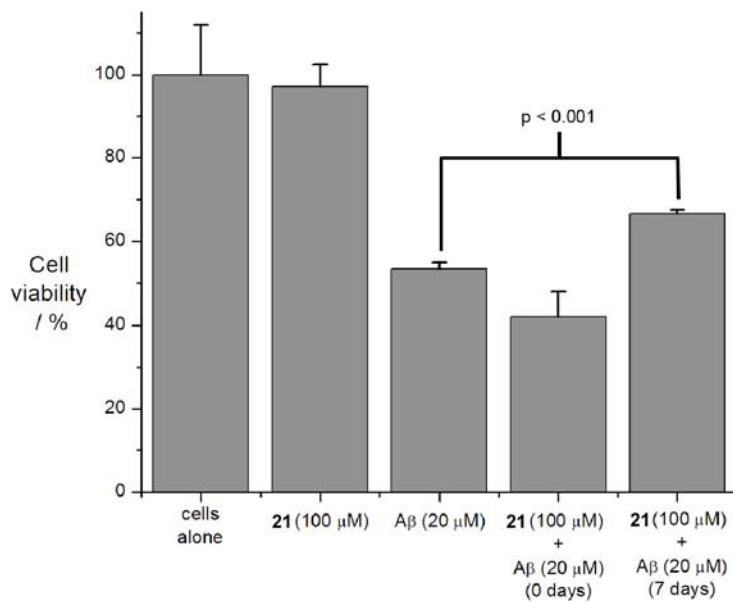


Figure 4.9: Relative cell viability of SH-SY5Y human neuroblastoma cells in the presence of aggregated A β peptides with or without incubation with molecule **21**. Cells incubated with **21** alone were treated with a solution of **21** that was incubated for 7 days in sterile water prior to exposure to cells. A β samples were prepared by incubation in sterile water for 4 days and: 1) incubated further for 7 days prior to exposure to cells, 2) incubated further for 7 days, mixed with **21**, and immediately exposed to cells (labeled as 0 days), or 3) incubated with **21** for 7 days prior to exposure to cells (labeled as 7 days). The data are expressed as mean values + standard deviations. The viability of cells exposed to A β incubated with molecule **21** for 7 days was significantly different than the viability of cells exposed to A β alone ($P < 0.001$).

4.7 Chapter summary

We demonstrate that a cyclic enediyne covalently attached to an A β -binding group can promote the degradation of A β peptides at physiological temperature in aqueous solution. This targeted enediyne exhibited partial cytoprotective properties of against A β toxicity in human neuroblastoma cells, and, hence, represents a first step towards a new strategy to combat AD through the chemical degradation of A β using synthetic molecules. A major challenge that remains is to develop such targeted

molecular warheads that can be administered safely in humans. One potential methods to improve the biocompatibility of warheads could be to use triggered enediynes¹⁵⁹ (i.e., that become activated only when bound to A β peptides). Several groups have developed chemical cleaving agents based on metal-chelating cyclen motifs that demonstrate the capability to affect degradation of A β peptides under aqueous conditions.^{122, 123} However, the method presented in this chapter uses a warhead that does not require activation by an external source such as a redox-active metal. A chemical method to degrade disease-related materials such as A β peptides under physiological conditions represents a promising new strategy for combating AD and other amyloid-related disorders.

4.8 Experimental Methods

All synthetic reagents were from Aldrich, Fisher Scientific, Alfa Aesar, Fluka, City Chemical, or Quanta Biosciences and were used without further purification. A β ₁₋₄₀ peptides were from Biopeptide, Inc., and used without further purification. All solvents used for reactions were obtained from Fisher scientific and dried prior to use. Solvents used for chromatography were ACS technical grade and used without further purification. All intermediates containing cyclic enediyne moieties described in this chapter were stored at -80 °C. SH-SY5Y human neuroblastoma cells (Product No: CRL-2266) and 3-(4,5-dimethylthiazolyl-2)-2, 5-diphenyltetrazolium bromide (MTT) cell proliferation assay (Product No: 30-1010K) were purchased from American Type Culture Collection

All NMR data was obtained on a 400 MHz Varian Mercury Spectrometer. Circular Dichroism (CD) experiments were performed on an Aviv Instruments Circular

Dichroism Spectrometer Model 215 using a quartz CD cell purchased from Hellma (0.2 mm path length). HPLC analyses were performed on a Hewlett-Packard (now Agilent) 1100 Series HPLC instrument. Water (18.2 $\mu\Omega/\text{cm}$) was filtered through a NANOPure DiamondTM (Barnstead) water purification system before use.

1-(*tert*-butyl)-1,1-dimethylsilyl (5-cyclodecen-3,7-diynylmethyl) ether (11)

A flame-dried 250 mL 3-necked round bottom flask was charged with dibromide **10** (872 mg, 2.0 mmol), hexamethylphosphoramide (8.8 g, 100.0 mmol, 8.5 mL) and 110 mL dry tetrahydrofuran (THF) and allowed to stir under a N₂ atmosphere at -40 °C. After the temperature had stabilized, Lithium hexamethyldisilazide (LiHMDS, 0.25 M in THF, 10.0 mmol, 20 mL) was added slowly via mechanical syringe pump over 5 h. The dark brown reaction mixture was poured without warming onto 120 mL of an aqueous saturated solution of NH₄Cl (containing 40 g of ice) and the solution was extracted with diethylether (Et₂O) (4 x 40 mL). The combined organic phase was washed with cold HCl (10%, 2 x 40 mL), DI H₂O (40 mL), saturated NaHCO₃ (40 mL) and saturated NaCl (20 mL), dried over sodium sulfate and concentrated *in vacuo*. Care was taken to use a low vacuum setting on the rotary evaporator and to keep the reaction flask cool. The residue was eluted using a plug of silica (95:5 hexanes:Et₂O as eluent) gave 220 mg of crude product as a yellow oil. The crude material was taken on to the next step without further purification. ¹H-NMR (400 MHz) of the crude in CDCl₃ showed the presence of the cyclized product **11** by the appearance of the olefinic protons of the enediyne at $\delta = 5.83$ ppm.

Cyclodeca-5-en-3,7-diynylmethanol (12).

Crude *tert*-butyl(cyclodeca-5-en-3,7-diynylmethoxy)dimethylsilane **11** (220 mg) was dissolved in 5 mL of dry THF and allowed to stir at 0 °C. A solution of tetrabutyl ammonium fluoride (1.0 M in THF, 1.2 mL, 1.2 mmol) was added dropwise to the reaction mixture over two minutes. The ice bath was removed and the solution was allowed to stir for a further 90 minutes while warming to room temperature. The reaction mixture was diluted with 75 mL of Et₂O and washed with HCl (10%, 1 x 15 mL), saturated NaHCO₃ (1 x 15 mL), DI H₂O (1 x 15 mL), and saturated NaCl (1 x 15 mL). The organic layer was dried over Na₂SO₄ and concentrated *in vacuo* to give a yellow residue. Column chromatography (60:40 Et₂O:hexane as eluent) gave the enediyne alcohol **12** as a yellow oil (54 mg, 17% over two steps from **10**). ¹H-NMR (400 MHz, CDCl₃); δ = 5.82 (s, 2H), 3.54 (m, 2H), 2.50-2.63 (m, 2H), 2.06-2.35 (m, 3H), 1.78-1.90 (m, 2H), 1.67 (s, 1H). ¹³C-NMR (400 MHz, CDCl₃): δ = 123.53, 123.48, 104.16, 102.97, 83.17, 83.08, 67.64, 44.59, 32.85, 24.68, 21.35. ESI-MS (*m/z*) calcd for C₁₁H₁₂O [M]⁺ 160.0888; found [M-H]⁻ 159.22.

***tert*-butyl-2-(cyclodeca-5-en-3,7-diynylmethoxy)acetate (13).**

Enediyne alcohol **12** (20 mg, 0.13 mmol) was dissolved in 0.25 mL benzene and allowed to stir in a 4 mL reaction vial at 10 °C. After 5 minutes, tetrabutyl ammonium hydrogen sulfate (21 mg, 0.06 mmol) and KOH (40% in H₂O, 0.25 mL) were added to the reaction vial and the biphasic reaction mixture was allowed to stir vigorously. After 5 minutes, *tert*-butyl bromoacetate (29 mg, 0.15 mmol, 22.2 μL) was rapidly added to the vial. The reaction was allowed to stir at 10 °C for 45 min, and then at room temperature

for an additional 60 min. The reaction was diluted to 30 mL with Et₂O, washed with DI H₂O (5 mL) and saturated NaCl (5 mL), dried over Na₂SO₄ and concentrated *in vacuo* to give a yellow oil. The residue was purified via flash column chromatography (using 90:10 hexanes:EtOAc (ethyl acetate) as eluent) giving a clear pale yellow oil (19 mg, 55%). ¹H-NMR (400 MHz, CDCl₃): δ = 5.81 (s, 2H), 3.95 (d, 1.2 Hz, 2H), 3.43 (m, 2H), 2.49-2.63 (m, 2H), 2.19-2.36 (m, 3H), 1.85-1.90 (m, 2H) 1.47 (s, 9H). ¹³C-NMR (400 MHz, CDCl₃); δ = 169.92, 123.52, 123.40, 104.24, 103.07, 83.10, 83.08, 81.92, 76.17, 69.02, 42.10, 33.03, 28.42 (3C), 25.08, 21.27. ESI-MS (*m/z*) calcd for C₁₇H₂₂O₃ [M]⁺ 274.1569; found [M+Na]⁺ 297.04.

2-(cyclodeca-5-en-3,7-diynylmethoxy)acetic acid (14).

An oven-dried 25 mL roundbottom flask was charged with tert-butyl ester **13** (39 mg, 0.14 mmol), 2,6-lutidine (304 mg, 2.84 mmol, 329 μL) and 10 mL dry dichloromethane (DCM) and allowed to stir under an N₂ atmosphere at 0 °C. After 15 minutes, tert-butyldimethylsilyl triflate (316 mg, 1.4 mmol, 257 μL) was added rapidly to the reaction flask. After 1 h, the icebath was removed and the solution was allowed to stir for a further 2 h while warming to room temperature. The reaction was diluted to 100 mL with Et₂O, washed with HCl (5%, 10 mL), and saturated NaCl (10 mL), dried over Na₂SO₄ and concentrated *in vacuo* to give a viscous yellow oil. The residue was purified via flash column chromatography (using 90:10 DCM:methanol as eluent) giving a yellow foam (24 mg, 77%). ¹H-NMR (400 MHz, CDCl₃): δ = 5.81 (s, 2H), 4.10 (s, 2H), 3.46 (m, 2H), 1.85-2.62 (m, 7H). ¹³C-NMR (400 MHz, CDCl₃); δ = 175.26, 123.51 (2C),

104.10, 102.76, 83.25 (2C), 76.34, 68.78, 41.96, 33.12, 25.01, 21.23. ESI-MS (m/z) calcd for $C_{13}H_{14}O_3$ $[M]^+$ 218.0943; found $[M-H]^-$ 217.10 and $[2M-H]^-$ 434.95.

3,6,9,12-tetraoxatetradecane-1,14-diyl bis(toluenesulfonate) (16)

Pentaethylene glycol (**15**) (4.0 g, 26.0 mmol) and tosyl chloride (12.4 g, 65.0 mmol) in 130 mL dry DCM was allowed to stir until complete dissolution. Pyridine (10.7 mL, 132 mmol) was then added to the reaction flask and allowed to stir at room temperature for 12 h. The reaction mixture was slowly poured onto a mixture of concentrated HCl (15 mL) and crushed ice (150 g). The mixture was left standing until the ice had melted and then organic layer was separated from the aqueous layer. The organic layer was washed with saturated NaCl (1 x 25 mL), dried over Na_2SO_4 and concentrated *in vacuo*. The residue was purified via silica column chromatography (using a gradient from 100% DCM to 55:45 DCM:ethyl acetate (EtOAc) as eluent) giving di-tosylate **16** as a clear pale yellow oil (9.8 g, 69%). 1H -NMR (400 MHz, $CDCl_3$): δ = 7.77 (d, 8.0 Hz, 4H), 7.33 (d, 8.0 Hz, 4H), 4.18 (t, 4.8 Hz, 4H), 3.56-3.68 (m, 18H), 2.43 (s, 6H). ^{13}C -NMR (400 MHz, $CDCl_3$): δ = 145.04 (2C), 133.17 (2C), 130.10 (4C), 128.19 (4C), 70.95 (2C), 70.79 (2C), 70.70 (2C), 69.49 (2C), 68.88 (2C), 21.87 (2C). ESI-MS (m/z) calcd for $C_{24}H_{34}O_{10}S_2$ $[M]^+$ 546.1593; found $[M+NH_4]^+$ 564.08 and $[M+Na]^+$ 569.13.

1,14-diiodo-3,6,9,12-tetraoxatetradecane (17)

3,6,9,12-tetraoxatetradecane-1,14-diyl bis(toluenesulfonate) (**16**) (3.03 g, 5.48 mmol) and dry sodium iodide (7.20 g, 48.0 mmol) were combined in an oven-dried round bottom flask. Anhydrous acetone (30 mL) was added to the flask. Upon dissolution of

the solid material, the reaction mixture was heated to reflux for 12 h. After cooling to room temperature, the solids were removed by filtration and washed with acetone until colorless. The mother liquor was concentrated *in vacuo* and the residue was re-dissolved in EtOAc (75 mL). The organic layer was then washed with Na₂S₂O₃ (10% in H₂O, 7 mL), saturated NaCl (1 x 10 mL), dried over Na₂SO₄ and concentrated *in vacuo* to give a pale yellow oil (2.46 g, 98%). ¹H-NMR (400 MHz, CDCl₃): δ = 3.56 (t, 6.8 Hz, 4H), 3.46 (m, 11H), 3.08 (t, 6.8 Hz, 3H). ESI-MS (*m/z*) calcd for C₁₀H₂₀I₂O₄ [M]⁺ 457.9451; found [M+H]⁺ 458.84

14-iodo-N-(4-(6-methylbenzothiazol-2-yl)phenyl)-3,6,9,12-tetraoxatetradecan-1-amine (18)

An oven-dried 2 L round bottom flask charged with 1,14-diiodo-3,6,9,12-tetraoxatetradecane **17** (23.4g, 51.0 mmol), 6-methylbenzothiazole aniline (BTA) (88g, 360 mmol), potassium carbonate (115 g, 820 mmol) and dry THF (1 L) was allowed to stir for 15 minutes while being purged with N₂ gas. The reaction flask was equipped with a condenser (and a drying tube) and was heated to reflux while stirring for 7 days. The reaction flask was then cooled to room temperature and the solvent removed *in vacuo*. The residue was dissolved in DCM (200 mL), and filtered to remove insoluble material. The organic phase was then washed with DI H₂O (2 x 30 mL), dried over Na₂SO₄, and concentrated *in vacuo* to give a dark yellow/brown residue. The residue was purified via silica column chromatography (98:2 EtOAc:MeOH) to yield a yellow oil (7.2 g, 25%). Note: This compound should be used immediately after preparation as it slowly spontaneously cyclizes to the aza-crown ether. ¹H-NMR (400 MHz, CDCl₃): δ = 7.88 (d,

8.4 Hz, 2H), 7.85 (d, 8.4 Hz, 1H), 7.62 (s, 1H), 7.23 (dd, 6.8 Hz, 1.4 Hz, 1H), 6.67 (d, 8.8 Hz, 2H), 3.65-3.75 (m, 17H), 3.37 (t, 5.2 Hz, 2H), 3.24 (t, 6.8 Hz, 2H), 2.47 (s, 3H). ^{13}C -NMR (400 MHz, CDCl_3): δ = 168.01, 152.57, 150.82, 134.86, 134.60, 129.22 (2C), 127.81, 122.99, 122.08, 121.48, 112.89 (2C), 72.23, 70.96, 70.90, 70.85 (2C), 70.63, 70.48, 69.59, 43.40, 21.77, 3.19. ESI-MS (m/z) calcd for $\text{C}_{24}\text{H}_{31}\text{IN}_2\text{O}_4\text{S}$ $[\text{M}]^+$ 570.1049; found $[\text{M}+\text{H}]^+$ 571.04.

14-azido-N-(4-(6-methylbenzothiazol-2-yl)phenyl)-3,6,9,12-tetraoxatetradecan-1-amine (19)

To a 50 mL round bottom flask equipped with a stirbar, 535 mg (938 μmol) BTA-EG₅-I **18** and NaN_3 (186 mg, 2.86 mmol) were dissolved in 25 mL of DMF. The reaction flask was stirred at 90 °C for 17 h. The reaction flask was allowed to cool to room temperature upon which the solvent was removed *in vacuo* to yield a yellow residue. The residue was diluted to 150 mL in EtOAc, washed with DI H₂O (4 x 15 mL), saturated NaCl (15 mL), dried over sodium sulfate and concentrated *in vacuo*. Purification via silica column chromatography (100% EtOAc) gave the azide **19** as a viscous yellow oil (419 mg, 91%). ^1H -NMR (400 MHz, CDCl_3): δ = 7.88 (d, 8.8 Hz, 2H), 7.84 (d, 8.4 Hz, 1H), 7.62 (s, 1H), 7.23 (dd, 6.8 Hz, 1.2 Hz, 1H), 6.66 (d, 8.8 Hz, 2H), 3.72 (t, 5.2 Hz, 2H), 3.65-3.75 (m, 15H), 3.24 (t, 5.2 Hz, 4H), 2.46 (s, 3H). ^{13}C -NMR (400 MHz, CDCl_3): δ = 167.99, 152.68, 150.81, 134.92, 134.56, 129.18 (2C), 127.78, 123.04, 122.09, 121.48, 112.86 (2C), 70.95, 70.88 (2C) 70.82, 70.61, 70.29, 69.59, 50.93, 43.37, 21.76. IR (KBr pellet): IR: 2102.7, 1608.4, 1484.6, 1454.5, 1180.6,

1120.4 cm^{-1} . ESI-MS (m/z) calcd for $\text{C}_{24}\text{H}_{31}\text{N}_5\text{O}_4\text{S}$ $[\text{M}]^+$ 485.2097; found $[\text{M}+\text{H}]^+$ 486.21.

***N'*-(4-(6-methylbenzothiazol-2-yl)phenyl)-3,6,9,12-tetraoxatetradecane-1,14-diamine
(20)**

In a 100 mL round bottom flask equipped with a stirbar, compound **19** (383 mg, 789 μmol) and triphenylphosphine (621 mg, 2.37 mmol) were dissolved in 25 mL of THF. The reaction was allowed to stir at room temperature for 20 minutes, at which time 2.5 mL of DI H_2O was added. The reaction flask was equipped with a reflux condenser and allowed to stir at 60 $^\circ\text{C}$. After 4 h, the reaction flask was allowed to cool to room temperature, concentrated *in vacuo* and immediately subjected to silica column chromatography (90:10:1 DCM:MeOH:conc. NH_4OH (aq) as eluent). The combined fractions were dried over Na_2SO_4 , filtered and concentrated *in vacuo* to give the amine **20** as a viscous yellow oil (351 mg, 97%). ^1H -NMR (400 MHz, CDCl_3): δ = 7.88 (d, 8.8 Hz, 2H), 7.85 (d, 8.0 Hz, 1H), 7.63 (s, 1H), 7.23 (dd, 7.2 Hz, 1.2 Hz, 1H), 6.67 (d, 8.8 Hz, 2H), 3.73 (t, 5.2 Hz, 2H), 3.61-3.67 (m, 13H), 3.50 (t, 5.2 Hz, 2H), 3.37 (t, 5.2 Hz, 2H), 2.86 (s, 2H), 2.47 (s, 3H), 1.77 (s, 2H). ^{13}C -NMR (400 MHz, CDCl_3): δ = 168.01, 152.71, 150.86, 134.94, 134.57, 129.20 (2C) 127.79, 123.05, 122.12, 121.49, 112.86 (2C), 73.58, 70.90 (2C), 70.86 (2C), 70.66, 70.54, 69.65, 43.42, 42.00, 21.78. HR-MS (m/z) calcd for $\text{C}_{24}\text{H}_{33}\text{N}_3\text{O}_4\text{S}$ $[\text{M}]^+$ 459.2186; found $[\text{M}]^+$ 459.2188.

(Cyclodeca-5-en-3,7-diynylmethoxy)-N-(14-(4-(6-methylbenzothiazol-2-yl)phenylamino)-3,6,9,12-tetraoxatetradecyl)acetamide (21)

2-(cyclodeca-5-en-3,7-diynylmethoxy)acetic acid **14** (6.5 mg, 30 μmol) was dissolved in 1 mL dry DCM and allowed to stir in a dry scintillation vial at 0 °C. After 5 minutes, BTA-EG₅-NH₂ **3** (16.5 mg, 36 μmol) in 1 mL dry DCM was added to the solution of the enediyne-carboxylic acid **7**. 4-Dimethylaminopyridine (DMAP) (5.5 mg, 45 μmol) and Ethyl (N,N-dimethylaminopropyl)carbodiimide hydrochloride (EDC•HCl) (8.6 mg, 45 μmol) were added to the vial. The reaction was allowed to stir at 0 °C for 2h, and then at room temperature for an additional 1h. The reaction mixture was immediately purified by silica column chromatography (using a gradient from 100% EtOAc to 97:3 EtOAc:MeOH as eluent) to give **21** as a yellow oil (3.9 mg, 20%). ¹H-NMR (400 MHz, CDCl₃): δ = 7.88 (d, 8.8 Hz, 2H), 7.85 (d, 8.0 Hz, 1H), 7.63 (s, 1H), 7.23 (dd, 7.2 Hz, 1.2 Hz, 1H), 6.87, (s, 1H), 6.67 (d, 8.8 Hz, 2H), 5.82 (s, 2H), 3.94 (s, 2H), 3.73 (t, Hz, 4.8 Hz, 2H), 3.63-3.67 (m, 13H), 3.57 (t, Hz, 4.8 Hz, 2H), 3.50 (m, 2H), 3.37 (m, 4H), 2.47-2.60 (m, 5H), 2.17-2.34 (m, 3H), 1.77-1.91 (m, 2H). HR-MS (*m/z*) calcd for C₃₇H₄₅N₃O₆S [M]⁺ 659.3024; found [M]⁺ 659.3016.

(Cyclodeca-5-en-3,7-diynylmethoxy)-N-(2,5,8,11-tetraoxatridecan-13-yl)acetamide (22)

2-(cyclodeca-5-en-3,7-diynylmethoxy)acetic acid **14** (6.5 mg, 30 μmol) was dissolved in 1 mL dry DCM and allowed to stir in a dry scintillation vial at 0 °C. After 5 minutes, 2,5,8,11-tetraoxatridecan-13-amine (9.3 mg, 45 μmol , from Quantabiodesign,

Ltd.) in 1 mL dry DCM was added to the solution of the enediyne-carboxylic acid **14**. DMAP (5.5 mg, 45 μ mol) and EDC•HCl (8.6 mg, 45 μ mol) were added to the vial. The reaction was allowed to stir at 0 °C for 2h, and then at room temperature for an additional 1h. The reaction mixture was immediately purified by silica column chromatography (using a gradient from 100% DCM to 95:5 DCM:MeOH as eluent) giving compound **22** as a yellow oil (6.8 mg, 57%). ¹H-NMR (400 MHz, CDCl₃): 6.90 (s, 1H), δ = 5.82 (s, 2H), 3.95 (s, 2H), 3.37-3.66 (m, 21H), 2.50-2.61 (m, 2H), 2.27-2.35 (m, 1H), 2.15-2.20 (m, 2H), 1.80-1.89 (m, 2H). ¹³C-NMR (400 MHz, CDCl₃); δ = 169.67, 123.57, 123.47, 103.91, 102.43, 83.36, 83.29, 76.17, 72.21, 70.79-70.89 (5C), 70.62, 70.06, 59.32, 42.04, 38.83, 33.09, 25.01, 21.23. HR-MS (*m/z*) calcd for C₂₂H₃₃NO₆ [M]⁺ 407.2302; found [M]⁺ 407.2304.

Circular dichroism analysis of aggregated A β ₁₋₄₀ samples

Optical rotation data was obtained at 1 nm intervals between 300-190 nm with an acquisition time of 3 s for each data point. Results of 4 runs were averaged and then corrected by subtracting out a blank sample containing only NANOPure water.

A 100 μ M solution of A β ₁₋₄₀ was prepared by dissolving 300 μ g A β ₁₋₄₀ in 693 μ L of deionized nanopure water. The solution was transferred to a quartz cuvette, which was then capped and sealed with parafilm. The sample was incubated at 37°C for 4 days and then subjected to CD analysis.

MTT Cell Viability Assay

The viability of SH-SY5Y cells exposed to different treatments was measured based on the ability of metabolically active cells to reduce yellow tetrazolium MTT to purple formazan, which can be measured at $\lambda = 570 \text{ nm}$.¹⁵⁹ The assay was performed in a 96-well plate format, where each sample was measured at least in triplicate. Cells were plated at a density of 50,000 cells/well (in 100 μL of culture media consisting of 1:1 mixture of Eagle's Minimum Essential Medium (Product No. 30-2003 from ATCC) and Ham's F12 supplemented with 10% Fetal Bovine Serum) and incubated overnight before treatment with 100 μL of various sample solutions. All incubation steps were performed in a humidified incubator at 37 °C and 5% carbon dioxide unless stated otherwise.

The cells were exposed to a final concentration of the following sample solutions:

- 1) 100 μM molecule **21** that had been incubated in sterile water for 7 days;
- 2) 20 μM aggregated A β prepared from a 100 μM stock solution of A β (incubated for 4 days) that was incubated further in sterile water for 7 days;
- 3) 20 μM aggregated A β prepared from a 100 μM stock solution of A β (incubated for 4 days) that was incubated further in sterile water for 7 days and mixed with 100 μM **21** immediately prior to exposure to cells; and
- 4) 20 μM aggregated A β prepared from a 100 μM stock solution of A β (incubated for 4 days) that was incubated with 100 μM **21** in sterile water for 7 days.

All sample solutions were supplemented with an equivalent volume of 2X culture media immediately prior to dosing cells. The cells were incubated with the sample solutions for 24 hours and after the 24-hour incubation period, 20 μL of the MTT reagent was added and cells incubated

further for 3 hours. The cells were subsequently solubilized with 100 μ L detergent reagent, incubated overnight at room temperature and cell viability determined by measuring the absorbance at 570 nm. All results were expressed as percent reduction of MTT relative to untreated controls (defined as 100% viability) and the average absorbance value for each treatment was subtracted with the absorbance reading of wells containing media, MTT reagent and detergent reagent.

Statistical Analysis

Independent two-tailed student's t-tests were performed using Origin 7.0 (Microcal Software, Inc., Northampton, MA) to evaluate the statistical significance of the difference between the control and experimental mean values. A p-value of < 0.05 was defined as statistically significant. All results were expressed as mean values + standard deviations.

Notes about this chapter

Chapter 4 is based on material currently being prepared for submission for publication: Mark Rubinshtein, Lila K. Habib, Mahealani R. Bautista, and Jerry Yang "Chemical Degradation of Alzheimer's-Related beta-Amyloid Peptides Using a Targeted Eneidyne." I was the primary investigator and author of this material.

Chapter 5

Efficient Synthesis and Applications of Oligoethylene glycol derivatives of Benzothiazole Anilines

5.1 Introduction

This chapter presents a highly improved general methodology for the synthesis of oligoethylene glycol derivatives of BTA. Previous syntheses of this class of compounds—such as those described in chapter 4 of this dissertation and by Inbar et al¹¹⁹—have been plagued by poor yields and long reaction times. Because of the interesting amyloid binding properties and potential utility of BTA-oligoethylene glycol (BTA-EG_x) derivatives, and the interest of examining their biological activity *in vivo*, it was imperative to develop a more efficient synthetic route to this family of compounds. The improved methodology we present for BTA-EG_x synthesis has both significantly decreased reaction times and increased yields, and has afforded facile access to multi-gram quantities of these molecules. The increased availability of the BTA-EG_x molecules has provided us with the opportunity to probe the possible uses of these compounds through collaboration with several other research groups. This chapter highlights several of the collaborative efforts that showcase the potential biomedical applications and fundamental studies of BTA-EG_x compounds.

5.2 Microwave-assisted synthesis of BTA-EG₄ and BTA-EG₆

The synthetic route we describe for the preparation of BTA-EG_x compounds utilizes commercially available oligoethylene glycols as starting materials. We successfully applied the methodology to the synthesis of two specific members of the BTA-EG_x family: BTA-EG₄, which is derived from tetraethylene glycol, and BTA-EG₆, which is made from hexaethylene glycol (Figure 5.1). These two molecules were chosen as targets due to their demonstrated ability to bind aggregated A β peptides with high density;¹¹⁹ however, this methodology can, in principle, be exploited to prepare any BTA-EG_x molecule from the corresponding oligoethylene glycol.

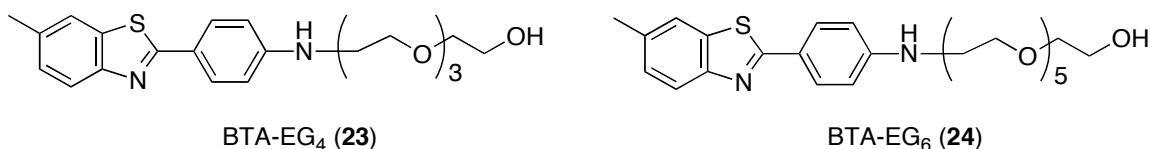
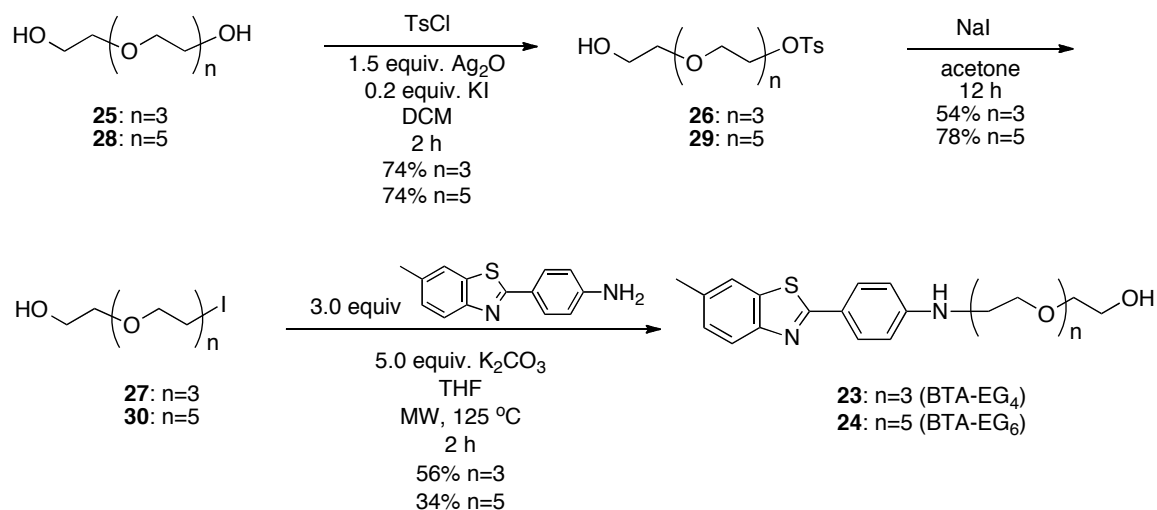


Figure 5.1: Structures of BTA-EG₄ (**23**) and BTA-EG₆ (**24**). BTA-EG₄ is synthesized using tetraethylene glycol as a starting material, while BTA-EG₆ is prepared from hexaethylene glycol.

The syntheses of BTA-EG₄ (**23**) and BTA-EG₆ (**24**), which are outlined in Scheme 5.1, begin with monotosylation of tetraethylene glycol **25** and hexaethylene glycol **26**, respectively. Although others have successfully monotosylated symmetric diols by using a large excess of the diol, we instead chose to prepare the desired intermediate using a protocol described by Bouzide and Sauv e.¹⁶⁰ Employing Ag₂O as the base affords the monotosylate in 74% yield and the di-tosylate as a minor side product. In addition to the high yield of desired product and the ease of purification,

introducing this synthetic step eliminates the need to use a large excess of diol, making it particularly suitable for monotosylation of costlier oligoethylene glycol starting materials in BTA-EG_x synthesis. The monotosylate is readily converted to the monoiodide via an S_N2 reaction with sodium iodide.



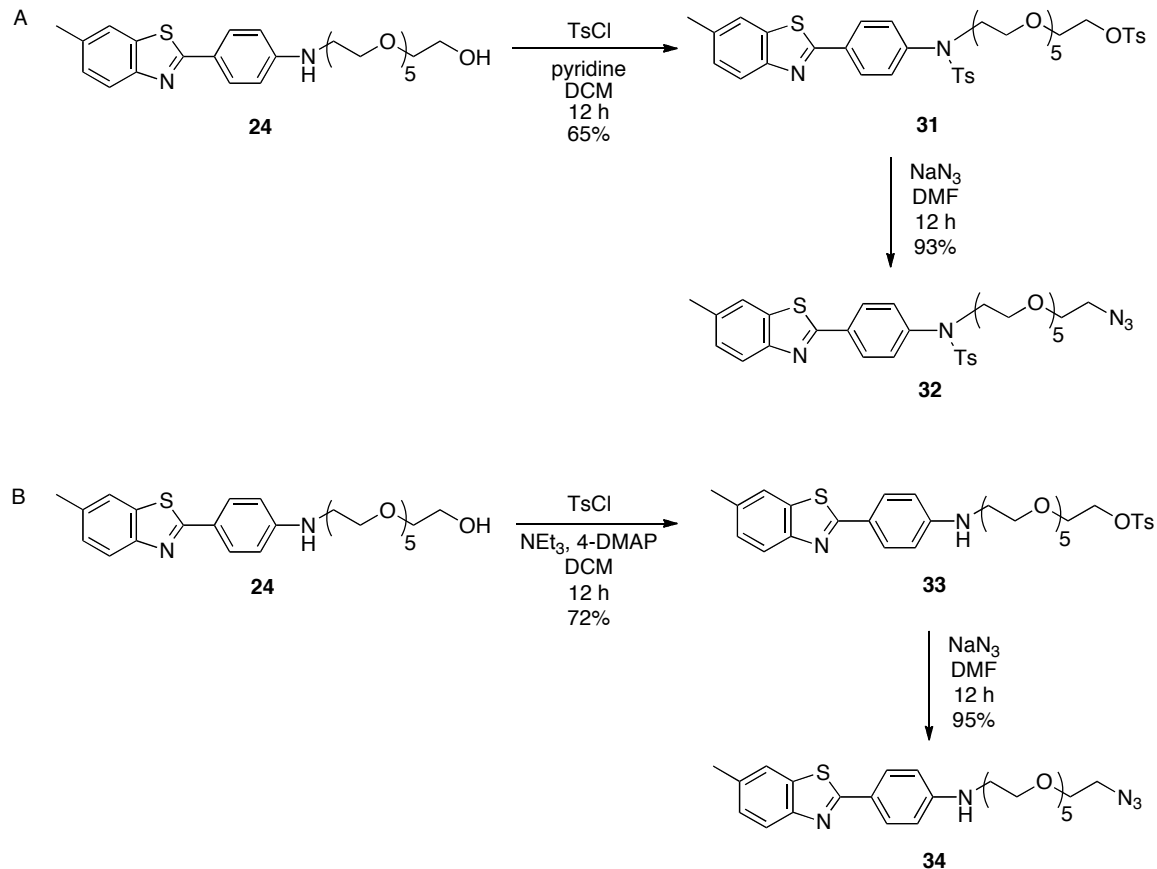
Scheme 5.1: Synthesis of BTA-EG₄ **23** and BTA-EG₆ **24** from tetraethylene glycol **25** and hexaethylene glycol **28**, respectively.

Substitution of BTA onto the monoiodide had been the most problematic step in the reaction sequence, and consequently required alteration to improve the overall efficiency of BTA-EG_x synthesis. Our previous attempts to affect this transformation result in low yields, even with reaction times of one week under reflux conditions. Instead of using conventional heated methods to affect the substitution reaction, we explored the possibility of using microwave-assisted synthesis¹⁶¹ to generate BTA-EG₄ and BTA-EG₆. Indeed, reacting BTA with the appropriate oligoethylene glycol monoiodide at 120°C in a microwave reactor resulted in a drastically increased yield of

BTA-EG₄ (from 25% to 56%) and a modest increase in yield for the BTA-EG₆ (from 25% to 34%) while lowering the reaction times from on the order of days to only two hours.

5.3 Further derivatization of BTA-EG₆

Upon successful preparation of the BTA-EG_x using microwave-assisted synthesis, we chose to evaluate the ease of further modification of the hydroxy terminus—specifically to the azide functionality—in order to create a BTA derivative compatible with CuAAC. In order to accomplish this transformation, we attempted to first convert the hydroxy group to the toluenesulfonyl ester. However, treating BTA-EG₆ **24** with 1.1 equivalents of toluenesulfonyl chloride and pyridine in DCM led to a significant sulfonamide formation at the aniline nitrogen. Indeed, adding 2.0 equivalents of toluenesulfonyl chloride to BTA-EG₆ with pyridine as the base led to complete consumption of the starting material and afforded the *N,O*-ditosylated product **31**, and subsequent substitution with sodium azide produce the hydrolytically stable sulfonamide **32** (Scheme 5.2A). Alternatively, treating BTA-EG₆ **24** with toluenesulfonyl chloride, triethylamine and catalytic 4-DMAP affords only toluenesulfonyl ester **33** in good yield. Azide **34** is readily prepared from toluenesulfonyl ester **33** via nucleophilic substitution (Scheme 5.2B). The azide derivative of BTA-EG₆ **34** is highly versatile, as it possesses click-compatible functionality and can covalently linked to a number of terminal alkyne containing partners. In addition, azide **34** can be easily converted to the primary amine via Staudinger reduction.^{155, 156}



Scheme 5.2: Tosylation of BTA-EG₆ **24** under different conditions. Treatment of BTA-EG₆ with TsCl in pyridine/DCM (A) affords the *N,O*-ditosylated product **31**, while using triethylamine/4-DMAP in DCM gives toluenesulfonyl ester **33** as the major product. Subsequent substitution of **31** and **33** with sodium azide affords the organoazide BTA derivatives **32** and **34**, respectively.

5.4 Blocking HIV-1 transmission with BTA-EG₆

Amyloid fibrils found in semen known as semen-derived enhancer of viral infection (SEVI) have been shown to enhance infectivity of HIV-1.¹⁶² Consequently, SEVI is a target for potential microbicidal agents that can decrease transmission of the virus. Our recent collaboration with Dewhurst and coworkers at the University of

Rochester explores the strategy of using BTA-EG₆ (**24**), a known amyloid-binding small molecule, to target SEVI and inhibit the infectivity of HIV (Figure 5.2).¹⁶³

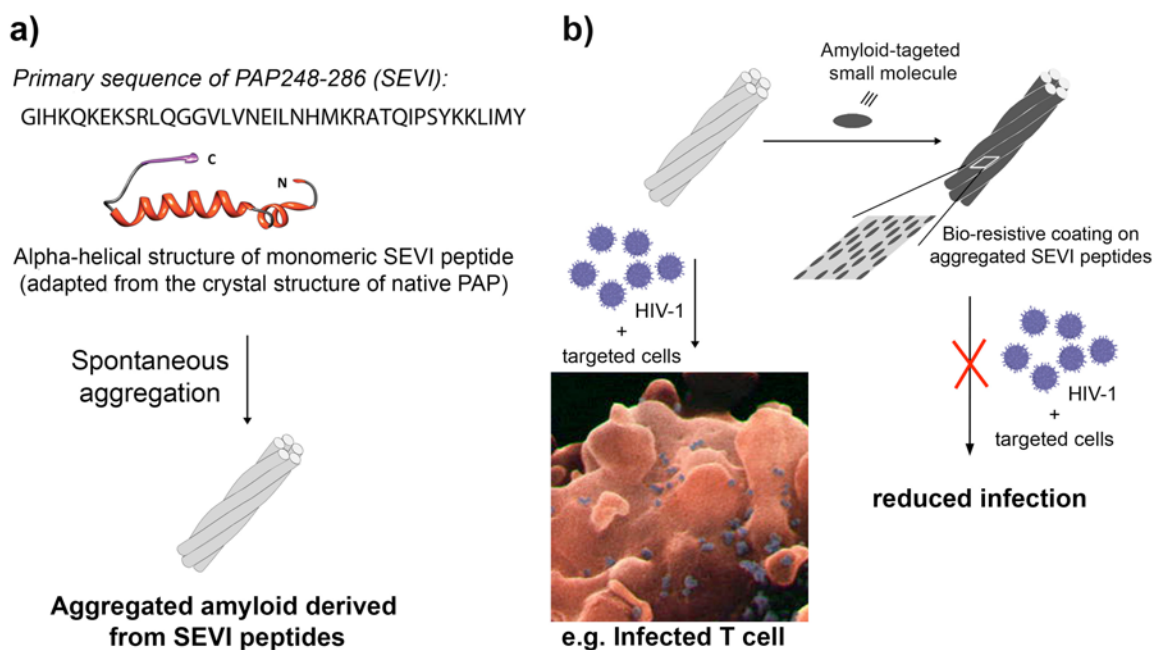


Figure 5.2: Schematic representation of the putative role of aggregated PAP248-286 peptides (also called SEVI peptides) in HIV-1 infection. a) Primary sequence and helical representation of PAP248-286 peptides;¹⁶⁴ these abundant peptides have been reported to spontaneously form aggregated amyloid fibrils in semen. b) Illustration of the SEVI amyloid-mediated infection of a T cell (pink/red) with HIV-1 (blue/purple).¹⁶⁵ Also depicted is the proposed method to attenuate SEVI-mediated infection by forming bio-resistive coatings on aggregated amyloids derived from PAP248-286.

In order to assess the viability of this approach, the binding affinity of BTA to SEVI fibrils was measured using a previously reported fluorescence-based assay (Figure 5.3).¹⁶⁶ This study demonstrated that BTA-EG₆ binds to SEVI fibrils with high affinity ($K_d = 127 \pm 22$ nM). In comparison, BTA-EG₆ has approximately the same binding affinity to AD-related A β ₁₋₄₂ ($K_d = 111 \pm 32$ nM). Accordingly, the extent of the interaction between BTA-EG₆ and SEVI prompted further investigation into the potential

of this targeting strategy. Indeed, it was found that BTA-EG₆ inhibits SEVI-mediated enhancement of HIV-1 infection in a dose-dependent manner (Figure 5.4A) with an IC₅₀ value of 13 μM. At high BTA-EG₆ concentrations (22.5 μg/mL), the infectivity of HIV was lowered to values only slightly higher than those detected in the absence of SEVI. Dewhurst and coworkers showed that BTA-EG₆ had no impact on the infectivity of the virus alone, implying that the reduction in infectivity is due to the interaction of BTA-EG₆ with SEVI rather than a result of general virus infectivity (Figure 5.4). In addition to its demonstrated inhibitive effect on SEVI-mediated infectivity of HIV-1, BTA-EG₆ is able to reduce the infection-enhancing properties of human semen (Figure 5.5). Treating pooled human semen samples with BTA-EG₆ inhibited semen-mediated infection at concentrations similar to those active against SEVI.

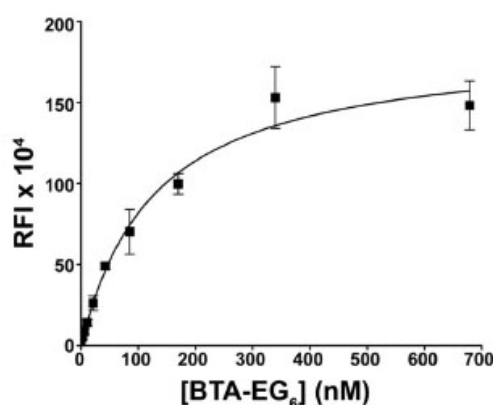


Figure 5.3: Binding of BTA-EG₆ to SEVI fibrils as determined by a previously reported centrifugation assay.¹⁶⁶ Briefly, various concentrations of BTA-EG₆ in PBS were incubated overnight at room temperature in the presence or absence of SEVI fibrils. After equilibration, each solution was centrifuged, and the supernatants were separated from the pelleted fibrils. The fluorescence of BTA-EG₆ was determined from the resuspended pellets in PBS solution. *Error bars* represent S.D. of duplicate measurements. The K_d was determined by fitting the data to a one-site specific binding algorithm: $Y = B_{\max}[X/(K_d+X)]$, where X is the concentration of BTA-EG₆, Y is the specific binding fluorescence intensity, and B_{\max} corresponds to the apparent maximal observable fluorescence upon binding of BTA-EG₆ to SEVI fibrils. *RFI*, relative fluorescence intensity.

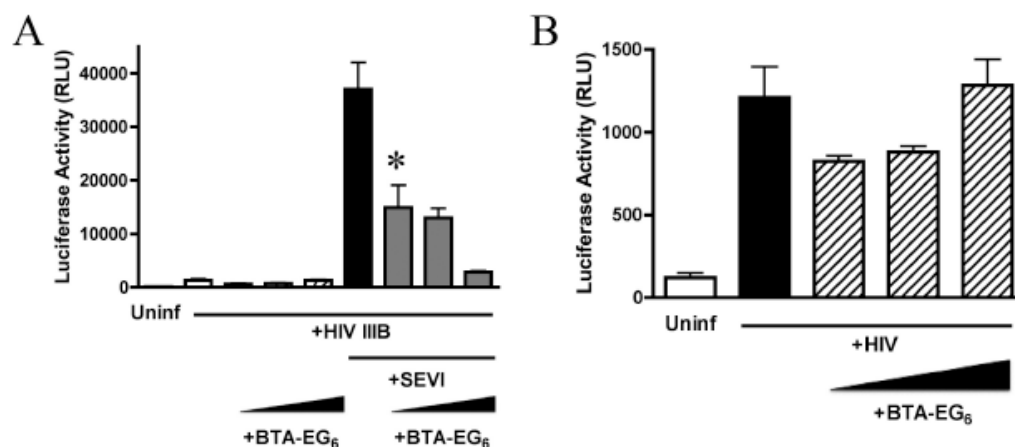


Figure 5.4: (A) HIV-1 III B virions were preincubated with increasing concentrations of BTA-EG₆ (**24**) (0, 5.5, 11, and 22.5 $\mu\text{g/ml}$) and with or without SEVI (15 $\mu\text{g/ml}$) as indicated. The samples were then added to CEM-M7 cells. Cells were washed at 2 h, and infection was assayed at 48 h by measuring Tat-driven luciferase expression. Results shown are average values \pm S.D. of triplicate measurements from one of four independent experiments that yielded equivalent results. * indicates $p < 0.05$ when compared with control cells exposed to HIV-1III B + SEVI alone by ANOVA with Tukey's post test. RLU, relative luciferase units; Uninf, uninfected. (B) B, zoom in of panel A to show data for cells treated with HIV-III B virions with and without increasing concentrations of BTA-EG₆, in the absence of SEVI. BTA-EG₆ had no effect on the infectivity of HIV alone; concentrations of BTA-EG₆ are noted above for panel A.

The inhibitive effect of BTA-EG₆ against both SEVI and semen mediated infectivity of HIV-1 makes it a potential candidate for addition to microbicide formulations that can be used to combat the spread of the virus. Furthermore, BTA-EG₆ exhibits no toxicity or inflammation to cervical cells, even after 24 hours of exposure at concentrations ten times the IC₅₀ (Figure 5.6). The non-toxic properties of BTA-EG₆ reinforces its potential as an ingredient in microbicide formulations, as it is well known that agents known to cause inflammation to cervical cells, such as the discontinued microbicide nonoxynol-9, may increase the risk of HIV transmission.^{167, 168} Accordingly,

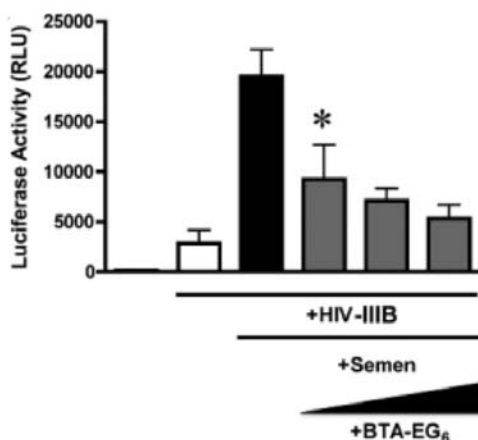


Figure 5.5: HIV-1III B virions were preincubated with 50% pooled human semen, with or without increasing concentrations of BTA-EG₆ (5.5, 11, and 22.5 µg/ml). After 10 min, these stocks were diluted 15-fold into CEM-M7 cells. Cells were washed after 1 h, and luciferase expression was measured at 48 h to quantify the extent of infection. Results shown are average values ± S.D. of triplicate measurements from one of three independent experiments that yielded equivalent results. * indicates $p < 0.05$ when compared with control cells exposed to HIV-1III B + semen alone, by ANOVA with Tukey's post test. RLU, relative luciferase units.

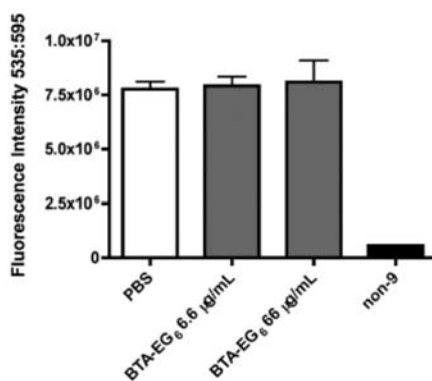


Figure 5.6: The cervical endothelial cell lines A2En (endocervical), 3EC1 (ectocervical), and SiHa were treated for 12 h with BTA-EG₆ at concentrations up to 10 times greater than the IC₅₀. Control cultures were treated with nonoxynol-9 (non-9) at 0.1% final concentration as a positive control for induction of cell death.¹⁶⁹ At 12 h, viability was measured by resazurin cytotoxicity assay (AlamarBlue™ assay). Representative results from A2En cells are shown; results from 3EC1 and SiHa cells were very similar (not shown).

BTA-EG₆ is a viable candidate for use as an antimicrobial agent for combating the spread of HIV-1 through sexual contact.

5.5 Self-assembled cation-selective ion channels formed from BTA-EG₄.

The formation of ion channels in cell membranes is critical for many biological properties including signal transduction and regulation of membrane potentials.^{170, 171} Accordingly synthetic molecules with ion-channel forming properties are garnering significant attention due to their potential use in biomedical applications. Because of its amphiphilic nature and demonstrated membrane permeability, we suspected that BTA-EG₄ might exhibit interesting activity in the presence of cell membranes. In collaboration with Mayer and coworkers at the University of Michigan, we explored the ion channel forming properties of BTA-EG₄.

Figure 5.7 shows that BTA-EG₄ indeed assembles into well-defined pores with quantized conductance levels at concentrations of 10 μ M in planar bilipid layers. These channels were found to have an average conductance of 37.8 ± 1.3 pS with an average lifetime of approximately 2 s in 1.0 M CsCl. Multiples of the main conductance level observed are presumably due to simultaneously open channels in the bilayer. The measured conductance values are only slightly less than those measured for the well-characterized pores formed by known ion channel-forming peptide gramicidin A under the same experimental conditions.^{172, 173} The pores formed by BTA-EG₄ **23** are selective for monovalent cations: while single-channel conductance values were measured for several alkali metal chlorides (Cs, K, Na and Li) and HCl, no single-channel conductance was observed in an electrolyte solution containing 1.0 M CaCl₂. Further investigation

into the behavior of the pores formed from BTA-EG₄ revealed that approximately four monomeric BTA-EG₄ are required to form the observed ion channels.

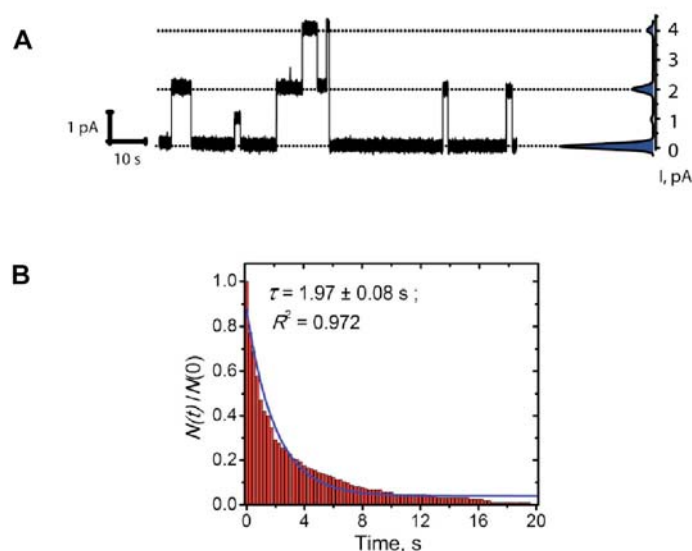


Figure 5.7: (A) Original current versus time trace from single ion channel recording through self-assembled pores from BTA-EG₄ in a planar lipid bilayer composed of 1,2-diphytanoyl-*sn*-glycero-3-phosphatidylcholine (DiphyPC) lipids. Histogram of current amplitudes reflects their number of occurrence in the corresponding current trace. (B) Normalized survival plot of the open channel lifetime determined from 174 single channel opening events under the same experimental conditions as in A). The average lifetime, τ , for BTA-EG₄ pores was determined from a fit of the histogram to the equation, $N(t)/N(0) = \exp(-t/\tau)$, where $N(t)$ represents the number of channels with lifetimes longer than the time t , and $N(0)$ represents the total number of channels with observable single conductance. BTA-EG₄ was added at a final concentration of 20 μM to both bilayer compartments, the applied voltage was +50 mV, and the electrolyte contained 1.0 M CsCl with 10 mM HEPES buffer, pH 7.4.

Because of the previously known antibiotic activity of the ion-channel forming peptide gramicidin A toward gram-positive bacteria,^{174, 175} the antibacterial effect of BTA-EG₄ was evaluated. Indeed, BTA-EG₄ retarded the growth of a strain of gram-positive bacteria (*Bacillus subtilis*) with an IC₅₀ value of 50 μM and completely suppressed growth at concentrations of 100 μM (Figure 5.8A). In addition, BTA-EG₄

was found to be toxic to SH-SY5Y human neuroblastoma cells in a dose-dependent manner with an IC_{50} value of 65 μM . Due to the ability of BTA-EG₄ to insert into cell membranes and exhibit similar toxicity as other ion channel-forming molecules suggests that the antibacterial activity and cellular toxicity of BTA-EG₄ may be directly related to its ability to form pores in cell membranes. Accordingly, the ion channel forming properties of BTA-EG₄ may shed light on both its mechanism of action and its potential utility (and drawbacks) for drug delivery and other biomedical applications.

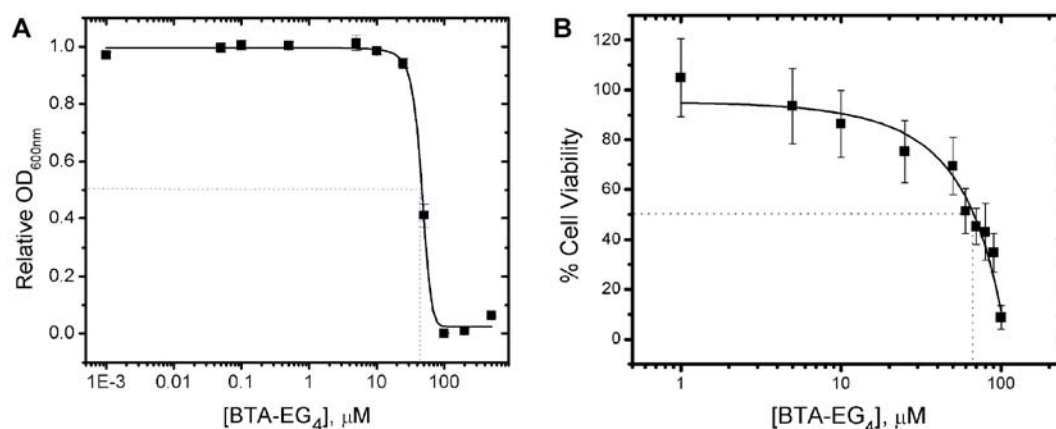


Figure 5.8: (A) Inhibitory effect of BTA-EG₄ **23** on the growth of *Bacillus subtilis* bacteria 22 h after exposure to LB media containing various concentrations of BTA-EG₄. Growth was quantified by the optical density at a wavelength of 600 nm relative to untreated control cells. The concentration of BTA-EG₄ molecules that inhibited growth by 50% (IC_{50} values) was 50 μM . Each point represents the mean of 2 experiments with 3 replicates in each experiment; error bars represent the standard error of the mean. (B) Cytotoxicity of BTA-EG₄ on human neuroblastoma (SH-SY5Y) cells 24 h after exposure. Each point represents the mean of 2 or 3 experiments with 6 replicates in each experiment. Error bars reflect the standard error of the mean. The IC_{50} value was 65 μM .

5.6 Chapter Summary

Through the use of microwave-assisted chemistry, we have developed an improved synthesis for BTA-EG₄ and BTA-EG₆—two demonstrated amyloid-binding

molecules—and a general methodology to efficiently access the BTA-EG_x family of compounds. The increased availability of BTA-EG₄ and BTA-EG₆ has led to several collaborative efforts geared toward investigating the properties and potential applications of these compounds. In addition to its previously known ability to bind Alzheimer's-related A β , BTA-EG₆ was found to be a possible candidate for antimicrobial formulations used to combat the sexual transmission of HIV-1 due to its ability to inhibit SEVI and semen-mediated infectivity of the virus. BTA-EG₄ was found to form monovalent cation selective pores in lipid membranes—a finding which may explain the mechanism of its antibacterial activity and cellular toxicity. Other collaborations involving BTA-EG_x are exploring their use as dendritic spine density promoters for the treatment of Alzheimer's disease. The ability to produce both known and novel derivatives of BTA-EG_x compounds in an easy and highly efficient manner will provide the quantities of material necessary to further explore their properties and may potentially lead to the discovery of a myriad of additional biomedical applications for these exceptional molecules.

5.7 Experimental methods

All synthetic reagents were from Aldrich, Fisher Scientific, Alfa Aesar, or Fluka, and were used without further purification. All solvents used for reactions were obtained from Fisher scientific and dried on Alumina columns prior to use. Solvents used for chromatography were ACS technical grade and used without further purification. Water (18.2 $\mu\Omega$ /cm) was filtered through a NANOPure DiamondTM (Barnstead) water

purification system before use. Microwave synthesis was performed with a Biotage Initiator Microwave synthesizer using high-pressure vessels.

All NMR spectra of BTA-EG_x compounds and precursors were recorded on a Varian Mercury Plus 400 MHz NMR spectrometer in CDCl₃. Low resolution MS analysis was performed on a ThermoFinnigan LCQdeca mass spectrometer with an atmospheric pressure electrospray ionization (APCI) source or an electrospray ionization (ESI) source. High resolution MS analysis was performed on a Thermo Scientific LTQ Orbitrap XL mass spectrometer with an electrospray ionization source.

2-(2-(2-(2-hydroxyethoxy)ethoxy)ethoxy)ethyl toluenesulfonate (26)

In a clean, dry 1L roundbottom flask equipped with a stirbar, tetraethylene glycol (10.0 g, 51.5 mmol) was dissolved in 500mL dry DCM and stirred at room temperature. After 5 minutes, KI (1.71 g, 10.3 mmol), Ag₂O (17.9 g, 77.2 mmol), and *p*-toluenesulfonyl chloride (10.8 g, 56.6 mmol) were successively added to the reaction flask. The reaction mixture was stirred vigorously for 2 h, filtered through celite to remove the solids and concentrated *in vacuo*. The residue was purified via silica column chromatography (100% DCM to 95:5 DCM:CH₃OH) giving 2-(2-(2-(2-hydroxyethoxy)ethoxy)ethoxy)ethyl toluenesulfonate as a colorless oil (13.2 g, 74%). ¹H-NMR (400 MHz, CDCl₃): δ = 7.74 (d, 8.0 Hz, 2H), 7.30 (d, 8.0 Hz, 2H), 4.11 (t, 4.8 Hz, 2H), 3.66-3.53 (m, 12H), 2.79 (s, 1H), 2.39 (s, 3H). ¹³C-NMR (100 MHz, CDCl₃): δ = 145.04, 133.17, 130.10 (2C), 128.19 (2C), 70.95, 70.79, 70.70, 69.49, 68.88, 21.87. ESI-MS (*m/z*) calcd for C₁₅H₂₄O₇S [M]⁺ 348.1243; found [M+H]⁺ 348.96, [M+NH₄]⁺ 365.94 and [M+Na]⁺ 371.08.

2-(2-(2-(2-iodoethoxy)ethoxy)ethoxy)ethanol (27)

2-(2-(2-(2-hydroxyethoxy)ethoxy)ethoxy)ethyl toluenesulfonate (12.01 g, 234.5 mmol), sodium iodide (207 g, 137.9 mmol) and 200 mL dry acetone were combined in a clean, dry roundbottom flask and heated to reflux with vigorous stirring. After 12h the reaction was cooled to room temperature and diluted with 100 mL ethyl acetate. The organic phase was washed with 10% Na₂S₂O₃, (2 x 10 mL), DI H₂O (1 x 20 mL), saturated NaCl (1 x 20 mL), dried over anhydrous Na₂SO₄, filtered, and concentrated *in vacuo* giving 2-(2-(2-(2-iodoethoxy)ethoxy)ethoxy)ethanol as a pale yellow oil (5.61 g, 54%). ¹H-NMR (400 MHz, CDCl₃): δ = 3.73-3.58 (m, 14H), 3.24 (t, 2H), 2.59 (s, 1H). ¹³C-NMR (100 MHz, CDCl₃): δ = 72.70, 72.19, 70.90, 70.76, 70.58, 70.39, 61.94, 3.07.

BTA-EG₄ (23)

A microwave reaction tube was charged with 2-(2-(2-(2-iodoethoxy)ethoxy)ethoxy)ethanol (1.47 g, 4.83 mmol), benzothiazole aniline (3.49 g, 14.5 mmol), potassium carbonate (3.34 g, 24.2 mmol) and 20 mL dry THF. The tube was then equipped with a small stirbar, sealed and placed in a microwave reactor. The reaction was heated at 125 °C for 2h. The reaction was cooled to room temperature and filtered to remove the solids. The solids washed several times with DCM until the filtrate was colorless. The combined organic layers were concentrated *in vacuo* and purified by column chromatography to give the desired BTA-EG₄ compound as a yellow solid. (1.13g, 56%). ¹H-NMR (400 MHz, CDCl₃): δ = 7.87 (d, 8.8 Hz, 2H), 7.83 (d, 8.4 Hz, 1H) 7.63 (s, 1H) 7.23 (d, 8.4 Hz, 1H), 6.68 (d, 8.8 Hz, 2H), 3.76-3.64 (m, 14H), 3.37 (t, 5.2 Hz, 2H), 2.47 (s, 3H). ¹³C-NMR (100 MHz, CDCl₃): δ = 168.03, 152.64, 150.92,

134.87, 134.47, 129.13 (2C), 127.70, 122.88, 122.03, 121.41, 112.82 (2C), 72.86, 70.88, 70.69, 70.43 (2C), 69.64, 61.91, 43.32, 21.70. HR-ESI-MS (m/z) calcd for $C_{22}H_{28}N_2O_4SNa$ $[M+Na]$ 439.1662; found $[M+Na]^+$ 439.1660.

17-hydroxy-3,6,9,12,15-pentaoxaheptadecyl toluenesulfonate (29)

In a clean, dry 1L roundbottom flask equipped with a stirbar, hexaethylene glycol (15.0 g, 53.1 mmol) was dissolved in 500mL dry DCM and stirred at room temperature. After 5 minutes, KI (1.76 g, 10.6 mmol), Ag_2O (18.5 g, 79.7mmol), and *p*-toluenesulfonyl chloride (11.1 g, 58.4 mmol) were successively added to the reaction flask. The reaction mixture was stirred vigorously for 2 h, filtered through celite to remove the solids and concentrated *in vacuo*. The residue was purified via silica column chromatography (100% DCM to 97:3 DCM:CH₃OH) giving 2-(2-(2-(2-hydroxyethoxy)ethoxy)ethoxy)ethyl toluenesulfonate as a colorless oil (15.2 g, 74%). ¹H-NMR (400 MHz, CDCl₃): δ = 7.79 (d, 8.4 Hz, 2H), 7.34 (d, 8.0 Hz, 2H), 4.16 (t, 4.8 Hz, 2H), 3.71-3.58 (m, 22H), 2.45 (s, 3H). ESI-MS (m/z) calcd for $C_{19}H_{32}O_9S$ $[M]^+$ 436.1767; found $[M+H]^+$ 437.00 and $[M+Na]^+$ 459.08.

17-iodo-3,6,9,12,15-pentaoxaheptadecan-1-ol (30)

17-hydroxy-3,6,9,12,15-pentaoxaheptadecyl toluenesulfonate **29** (15.2 g, 34.8 mmol), sodium iodide (15.6 g, 104.3 mmol) and 300 mL dry acetone were combined in a clean, dry roundbottom flask and heated to reflux with vigorous stirring. After 12 h the reaction was cooled to room temperature, filtered and the solids washed with acetone. The filtrate was concentrated *in vacuo* and redissolved in 300 mL ethyl acetate. The

organic phase was washed with 10% Na₂S₂O₃, (2 x 10 mL), DI H₂O (1 x 30 mL), saturated NaCl (1 x 30 mL), dried over anhydrous Na₂SO₄, filtered, and concentrated *in vacuo* giving 17-iodo-3,6,9,12,15-pentaoxaheptadecan-1-ol (**30**) as a pale yellow oil (10.6 g, 78%). ¹H-NMR (400 MHz, CDCl₃): δ = 3.77-3.60 (m, 22H), 3.25 (t, 7.2 Hz, 2H), 2.97 (s, 1H). ¹³C-NMR (100 MHz, CDCl₃): δ = 72.85, 72.18, 70.86, 70.81, 70.78, 70.76, 70.75, 70.73, 70.46, 70.37, 61.93, 3.23. ESI-MS (*m/z*) calcd for C₁₂H₂₅IO₆ [M]⁺ 392.0696; found [M+H]⁺ 393.10, [M+NH₄]⁺ 410.01 and [M+Na]⁺ 415.04.

BTA-EG₆ (24)

17-iodo-3,6,9,12,15-pentaoxaheptadecan-1-ol (10.62 g, 27.1 mmol), benzothiazole aniline (19.51 g, 81.2 mmol), potassium carbonate (18.71 g, 135.4 mmol) were split into two batches. Two identical microwave reaction tubes were charged with 17-iodo-3,6,9,12,15-pentaoxaheptadecan-1-ol (5.31 g, 13.55 mmol), benzothiazole aniline (9.76 g, 40.6 mmol), potassium carbonate (9.36 g, 24.2 mmol) and 9 mL dry THF. The tubes were then equipped with a small stirbar, sealed and placed in a microwave reactor. The reaction was heated at 125 °C for 2h, cooled to room temperature and filtered to remove the solids. The solids washed several times with several portions of DCM and the combined organic layers were concentrated *in vacuo*. Purification by column chromatography gave the desired BTA-EG₆ compound as a tacky yellow oil. (4.16 g, 34%). ¹H-NMR (400 MHz, CDCl₃): δ = 7.83-7.79 (m, 3H), 7.54 (s, 1H), 7.17 (dd, 8.8 Hz, 1.0 Hz, 1H), 6.61 (d, 8.8 Hz, 2H), 3.67-3.51 (m, 24H), 3.28 (t, 5.2 Hz, 2H), 2.39 (s, 3H). ¹³C-NMR (100 MHz, CDCl₃): δ = 168.04, 151.82, 151.03, 134.50, 134.29, 129.14 (2C), 127.80, 121.93, 121.65, 121.39, 112.68 (2C), 72.73, 70.64 (6C), 70.40 (2C),

69.35, 61.61, 43.16, 21.63. HR-ESI-MS (m/z) calcd for $C_{26}H_{36}N_2O_6SNa$ $[M+Na]^+$ 527.2186; found $[M+Na]^+$ 527.2184.

17-(4-methyl-*N*-(4-(6-methylbenzothiazol-2-yl)phenyl)phenyl)sulfonamido)

3,6,9,12,15-pentaoxaheptadecyl toluenesulfonate (31)

In a clean, oven-dried 100 mL round bottom flask, BTA-EG₆ **24** (1.15 g, 2.28 mmol) was dissolved in 20 mL DCM. The flask was cooled on an ice bath to 0°C and pyridine (361 mg, 367 μ L, 4.56 mmol) was added. After 10 min, *p*-toluenesulfonyl chloride (652 mg, 3.52 mmol) was added to the reaction flask and the contents were allowed to warm up to room temperature while stirring. After 12 h, the contents of the reaction flask were concentrated in vacuo and immediately purified via flash chromatography (100% DCM to 95:5 DCM:methanol) to afford a pale yellow oil (902 mg, 65%). ¹H-NMR (400 MHz, CDCl₃): δ = 7.99 (d, 8.4 Hz, 2H), 7.92 (d, 8.4 Hz, 1H), 7.78 (d, 8.4 Hz, 2H), 7.69 (s, 1H), 7.49 (d, 8.4 Hz, 2H), 7.33-7.18 (m, 7H), 4.14 (t, 3.2 Hz, 2H), 3.77 (t, 6.4 Hz, 2H), 3.67-3.53 (m, 20H), 2.50 (s, 3H), 2.42 (s, 3H), 2.41 (s, 3H). ¹³C-NMR (100 MHz, CDCl₃): δ = 165.94, 152.42, 145.01, 143.93, 142.04, 135.90, 135.53, 135.28, 133.26, 133.15, 130.04 (2C), 129.77 (2C), 129.40 (2C), 128.33, 128.20 (2C), 128.17 (2C), 127.89, 123.00, 121.65, 70.93, 70.78 (2C), 70.73 (2C), 70.69, 70.67, 70.60, 69.47, 69.20, 68.88, 60.64, 50.32, 21.88, 21.82, 21.81. ESI-MS (m/z) calcd for $C_{40}H_{48}N_2O_{10}S_3$ $[M]^+$ 812.2471; found $[M+H]^+$ 813.2 and $[M+Na]^+$ 835.2.

17-azido-*N*-(4-(6-methylbenzothiazol-2-yl)phenyl)-3,6,9,12,15-pentaoxaheptadecan-1-amine (32)

A clean, oven-dried roundbottom flask was charged with *N,O*-ditosylated compound **31** (884 mg, 1.34 mmol), NaN₃ (262 mg, 4.03 mmol) and 5 mL dry DMF and allowed to stir at 70°C. After 12 h., the contents of the reaction flask were diluted with 100 mL Et₂O and washed with DI H₂O (2 x 10 mL), saturated NaCl (1 x 10 mL), dried over anhydrous Na₂SO₄, filtered, and concentrated *in vacuo* to afford organoazide **32** as a yellow oil (688mg, 93%). ¹H-NMR (400 MHz, CDCl₃): δ = 7.99 (d, 8.4 Hz, 2H), 7.92 (d, 8.4 Hz, 1H), 7.69 (s, 1H), 7.49 (d, 8.4 Hz, 2H), 7.31-7.18 (m, 5H), 3.77 (t, 6.4 Hz, 2H), 3.73-3.53 (m, 20H), 3.36 (t, 4.8 Hz, 2H), 2.49 (s, 3H), 2.41 (s, 3H). ¹³C-NMR (100 MHz, CDCl₃); δ = 165.94, 152.44, 143.92, 142.07, 135.90, 135.54, 135.31, 133.27, 129.77 (2C), 129.40 (2C), 128.33, 128.18 (2C), 127.91 (2C), 123.02, 121.65, 70.90, 70.86, 70.83, 70.81, 70.79, 70.77, 70.69, 70.62, 70.24, 69.23, 50.89, 50.32, 21.83, 21.81. ESI-MS (*m/z*) calcd for C₃₃H₄₁N₅O₇S₂ [M]⁺ 683.2447; found [M+H]⁺ 684.22 and [M+Na]⁺ 706.19.

17-((4-(6-methylbenzothiazol-2-yl)phenyl)amino)-3,6,9,12,15-pentaoxaheptadecyl toluenesulfonate (33)

In a clean, oven-dried 25 mL roundbottom flask, BTA-EG₆ **24** (440 mg, 872 μmol) was dissolved in 5 mL dry DCM. The flask was cooled on an ice bath to 0°C and triethylamine (106 mg, 146 μL, 1.05 mmol) and 4-DMAP (21.3 mg, 174 μmol) were added. After 5 min, *p*-toluenesulfonyl chloride (199 mg, 1.05 mmol) was added to the reaction flask and the contents were allowed to stir at 0°C for an additional hour. The

reaction was then concentrated *in vacuo* and immediately purified via flash chromatography (100% DCM to 95:5 DCM:methanol) to afford **33** as a yellow oil (417 mg, 72%) ¹H-NMR (400 MHz, CDCl₃): δ = 7.87 (d, 8.8 Hz, 2H) 7.84 (d, 8.4 Hz, 1H), 7.78 (d, 8.4 Hz, 2H), 7.63 (m, 1H), 7.31 (d, 8.4 Hz, 2H) 7.23 (d, 8.4 Hz, 1H), 6.66 (d, 8.8 Hz, 2H), 4.14 (t, 5.2 Hz, 2H), 3.73 (t, 5.2 Hz, 2H), 3.66-3.57 (m, 19H), 3.37 (m, 2H), 2.47 (s, 3H), 2.42 (s, 3H). ¹³C-NMR (100 MHz, CDCl₃): δ = 167.96, 152.63, 150.79, 145.01 134.86, 134.51, 133.18, 130.04 (2C), 129.12 (2C), 128.19 (2C), 127.73, 122.93, 122.04, 121.43, 112.79 (2C), 70.94, 70.83-70.72 (7C), 70.56, 69.53, 68.89, 43.31, 21.87, 21.71. ESI-MS (*m/z*) calcd for C₃₃H₄₂N₂O₈S₂ [M]⁺ 658.2383; found [M+H]⁺ 659.27 and [M+Na]⁺ 681.23.

***N*-(17-azido-3,6,9,12,15-pentaoxaheptadecyl)-4-methyl-*N*-(4-(6-methylbenzothiazol-2-yl)phenyl)benzenesulfonamide (34)**

A clean, oven-dried roundbottom flask was charged with *N,O*-ditosylated compound **31** (414 mg, 628 μmol), NaN₃ (123 mg, 1.89 mmol) and 5 mL dry DMF and allowed to stir at 70°C. After 12 h., the contents of the reaction flask were diluted with 100 mL Et₂O and washed with DI H₂O (2 x 10 mL), saturated NaCl (1 x 10 mL), dried over anhydrous Na₂SO₄, filtered, and concentrated *in vacuo* to afford organoazide **34** as a yellow oil (316 mg, 95%). ¹H-NMR (400 MHz, CDCl₃): δ = ¹H-NMR (400 MHz, CDCl₃): δ = 7.88 (d, 8.4 Hz, 2H), 7.84 (d, 8.4 Hz, 1H), 7.63 (s, 1H), 7.23 (d, 8.4 Hz, 1H), 6.66 (d, 8.4 Hz, 2H), 4.74 (s, 1H) 3.77-3.63 (m, 23H), 3.34 (t, 5.2 Hz, 2H), 2.47 (s, 3H). ¹³C-NMR (100 MHz, CDCl₃): δ = 167.99, 152.62, 150.80, 134.85, 134.51, 129.13 (2C), 127.73, 122.91, 122.03, 121.43, 112.79 (2C), 70.89-70.78 (5C), 70.55, 70.24, 69.54,

50.88, 43.31, 21.72. HR-ESI-MS (m/z) calcd for $C_{26}H_{36}N_5O_5S$ $[M+H]^+$ 530.2432; found $[M+H]^+$ 530.2433.

Notes about this chapter

This contains material that appears in "Amyloid binding small molecules efficiently block SEVI (semen-derived enhancer of infection) and semen mediated enhancement of HIV-1 infection." Olsen, J. S.; Brown, C.; Capule, C. C.; Rubinshtein, M.; Doran, T. M.; Srivastava, R. K.; Feng, C.; Nilsson, B. L.; Yang, J.; Dewhurst, S. J. *Biol. Chem.* **2010**, 285, 35488-35496. I am a co-author on this paper. Additionally, this chapter contains material as it may appear in a paper recently submitted for publication: "Self-assembled, cation-selective ion channels from oligo(ethylene glycol) derivatives of benzothiazole aniline." Prangkio, P.; Rao, D.; Lance, K.; Rubinshtein, M.; Yang, J.; Mayer, M. I am a co-author on this paper.

Appendix A

Light scattering and differential refractive index data for 5a-5d

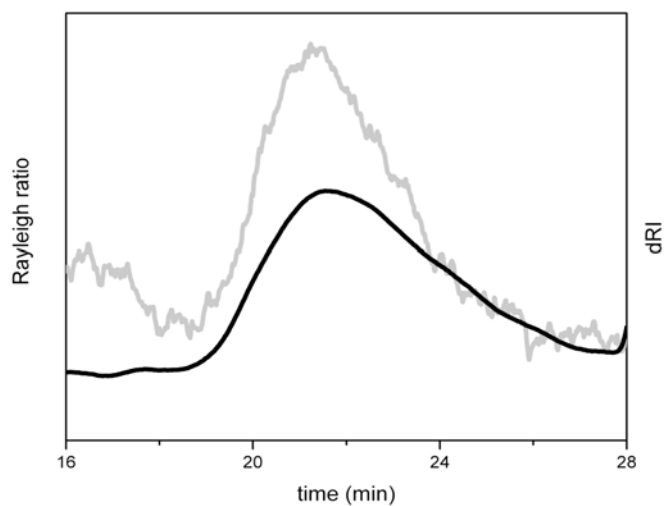


Figure A.1. Size exclusion chromatogram of unfractionated polymer **6a** monitored by light scattering (gray) and differential refractive index (black) from retention times of 18-28 minutes. This data was used to calculate M_n and M_w/M_n (PDI) of the sample using ASTRA software, Wyatt Technologies, Santa Barbara, CA. This polymeric species had a value of $M_n = 27.4 \times 10^4$ g/mol and a PDI of 1.19.

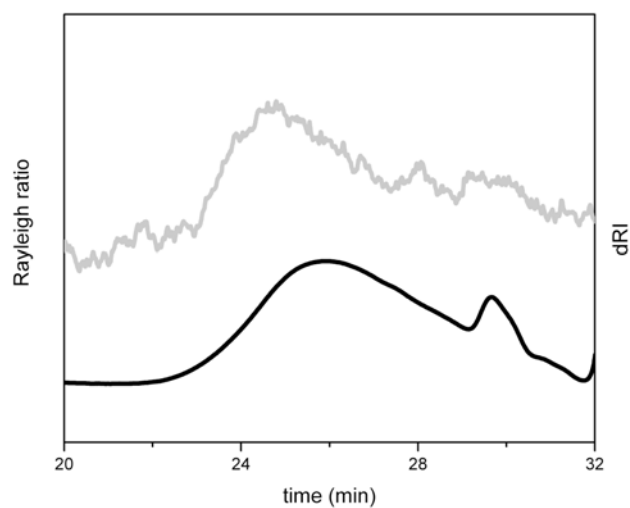


Figure A.2. Size exclusion chromatogram of alkyne-functionalized polymer **6b** monitored by light scattering (gray) and differential refractive index (black) from retention times of 20-32 minutes. This data was used to calculate the value M_n and M_w/M_n (PDI) of the sample using ASTRA software, Wyatt Technologies, Santa Barbara, CA. This polymeric species had a value of $M_n = 22.6 \times 10^4$ g/mol and a PDI of 1.11.

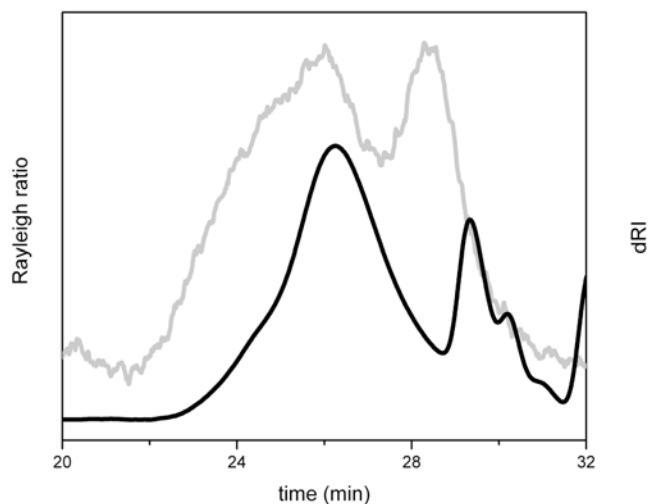


Figure A.3. Size exclusion chromatogram of azide-functionalized polymer **6c** monitored by light scattering (gray) and differential refractive index (black) from retention times of 20-32 minutes. This data was used to calculate the value M_n and M_w/M_n (PDI) of the sample using ASTRA software, Wyatt Technologies, Santa Barbara, CA. This chromatogram shows at least two main populations of polymers; the polymer represented by the peak at ~26 minutes had a value of $M_n = 34.5 \times 10^4$ g/mol and a PDI of 1.12, while the polymeric species represented by the peak at ~29.5 minutes (plus the shoulder peak) had a value of $M_n = 38.8 \times 10^4$ g/mol and a PDI of 1.27.

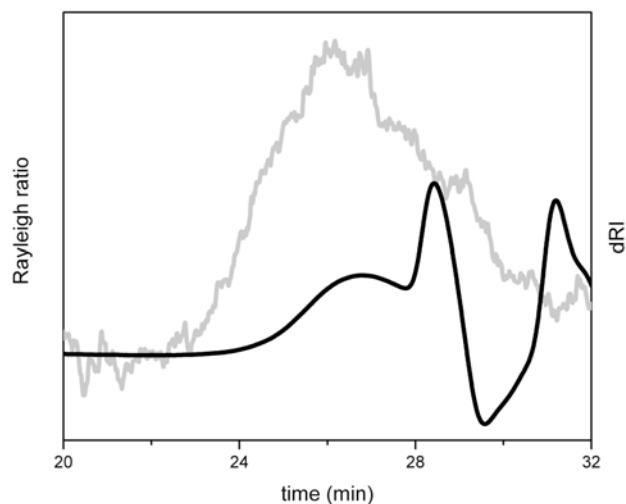


Figure A.4. Size exclusion chromatogram of oligoethylene glycol/azide-functionalized polymer **6d** monitored by light scattering (gray) and differential refractive index (black) from retention times of 20-32 minutes. This data was used to calculate the value M_n and M_w/M_n (PDI) of the sample using ASTRA software, Wyatt Technologies, Santa Barbara, CA. This chromatogram shows two populations of polymers; the polymer represented by the broad peak at ~ 26.5 min had a value of $M_n = 23.1 \times 10^4$ g/mol and a PDI of 1.17, while the polymer represented by the narrower peak at ~ 28.5 min had a value of $M_n = 7.38 \times 10^3$ g/mol and a PDI of 1.23.

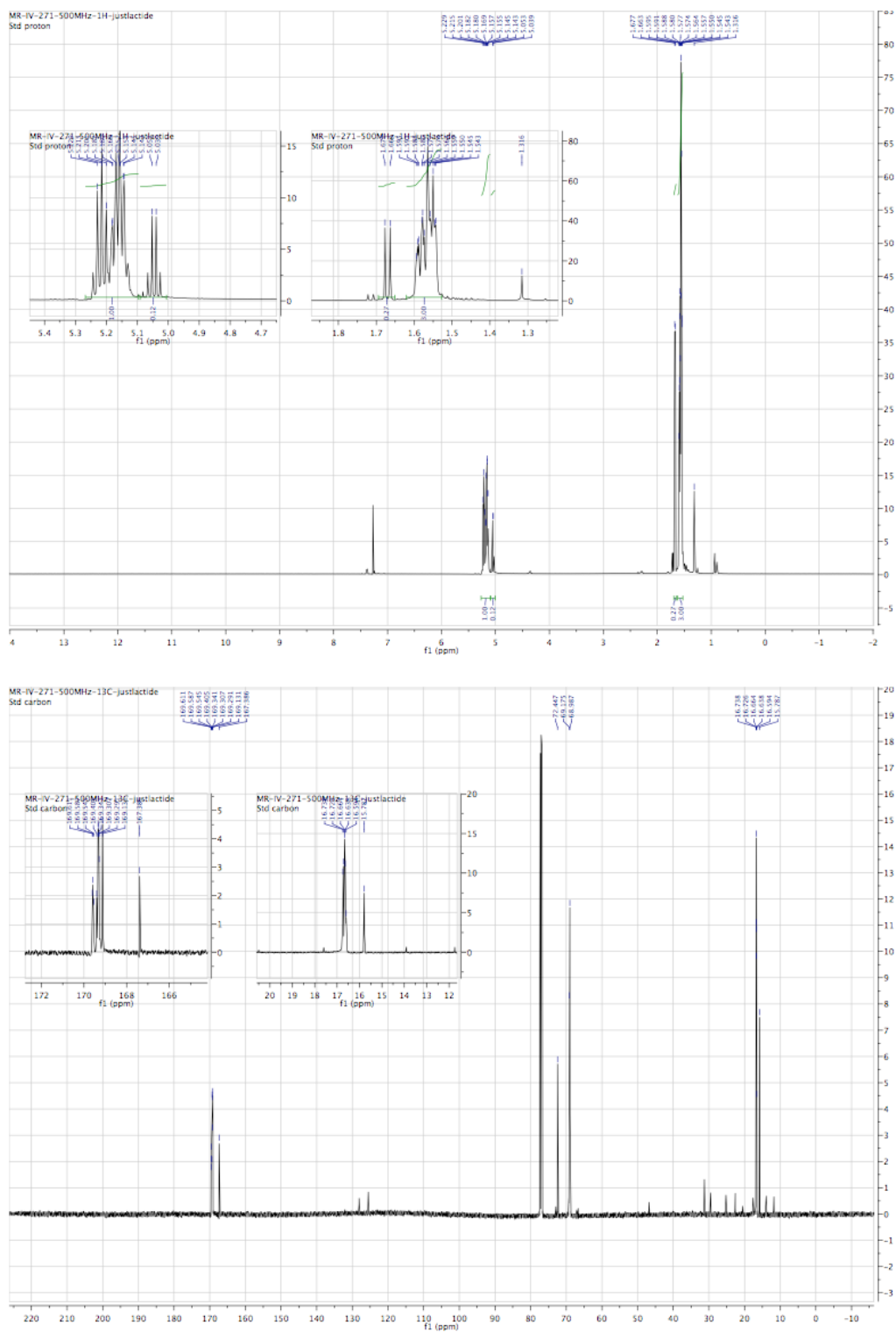


Figure A.5: ^1H and ^{13}C NMR spectral data for crude polymer **6a**.

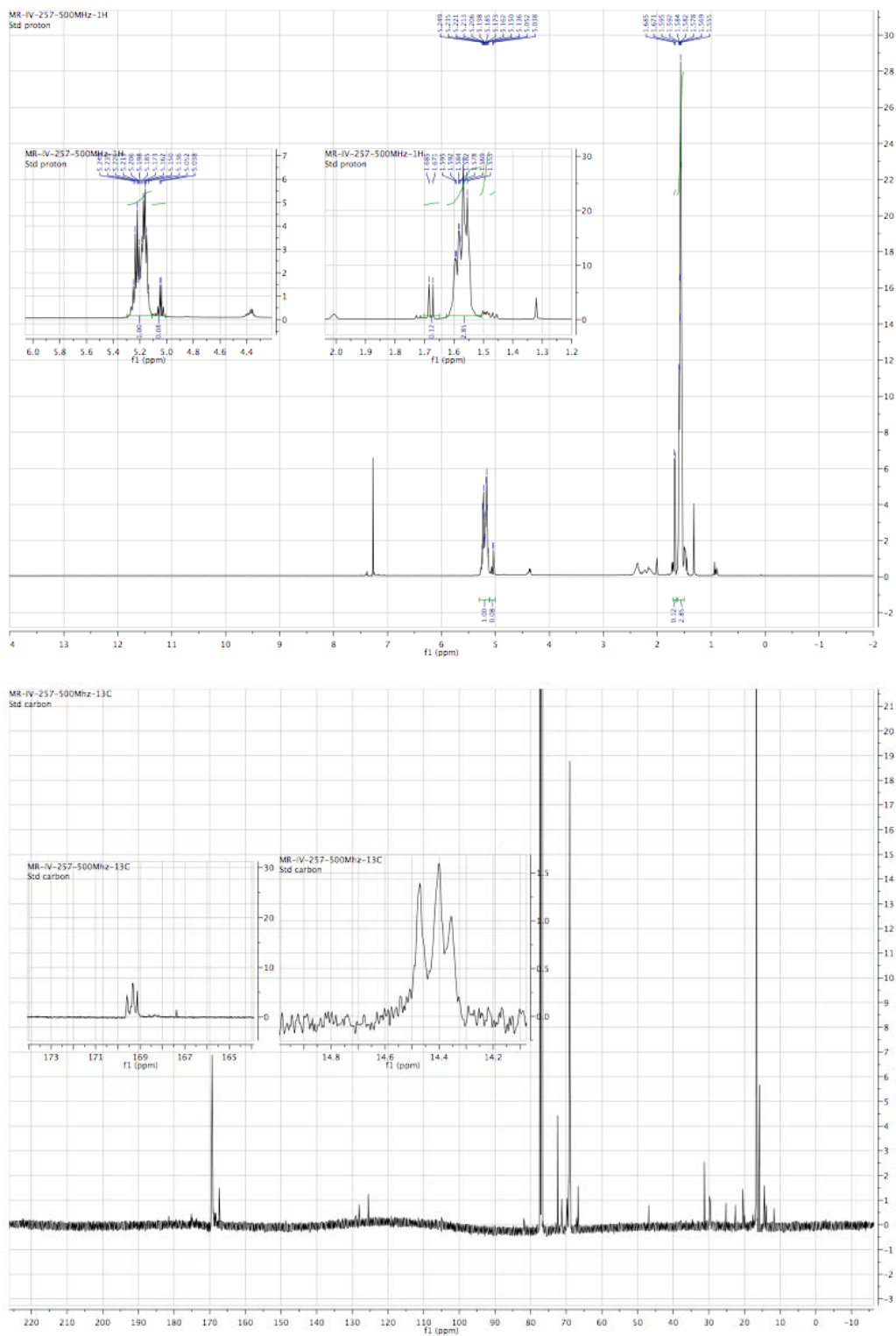


Figure A.6: ^1H and ^{13}C NMR spectral data for crude polymer **6b**.

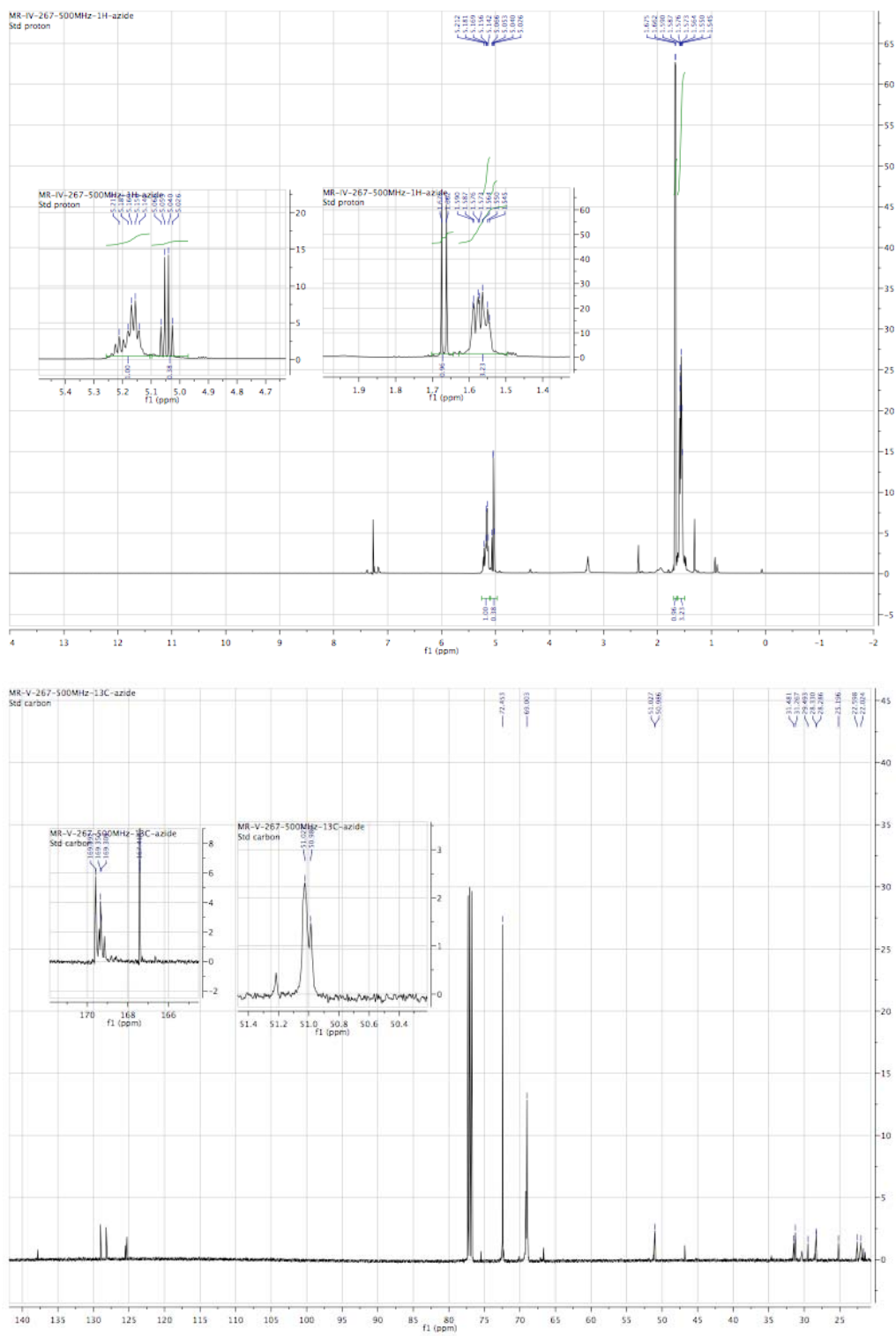


Figure A.7. ^1H and ^{13}C NMR spectral data for crude polymer **6c**.

REFERENCES

1. Lunt, J., Large-scale production, properties and commercial applications of polylactic acid polymers. *Polymer Degradation and Stability* **1998**, *59* (1-3), 145-152.
2. Drumright, R.; Gruber, P.; Henton, D., Polylactic acid technology. *Advanced Materials* **2000**, *12*, 1841-1846.
3. Siracusa, V.; Rocculi, P.; Romani, S.; Rosa, M. D., Biodegradable polymers for food packaging: a review. *Trends in Food Science & Technology* **2008**, *19* (12), 634-643.
4. Jarosiewicz, A.; Tomaszewska, M., Controlled-release NPK fertilizer encapsulated by polymeric membranes. *Journal of Agricultural and Food Chemistry* **2003**, *51* (2), 413-417.
5. Zhao, J.; Wilkins, R. M., Low molecular weight polylactic acid as a matrix for the delayed release of pesticides. *Journal of Agricultural and Food Chemistry* **2005**, *53* (10), 4076-4082.
6. Gilding, D. K.; Reed, A. M., Biodegradable Polymers for Use in Surgery - Poly(Ethylene Oxide) Poly(Ethylene-Terephthalate) (Peo-Pet) Copolymers .1. *Polymer* **1979**, *20* (12), 1454-1458.
7. Reed, A. M.; Gilding, D. K., Biodegradable Polymers for Use in Surgery - Poly(Glycolic)-Poly(Lactic Acid) Homo and Co-Polymers .2. Invitro Degradation. *Polymer* **1981**, *22* (4), 494-498.
8. Langer, R., Biomaterials in drug delivery and tissue engineering: One laboratory's experience. *Accounts of Chemical Research* **2000**, *33* (2), 94-101.
9. Temenoff, J. S.; Mikos, A. G., Injectable biodegradable materials for orthopedic tissue engineering. *Biomaterials* **2000**, *21* (23), 2405-2412.
10. Agrawal, C. M.; Ray, R. B., Biodegradable polymeric scaffolds for musculoskeletal tissue engineering. *Journal of Biomedical Materials Research* **2001**, *55* (2), 141-150.
11. Martina, M.; Hutmacher, D. W., Biodegradable polymers applied in tissue engineering research: a review. *Polymer International* **2007**, *56* (2), 145-157.
12. <http://20minutegarden.com/2010/10/16/good-bye-mr-sun-chips-bag/>.
13. Driscoll, P. Biodegradable coronary stent development: A hurdle with big rewards. <http://mediligence.com/blog/2009/07/14/biodegradable-coronary-stent-development-a-hurdle-with-big-rewards/>.

14. Athanasiou, K. A.; Niederauer, G. G.; Agrawal, C. M., Sterilization, toxicity, biocompatibility and clinical applications of polylactic acid polyglycolic acid copolymers. *Biomaterials* **1996**, *17* (2), 93-102.
15. Middleton, J. C.; Tipton, A. J., Synthetic biodegradable polymers as orthopedic devices. *Biomaterials* **2000**, *21* (23), 2335-2346.
16. Serruys, P. W.; Ormiston, J. A.; Onuma, Y.; Regar, E.; Gonzalo, N.; Garcia-Garcia, H. M.; Nieman, K.; Bruining, N.; Dorange, C.; Miquel-Hebert, K.; Veldhof, S.; Webster, M.; Thuesen, L.; Dudek, D., A bioabsorbable everolimus-eluting coronary stent system (ABSORB): 2-year outcomes and results from multiple imaging methods. *Lancet* **2009**, *373* (9667), 897-910.
17. Uurto, I.; Mikkonen, J.; Parkkinen, J.; Keski-Nisula, L.; Nevalainen, T.; Kellomaki, M.; Tormala, P.; Salenius, J. P., Drug-eluting biodegradable poly-D/L-lactic acid vascular stents: An experimental pilot study. *Journal of Endovascular Therapy* **2005**, *12* (3), 371-379.
18. Morice, M.; Serruys, P. W.; Sousa, J. E.; Fajadet, J.; Hayashi, E. B.; Perin, M.; Colombo, A.; Schuler, G.; Barragan, P.; Guagliumi, G.; Molnar, F.; Falotico, R.; Grp, R. S., A randomized comparison of a sirolimus-eluting stent with a standard stent for coronary revascularization. *New England Journal of Medicine* **2002**, *346* (23), 1773-1780.
19. Acharya, G.; Park, K., Mechanisms of controlled drug release from drug-eluting stents. *Advanced Drug Delivery Reviews* **2006**, *58* (3), 387-401.
20. Musumeci, T.; Ventura, C. A.; Giannone, I.; Ruozi, B.; Montenegro, L.; Pignatello, R.; Puglisi, G., PLA/PLGA nanoparticles for sustained release of docetaxel. *International Journal of Pharmaceutics* **2006**, *325* (1-2), 172-179.
21. Ogawa, Y.; Yamamoto, M.; Okada, H.; Yashiki, T.; Shimamoto, T., A New Technique to Efficiently Entrap Leuprolide Acetate into Microcapsules of Polylactic Acid or Copoly(Lactic Glycolic) Acid. *Chemical & Pharmaceutical Bulletin* **1988**, *36* (3), 1095-1103.
22. Brown, D. M., *Drug Delivery Systems in Cancer Therapy*. Humana Press: Totowa, 2004.
23. Gilding, D. K., *Biodegradable Polymers*. Williams, D.F. ed.; CRC: Boca Raton, 1981; p 209-232.
24. Hartmann, M. H., *Biopolymers from Renewable Resources*. Kaplan, D. L., ed.; Springer-Verlag: Berlin, 1998; p. 367-411.

25. Kricheldorf, H. R.; Kreiser-Saunders, I.; Stricker, A., Poly lactones 48. SnOct(2)-initiated polymerizations of lactide: A mechanistic study. *Macromolecules* **2000**, *33* (3), 702-709.
26. Kowalski, A.; Duda, A.; Penczek, S., Kinetics and mechanism of cyclic esters polymerization initiated with tin(II) octoate. 3. Polymerization of L,L-dilactide. *Macromolecules* **2000**, *33* (20), 7359-7370.
27. Kricheldorf, H. R.; Serra, A., Poly lactones .6. Influence of Various Metal-Salts on the Optical Purity of Poly(L-Lactide). *Polymer Bulletin* **1985**, *14* (6), 497-502.
28. Katiyar, V.; Nanavati, H., Ring-opening polymerization of L-lactide using N-heterocyclic molecules: mechanistic, kinetics and DFT studies. *Polymer Chemistry* **2010**, *1* (9), 1491-1500.
29. Sodergard, A.; Stolt, M., Properties of lactic acid based polymers and their correlation with composition. *Progress in Polymer Science* **2002**, *27* (6), 1123-1163.
30. Ikada, Y.; Jamshidi, K.; Tsuji, H.; Hyon, S. H., Stereocomplex Formation between Enantiomeric Poly(Lactides). *Macromolecules* **1987**, *20* (4), 904-906.
31. Kricheldorf, H. R.; Boettcher, C., Poly lactones .24. Polymerizations of Racemic and Meso-D,L-Lactide with Al-O Initiators - Analyses of Stereosequences. *Makromolekulare Chemie-Macromolecular Chemistry and Physics* **1993**, *194* (6), 1653-1664.
32. Ovitt, T. M.; Coates, G. W., Stereoselective ring-opening polymerization of rac-lactide with a single-site, racemic aluminum alkoxide catalyst: Synthesis of stereoblock poly(lactic acid). *Journal of Polymer Science Part A-Polymer Chemistry* **2000**, *38*, 4686-4692.
33. Radano, C. P.; Baker, G. L.; Smith, M. R., Stereoselective polymerization of a racemic monomer with a racemic catalyst: Direct preparation of the polylactic acid stereocomplex from racemic lactide. *Journal of the American Chemical Society* **2000**, *122* (7), 1552-1553.
34. Ovitt, T. M.; Coates, G. W., Stereoselective ring-opening polymerization of meso-lactide: Synthesis of syndiotactic poly(lactic acid). *Journal of the American Chemical Society* **1999**, *121* (16), 4072-4073.
35. Chu, C. C., Hydrolytic Degradation of Polyglycolic Acid - Tensile-Strength and Crystallinity Study. *Journal of Applied Polymer Science* **1981**, *26* (5), 1727-1734.
36. Shih, C., Chain-End Scission in Acid-Catalyzed Hydrolysis of Poly(D,L-Lactide) in Solution. *Journal of Controlled Release* **1995**, *34* (1), 9-15.

37. Joziassse, C. A. P.; Grijpma, D. W.; Bergsma, J. E.; Cordewener, F. W.; Bos, R. R. M.; Pennings, A. J., The influence of morphology on the (hydrolytic degradation of as-polymerized and hot-drawn poly (L-lactide)). *Colloid and Polymer Science* **1998**, *276* (11), 968-975.
38. Alberts, B.; Johnson, A.; Lewis, J.; Raff, M.; Roberts, K.; Walter, P., *Molecular Biology of the Cell*. Fourth ed.; Garland Science, Taylor & Francis Group: New York, 2002.
39. Ouchi, T.; Nozaki, T.; Okamoto, Y.; Shiratani, M.; Ohya, Y., Synthesis and enzymatic hydrolysis of polydepsipeptides with functionalized pendant groups. *Macromolecular Chemistry and Physics* **1996**, *197* (6), 1823-1833.
40. Veld, P. J. A. I.; Dijkstra, P. J.; Feijen, J., Synthesis of Biodegradable Polyesteramides with Pendant Functional-Groups. *Makromolekulare Chemie-Macromolecular Chemistry and Physics* **1992**, *193* (11), 2713-2730.
41. Barrera, D. A.; Zylstra, E.; Lansbury, P. T.; Langer, R., Synthesis and RGD Peptide Modification of a New Biodegradable Copolymer - Poly(Lactic Acid-Co-Lysine). *Journal of the American Chemical Society* **1993**, *115* (23), 11010-11011.
42. Barrera, D. A.; Zylstra, E.; Lansbury, P. T.; Langer, R., Copolymerization and Degradation of Poly(Lactic Acid Co-Lysine). *Macromolecules* **1995**, *28* (2), 425-432.
43. Jiang, X.; Vogel, E. B.; Smith, M. R.; Baker, G. L., "Clickable" polyglycolides: Tunable synthons for thermoresponsive, degradable polymers. *Macromolecules* **2008**, *41* (6), 1937-1944.
44. Yin, M.; Baker, G. L., Preparation and characterization of substituted polylactides. *Macromolecules* **1999**, *32* (23), 7711-7718.
45. Ugi, I.; Fetzer, U.; Eholzer, U.; Knupfer, H.; Offerman, K., Isonitrile Syntheses. *Angewandte Chemie-International Edition* **1965**, *4* (6), 472-484.
46. Passerini, M., On the effect of cyan potassium on per-nitroso derivatives. *Berichte Der Deutschen Chemischen Gesellschaft* **1927**, *60*, 1201-1202.
47. Schwarz, J. S. P., Preparation of acyclic isoimides and their rearrangement rates to imides. *The Journal of Organic Chemistry* **1972**, *37* (18), 2906-2908.
48. Gilley, C. B.; Buller, M. J.; Kobayashi, Y., New entry to convertible isocyanides for the ugi reaction and its application to the stereocontrolled formal total synthesis of the proteasome inhibitor Omuralide. *Organic Letters* **2007**, *9* (18), 3631-3634.
49. Kolb, H. C.; Finn, M. G.; Sharpless, K. B., Click chemistry: Diverse chemical function from a few good reactions. *Angewandte Chemie-International Edition* **2001**, *40* (11), 2004-2021.

50. Rostovtsev, V. V.; Green, L. G.; Fokin, V. V.; Sharpless, K. B., A stepwise Huisgen cycloaddition process: Copper(I)-catalyzed regioselective "ligation" of azides and terminal alkynes. *Angewandte Chemie-International Edition* **2002**, *41* (14), 2596-2599.
51. Meldal, M.; Tornøe, C. W., Cu-catalyzed azide-alkyne cycloaddition. *Chemical Reviews* **2008**, *108* (8), 2952-3015.
52. Van Hoof, S.; Lacey, C. J.; Rohrich, R. C.; Wiesner, J.; Jomaa, H.; Van Calenbergh, S., Synthesis of analogues of (E)-1-Hydroxy-2-methylbut-2-enyl 4-diphosphate, an isoprenoid precursor and human gamma delta T cell activator. *Journal of Organic Chemistry* **2008**, *73* (4), 1365-1370.
53. Greene, T. W.; Wuts, P. G. M., *Protective Groups in Organic Synthesis*. Third ed.; John Wiley & Sons, Inc: 1999.
54. Odian, G., *Principles of Polymerization*. 3rd ed.; Wiley and Sons: New York, 1991.
55. Kumari, A.; Yadav, S. K.; Yadav, S. C., Biodegradable polymeric nanoparticles based drug delivery systems. *Colloids Surf B Biointerfaces* **2010**, *75* (1), 1-18.
56. Okada, H.; Toguchi, H., Biodegradable Microspheres in Drug-Delivery. *Critical Reviews in Therapeutic Drug Carrier Systems* **1995**, *12* (1), 1-99.
57. Gorner, T.; Gref, R.; Michenot, D.; Sommer, F.; Tran, M. N.; Dellacherie, E., Lidocaine-loaded biodegradable nanospheres. I. Optimization of the drug incorporation into the polymer matrix. *Journal of Controlled Release* **1999**, *57* (3), 259-268.
58. Polakovic, M.; Gorner, T.; Gref, R.; Dellacherie, E., Lidocaine loaded biodegradable nanospheres II. Modelling of drug release. *Journal of Controlled Release* **1999**, *60* (2-3), 169-177.
59. Paul, M.; Laatiris, A.; Fessi, H.; Dufeu, B.; Durand, R.; Deniau, M.; Astier, A., Pentamidine-loaded poly(D,L-lactide) nanoparticles: Adsorption and drug release. *Drug Development Research* **1998**, *43* (2), 98-104.
60. Budhian, A.; Siegel, S. J.; Winey, K. I., Production of haloperidol-loaded PLGA nanoparticles for extended controlled drug release of haloperidol. *Journal of Microencapsulation* **2005**, *22* (7), 773-785.
61. Budhian, A.; Siegel, S. J.; Winey, K. I., Haloperidol-loaded PLGA nanoparticles: Systematic study of particle size and drug content. *International Journal of Pharmaceutics* **2007**, *336* (2), 367-375.
62. Dadashzadeh, S.; Derakhshandeh, K.; Erfan, M., Encapsulation of 9-nitrocamptothecin, a novel anticancer drug, in biodegradable nanoparticles: Factorial

design, characterization and release kinetics. *European Journal of Pharmaceutics and Biopharmaceutics* **2007**, 66 (1), 34-41.

63. Yadav, S. C.; Kumari, A.; Yadav, S. K., Biodegradable polymeric nanoparticles based drug delivery systems. *Colloids and Surfaces B-Biointerfaces* **2010**, 75 (1), 1-18.

64. Lassalle, V.; Ferreira, M. L., PLA nano- and microparticles for drug delivery: An overview of the methods of preparation. *Macromolecular Bioscience* **2007**, 7 (6), 767-783.

65. Jeffery, H.; Davis, S. S.; Ohagan, D. T., The Preparation and Characterization of Poly(Lactide-Co-Glycolide) Microparticles .1. Oil-in-Water Emulsion Solvent Evaporation. *International Journal of Pharmaceutics* **1991**, 77 (2-3), 169-175.

66. Faisant, N.; Akiki, J.; Siepmann, F.; Benoit, J. P.; Siepmann, J., Effects of the type of release medium on drug release from PLIGA-based microparticles: Experiment and theory. *International Journal of Pharmaceutics* **2006**, 314 (2), 189-197.

67. Fessi, H.; Puisieux, F.; Devissaguet, J. P.; Ammoury, N.; Benita, S., Nanocapsule Formation by Interfacial Polymer Deposition Following Solvent Displacement. *International Journal of Pharmaceutics* **1989**, 55 (1), R1-R4.

68. Perry, M. C., *The Chemotherapy Source Book*. 3rd ed.; Lipincott, Williams & Wilkins: Philadelphia, 2001.

69. Ulukan, H.; Swaan, P. W., Camptothecins - A review of their chemotherapeutic potential. *Drugs* **2002**, 62 (14), 2039-2057.

70. Kong, S. D.; Luong, A.; Manorek, G.; Howell, S. B.; Yang, J., Acidic hydrolysis of N-Ethoxybenzylimidazoles (NEBIs): potential applications as pH-sensitive linkers for drug delivery. *Bioconjugate Chem* **2007**, 18 (2), 293-296.

71. Luong, A.; Issarapanichkit, T.; Kong, S. D.; Fong, R.; Yang, J., pH-Sensitive, N-ethoxybenzylimidazole (NEBI) bifunctional crosslinkers enable triggered release of therapeutics from drug delivery carriers. *Org Biomol Chem* **2010**, 8 (22), 5105-5109.

72. *2011 Alzheimer's Disease Facts and Figures*. Alzheimer's Association: Washington, D.C., 2011.

73. Mebane-Sims, I., 2009 Alzheimer's disease facts and figures. *Alzheimer's & Dementia* **2009**, 5 (3), 234-270.

74. Ferri, C. P.; Prince, M.; Brayne, C.; Brodaty, H.; Fratiglioni, L.; Ganguli, M.; Hall, K.; Hasegawa, K.; Hendrie, H.; Huang, Y. Q.; Jorm, A.; Mathers, C.; Menezes, P. R.; Rimmer, E.; Sczuzufca, M.; Intl, A. D., Global prevalence of dementia: a Delphi consensus study. *Lancet* **2005**, 366 (9503), 2112-2117.

75. Wimo, A.; Prince, M., *World Alzheimer's Report 2010: The Global Economic Impact of Dementia*. Alzheimer's Disease International: London, 2010.
76. Amano, N.; Iseki, E., Introduction: Pick's disease and frontotemporal dementia. *Neuropathology* **1999**, *19* (4), 417-421.
77. Brat, D. J.; Gearing, M.; Goldthwaite, P. T.; Wainer, B. H.; Burger, P. C., Tau-associated neuropathology in ganglion cell tumours increases with patient age but appears unrelated to ApoE genotype. *Neuropathology and Applied Neurobiology* **2001**, *27* (3), 197-205.
78. LaFerla, F. M.; Green, K. N.; Oddo, S., Intracellular amyloid-beta in Alzheimer's disease. *Nature Reviews Neuroscience* **2007**, *8* (7), 499-509.
79. Burdick, D.; Soreghan, B.; Kwon, M.; Kosmoski, J.; Knauer, M.; Henschen, A.; Yates, J.; Cotman, C.; Glabe, C., Assembly and Aggregation Properties of Synthetic Alzheimers A4/Beta Amyloid Peptide Analogs. *Journal of Biological Chemistry* **1992**, *267* (1), 546-554.
80. Clippingdale, A. B.; Wade, J. D.; Barrow, C. J., The amyloid-beta peptide and its role in Alzheimer's disease. *Journal of Peptide Science* **2001**, *7* (5), 227-249.
81. Mattson, M. P., Cellular actions of beta-amyloid precursor protein and its soluble and fibrillogenic derivatives. *Physiological Reviews* **1997**, *77* (4), 1081-1132.
82. Walsh, D. M.; Selkoe, D. J., A beta Oligomers - a decade of discovery. *Journal of Neurochemistry* **2007**, *101* (5), 1172-1184.
83. Yankner, B. A.; Duffy, L. K.; Kirschner, D. A., Neurotrophic and Neurotoxic Effects of Amyloid Beta-Protein - Reversal by Tachykinin Neuropeptides. *Science* **1990**, *250* (4978), 279-282.
84. Olson, M. I.; Shaw, C. M., Presenile Dementia and Alzheimers Disease in Mongolism. *Brain* **1969**, *92*, 147-156.
85. Mori, C.; Spooner, E. T.; Wisniewski, K. E.; Wisniewski, T. M.; Yamaguchi, H.; Saido, T. C.; Tolan, D. R.; Selkoe, D. J.; Lemere, C. A., Intraneuronal A beta 42 accumulation in Down syndrome brain. *Amyloid-Journal of Protein Folding Disorders* **2002**, *9* (2), 88-102.
86. Hardy, J.; Higgins, G., Alzheimer's disease: the amyloid cascade hypothesis. *Science* **1992**, *256* (5054), 184-185.
87. Selkoe, D. J., The Molecular Pathology of Alzheimers-Disease. *Neuron* **1991**, *6* (4), 487-498.

88. Hardy, J.; Selkoe, D. J., The amyloid hypothesis of Alzheimer's disease: progress and problems on the road to therapeutics. *Science* **2002**, *297* (5580), 353-356.
89. Hardy, J., Testing times for the "amyloid cascade hypothesis". *Neurobiology of Aging* **2002**, *23* (6), 1073-1074.
90. Burdick, D.; Kosmoski, J.; Knauer, M. F.; Glabe, C. G., Preferential adsorption, internalization and resistance to degradation of the major isoform of the Alzheimer's amyloid peptide, A beta 1-42, in differentiated PC12 cells. *Brain Research* **1997**, *746* (1-2), 275-284.
91. Knauer, M. F.; Soreghan, B.; Burdick, D.; Kosmoski, J.; Glabe, C. G., Intracellular Accumulation and Resistance to Degradation of the Alzheimer Amyloid A4/Beta-Protein. *Proceedings of the National Academy of Sciences of the United States of America* **1992**, *89* (16), 7437-7441.
92. Zhao, X. B.; Yang, J., Amyloid-beta Peptide Is a Substrate of the Human 20S Proteasome. *ACS Chemical Neuroscience* **2010**, *1* (10), 655-660.
93. Huang, X. D.; Cuajungco, M. P.; Atwood, C. S.; Hartshorn, M. A.; Tyndall, J. D. A.; Hanson, G. R.; Stokes, K. C.; Leopold, M.; Multhaup, G.; Goldstein, L. E.; Scarpa, R. C.; Saunders, A. J.; Lim, J.; Moir, R. D.; Glabe, C.; Bowden, E. F.; Masters, C. L.; Fairlie, D. P.; Tanzi, R. E.; Bush, A. I., Cu(II) potentiation of Alzheimer A beta neurotoxicity - Correlation with cell-free hydrogen peroxide production and metal reduction. *Journal of Biological Chemistry* **1999**, *274* (52), 37111-37116.
94. Rauk, A., Why is the amyloid beta peptide of Alzheimer's disease neurotoxic? *Dalton Transactions* **2008**, *10*, 1273-1282.
95. Habib, L. K.; Lee, M. T. C.; Yang, J., Inhibitors of Catalase-Amyloid Interactions Protect Cells from beta-Amyloid-Induced Oxidative Stress and Toxicity. *Journal of Biological Chemistry* **2010**, *285* (50), 38933-38943.
96. Takuma, K.; Yao, J.; Huang, J. M.; Xu, H. W.; Chen, X.; Luddy, J.; Trillat, A. C.; Stern, D. M.; Arancio, O.; Yan, S. S. D., ABAD enhances A beta-induced cell stress via mitochondrial dysfunction. *FASEB Journal* **2005**, *19* (1), 597-598.
97. Yan, S. D.; Chen, J. X., Amyloid-beta-induced mitochondrial dysfunction. *Journal of Alzheimers Disease* **2007**, *12* (2), 177-184.
98. Nussinov, R.; Jang, H.; Zheng, J., Models of beta-amyloid ion channels in the membrane suggest that channel formation in the bilayer is a dynamic process. *Biophysical Journal* **2007**, *93* (6), 1938-1949.
99. Lleo, A., Current therapeutic options for Alzheimer's disease. *Current Genomics* **2007**, *8* (8), 550-558.

100. Lanctôt, K. L.; Herrmann, N.; Yau, K. K.; Khan, L. R.; Liu, B. A.; LouLou, M. M.; Einarson, T. R., Efficacy and safety of cholinesterase inhibitors in Alzheimer's disease: a meta-analysis. *Canadian Medical Association Journal* **2003**, *169* (6), 557-564.
101. Williams, B. R.; Nazarians, A.; Gill, M. A., A review of rivastigmine: A reversible cholinesterase inhibitor. *Clinical Therapeutics* **2003**, *25* (6), 1634-1653.
102. Castellani, R. J.; Shah, R. S.; Lee, H. G.; Zhu, X. W.; Perry, G.; Smith, M. A., Current approaches in the treatment of Alzheimer's disease. *Biomedicine & Pharmacotherapy* **2008**, *62* (4), 199-207.
103. Orhan, G.; Orhan, I.; Sener, B., Recent developments in natural and synthetic drug research for Alzheimer's disease. *Letters in Drug Design & Discovery* **2006**, *3* (4), 268-274.
104. Danysz, W.; Parsons, C. G., The NMDA receptor antagonist memantine as a symptomatological and neuroprotective treatment for Alzheimer's disease: preclinical evidence. *International Journal of Geriatric Psychiatry* **2003**, *18*, S23-S32.
105. Danysz, W.; Parsons, C. G.; Stoffler, A., Memantine: a NMDA receptor antagonist that improves memory by restoration of homeostasis in the glutamatergic system - too little activation is bad, too much is even worse. *Neuropharmacology* **2007**, *53* (6), 699-723.
106. Bezprozvanny, I.; Mattson, M. P., Neuronal calcium mishandling and the pathogenesis of Alzheimer's disease. *Trends in Neurosciences* **2008**, *31* (9), 454-463.
107. Ghosh, A. K.; Kumaragurubarana, N.; Hong, L.; Kulkarni, S.; Xu, X. M.; Miller, H. B.; Reddy, D. S.; Weerasena, V.; Turner, R.; Chang, W.; Koelsch, G.; Tang, J., Potent memapsin 2 (beta-secretase) inhibitors: Design, synthesis, protein-ligand X-ray structure, and in vivo evaluation. *Bioorganic & Medicinal Chemistry Letters* **2008**, *18* (3), 1031-1036.
108. Ghosh, A. K.; Kumaragurubaran, N.; Hong, L.; Koelsh, G.; Tang, J., Memapsin 2 (beta-secretase) inhibitors: Drug development. *Current Alzheimer Research* **2008**, *5* (2), 121-131.
109. Citron, M., Strategies for disease modification in Alzheimer's disease. *Nature Reviews Neuroscience* **2004**, *5* (9), 677-685.
110. De Strooper, B.; Annaert, W.; Cupers, P.; Saftig, P.; Craessaerts, K.; Mumm, J. S.; Schroeter, E. H.; Schrijvers, V.; Wolfe, M. S.; Ray, W. J.; Goate, A.; Kopan, R., A presenilin-1-dependent gamma-secretase-like protease mediates release of Notch intracellular domain. *Nature* **1999**, *398* (6727), 518-522.
111. Weggen, S.; Eriksen, J. L.; Das, P.; Sagi, S. A.; Wang, R.; Pietrzik, C. U.; Findlay, K. A.; Smith, T. E.; Murphy, M. P.; Butler, T.; Kang, D. E.; Marquez-Sterling,

N.; Golde, T. E.; Koo, E. H., A subset of NSAIDs lower amyloidogenic A beta 42 independently of cyclooxygenase activity. *Nature* **2001**, *414* (6860), 212-216.

112. Eriksen, J. L.; Sagi, S. A.; Smith, T. E.; Weggen, S.; Das, P.; McLendon, D. C.; Ozols, V. V.; Jessing, K. W.; Zavitz, K. H.; Koo, E. H.; Golde, T. E., NSAIDs and enantiomers of flurbiprofen target gamma-secretase and lower A beta 42 in vivo. *Journal of Clinical Investigation* **2003**, *112* (3), 440-449.

113. Kukar, T. L.; Ladd, T. B.; Bann, M. A.; Fraering, P. C.; Narlawar, R.; Maharvi, G. M.; Healy, B.; Chapman, R.; Welzel, A. T.; Price, R. W.; Moore, B.; Rangachari, V.; Cusack, B.; Eriksen, J.; Jansen-West, K.; Verbeeck, C.; Yager, D.; Eckman, C.; Ye, W. J.; Sagi, S.; Cottrell, B. A.; Torpey, J.; Rosenberry, T. L.; Fauq, A.; Wolfe, M. S.; Schmidt, B.; Walsh, D. M.; Koo, E. H.; Golde, T. E., Substrate-targeting gamma-secretase modulators. *Nature* **2008**, *453* (7197), 925-929.

114. Weggen, S.; Eriksen, J. L.; Sagi, S. A.; Pietrzik, C. U.; Ozols, V.; Fauq, A.; Golde, T. E.; Koo, E. H., Evidence that nonsteroidal anti-inflammatory drugs decrease amyloid beta 42 production by direct modulation of gamma-secretase activity. *Journal of Biological Chemistry* **2003**, *278* (34), 31831-31837.

115. Kukar, T.; Murphy, M. P.; Eriksen, J. L.; Sagi, S. A.; Weggen, S.; Smith, T. E.; Ladd, T.; Khan, M. A.; Kache, R.; Beard, J.; Dodson, M.; Merit, S.; Ozols, V. V.; Anastasiadis, P. Z.; Das, P.; Fauq, A.; Koo, E. H.; Golde, T. E., Diverse compounds mimic Alzheimer disease-causing mutations by augmenting A beta 42 production. *Nature Medicine* **2005**, *11* (5), 545-550.

116. Phase III clinical trials of (R)-flurbiprofen (trade name Flurizan) on nearly 1700 individuals concluded that the drug did not increase cognitive function of patients significantly more than placebo. Accordingly, the drug was discontinued from further development by Myriad Genetics in June, 2008.

117. Gestwicki, J. E.; Crabtree, G. R.; Graef, I. A., Harnessing Chaperones to Generate Small-Molecule Inhibitors of Amyloid β Aggregation. *Science* **2004**, *306* (5697), 865-869.

118. Yang, F.; Lim, G. P.; Begum, A. N.; Ubeda, O. J.; Simmons, M. R.; Ambegaokar, S. S.; Chen, P. P.; Kaye, R.; Glabe, C. G.; Frautschy, S. A.; Cole, G. M., Curcumin inhibits formation of amyloid beta oligomers and fibrils, binds plaques, and reduces amyloid in vivo. *Journal of Biological Chemistry* **2005**, *280* (7), 5892-5901.

119. Inbar, P.; Li, C. Q.; Takayama, S. A.; Bautista, M. R.; Yang, J., Oligo(ethylene glycol) derivatives of thioflavin T as inhibitors of protein-amyloid interactions. *Chembiochem* **2006**, *7* (10), 1563-1566.

120. Inbar, P.; Yang, J., Inhibiting protein-amyloid interactions with small molecules: A surface chemistry approach. *Bioorganic & Medicinal Chemistry Letters* **2006**, *16* (4), 1076-1079.
121. Glabe, C., Does Alzheimer disease tilt the scales of amyloid degradation versus accumulation? *Nature Medicine* **2000**, *6* (2), 133-134.
122. Suh, J.; Yoo, S. H.; Kim, M. G.; Jeong, K.; Ahn, J. Y.; Kim, M. S.; Chae, P. S.; Lee, T. Y.; Lee, J.; Jang, Y. A.; Ko, E. H., Cleavage agents for soluble oligomers of amyloid beta peptides. *Angew Chem Int Ed Engl* **2007**, *46* (37), 7064-7067.
123. Wu, W. H.; Lei, P.; Liu, Q.; Hu, J.; Gunn, A. P.; Chen, M. S.; Rui, Y. F.; Su, X. Y.; Xie, Z. P.; Zhao, Y. F.; Bush, A. I.; Li, Y. M., Sequestration of Copper from beta-Amyloid Promotes Selective Lysis by Cyclen-Hybrid Cleavage Agents. *Journal of Biological Chemistry* **2008**, *283* (46), 31657-31664.
124. Zagorski, M. G.; Yang, J.; Shao, H. Y.; Ma, K.; Zeng, H.; Hong, A., Methodological and chemical factors affecting amyloid beta peptide amyloidogenicity. *Amyloid, Prions, and Other Protein Aggregates* **1999**, *309*, 189-204.
125. Koo, E. H.; Lansbury, P. T.; Kelly, J. W., Amyloid diseases: Abnormal protein aggregation in neurodegeneration. *Proceedings of the National Academy of Sciences of the United States of America* **1999**, *96* (18), 9989-9990.
126. Ryu, J.; Kanapathipillai, M.; Lentzen, G.; Park, C. B., Inhibition of beta-amyloid peptide aggregation and neurotoxicity by alpha-D-mannosylglycerate, a natural extremolyte. *Peptides* **2008**, *29* (4), 578-584.
127. Reinke, A. A.; Gestwicki, J. E., Structure-activity relationships of amyloid beta-aggregation inhibitors based on curcumin: Influence of linker length and flexibility. *Chemical Biology & Drug Design* **2007**, *70* (3), 206-215.
128. Necula, M.; Kaye, R.; Milton, S.; Glabe, C. G., Small Molecule Inhibitors of Aggregation Indicate That Amyloid beta Oligomerization and Fibrillization Pathways Are Independent and Distinct. *Journal of Biological Chemistry* **2007**, *282* (14), 10311-10324.
129. Ono, K.; Hasegawa, K.; Naiki, H.; Yamada, M., Curcumin has potent anti-amyloidogenic effects for Alzheimer's beta-amyloid fibrils in vitro. *Journal of Neuroscience Research* **2004**, *75* (6), 742-750.
130. Ono, K.; Hasegawa, K.; Naiki, H.; Yamada, M., Anti-amyloidogenic activity of tannic acid and its activity to destabilize Alzheimer's beta-amyloid fibrils in vitro. *Biochimica Et Biophysica Acta-Molecular Basis of Disease* **2004**, *1690* (3), 193-202.

131. Inbar, P.; Bautista, M. R.; Takayama, S. A.; Yang, J., Assay to screen for molecules that associate with Alzheimer's related beta-amyloid fibrils. *Analytical Chemistry* **2008**, *80* (9), 3502-3506.
132. Knauer, M. F.; Soreghan, B.; Burdick, D.; Kosmoski, J.; Glabe, C. G., Intracellular accumulation and resistance to degradation of the Alzheimer amyloid A4/beta protein. *Proceedings of the National Academy of Sciences of the United States of America* **1992**, *89* (16), 7437-7441.
133. Burdick, D.; Kosmoski, J.; Knauer, M. F.; Glabe, C. G., Preferential adsorption, internalization and resistance to degradation of the major isoform of the Alzheimer's amyloid peptide, A beta 1-42, in differentiated PC12 cells. *Brain Research* **1997**, *746* (1-2), 275-84.
134. Gross, E.; Witkop, B., Selective Cleavage of Methionyl Peptide Bonds in Ribonuclease with Cyanogen Bromide. *Journal of the American Chemical Society* **1961**, *83* (6), 1510-1511.
135. Hoyer, D.; Cho, H.; Schultz, P. G., A new strategy for selective protein cleavage. *Journal of the American Chemical Society* **1990**, *112* (8), 3249-3250.
136. Green, N. M., Avidin. 1. The Use of (14-C)Biotin for Kinetic Studies and for Assay. *Biochemical Journal* **1963**, *89*, 585-591.
137. Schepartz, A.; Cuenoud, B., Site-specific cleavage of the protein calmodulin using a trifluoperazine-based affinity reagent. *Journal of the American Chemical Society* **1990**, *112* (8), 3247-3249.
138. Cuenoud, B.; Tarasow, T. M.; Schepartz, A., A New Strategy for Directed Protein Cleavage. *Tetrahedron Letters* **1992**, *33* (7), 895-898.
139. Nicolaou, K. C.; Dai, W. M., Chemistry and Biology of the Eneidyne Anticancer Antibiotics. *Angewandte Chemie-International Edition* **1991**, *30* (11), 1387-1416.
140. Smith, A. L.; Nicolaou, K. C., The enedyne antibiotics. *Journal of Medicinal Chemistry* **1996**, *39* (11), 2103-2117.
141. Nicolaou, K. C.; Smith, A. L., Molecular Design, Chemical Synthesis, and Biological Action of Eneidyne. *Accounts of Chemical Research* **1992**, *25* (11), 497-503.
142. Zein, N.; Solomon, W.; Casazza, A. M.; Kadow, J. F.; Krishnan, B. S.; Tun, M. M.; Vyas, D. M.; Doyle, T. W., Protein Damage Caused by a Synthetic Eneidyne Core. *Bioorganic & Medicinal Chemistry Letters* **1993**, *3* (6), 1351-1356.
143. Jones, G. B.; Wright, J. M.; Hynd, G.; Wyatt, J. K.; Yancisin, M.; Brown, M. A., Protein-degrading enediynes: Library screening of Bergman cycloaromatization products. *Organic Letters* **2000**, *2* (13), 1863-1866.

144. Plourde, G.; El-Shafey, A.; Fouad, F. S.; Purohit, A. S.; Jones, G. B., Protein degradation with photoactivated enediyne-amino acid conjugates. *Bioorganic & Medicinal Chemistry Letters* **2002**, *12* (20), 2985-2988.
145. Zein, N.; Colson, K. L.; Leet, J. E.; Schroeder, D. R.; Solomon, W.; Doyle, T. W.; Casazza, A. M., Kedarcidin Chromophore - an Enediyne That Cleaves DNA in a Sequence-Specific Manner. *Proceedings of the National Academy of Sciences of the United States of America* **1993**, *90* (7), 2822-2826.
146. Semmelhack, M. F.; Gallagher, J. J.; Ding, W. D.; Krishnamurthy, G.; Babine, R.; Ellestad, G. A., The Effect on DNA Cleavage Potency of Tethering a Simple Cyclic Enediyne to a Netropsin Analog. *Journal of Organic Chemistry* **1994**, *59* (16), 4357-4359.
147. Hamann, P. R.; Hinman, L. M.; Hollander, I.; Beyer, C. F.; Lindh, D.; Holcomb, R.; Hallett, W.; Tsou, H. R.; Upeslakis, J.; Shochat, D.; Mountain, A.; Flowers, D. A.; Bernstein, I., Gemtuzumab ozogamicin, a potent and selective anti-CD33 antibody-calicheamicin conjugate for treatment of acute myeloid leukemia. *Bioconjugate Chemistry* **2002**, *13* (1), 47-58.
148. Fouad, F. S.; Wright, J. M.; Plourde, G.; Purohit, A. D.; Wyatt, J. K.; El-Shafey, A.; Hynd, G.; Crasto, C. F.; Lin, Y. Q.; Jones, G. B., Synthesis and protein degradation capacity of photoactivated enediynes. *Journal of Organic Chemistry* **2005**, *70* (24), 9789-9797.
149. Headlam, H. A.; Davies, M. J., Beta-scission of side-chain alkoxy radicals on peptides and proteins results in the loss of side-chains as aldehydes and ketones. *Free Radical Biology and Medicine* **2002**, *32* (11), 1171-1184.
150. Jones, G. B.; Wright, J. M.; Plourde, G. W.; Hynd, G.; Huber, R. S.; Mathews, J. E., A direct and stereocontrolled route to conjugated enediynes. *Journal of the American Chemical Society* **2000**, *122* (9), 1937-1944.
151. Pietraszkiewicz, M.; Jurczak, J., Synthesis of Chiral Diaza Crown Ethers Incorporating Carbohydrate Units. *Tetrahedron* **1984**, *40* (15), 2967-2970.
152. Asaki, T.; Hamamoto, T.; Sugiyama, Y.; Kuwano, K.; Kuwabara, K., Structure-activity studies on diphenylpyrazine derivatives: A novel class of prostacyclin receptor agonists. *Bioorganic & Medicinal Chemistry* **2007**, *15* (21), 6692-6704.
153. Waters, S. P.; Tian, Y.; Li, Y. M.; Danishefsky, S. J., Total synthesis of (-)-scabronine G, an inducer of neurotrophic factor production. *Journal of the American Chemical Society* **2005**, *127* (39), 13514-13515.
154. Lockhart, A.; Ye, L.; Judd, D. B.; Merritt, A. T.; Lowe, P. N.; Morgenstern, J. L.; Hong, G.; Gee, A. D.; Brown, J., Evidence for the presence of three distinct binding sites

for the thioflavin T class of Alzheimer's disease PET imaging agents on beta-amyloid peptide fibrils. *Journal of Biological Chemistry* **2005**, 280 (9), 7677-7684.

155. Gololobov, Y. G.; Zhmurova, I. N.; Kasukhin, L. F., 60 Years of Staudinger Reaction. *Tetrahedron* **1981**, 37 (3), 437-472.

156. Kasukhin, L. F.; Ponomarchuk, M. P.; Gololobov, I. G., The Staudinger Reaction - a New Reaction System for the Determination of the Substituent Sigma-Iota-Parameters. *Doklady Akademii Nauk SSSR (Доклады Академии Наук СССР)* **1981**, 257 (1), 119-122.

157. Gursky, O.; Aleshkov, S., Temperature-dependent beta-sheet formation in beta-amyloid A beta(1-40) peptide in water: uncoupling beta-structure folding from aggregation. *Biochimica Et Biophysica Acta-Protein Structure and Molecular Enzymology* **2000**, 1476 (1), 93-102.

158. Mosmann, T., Rapid colorimetric assay for cellular growth and survival: application to proliferation and cytotoxicity assays. *Journal of Immunological Methods* **1983**, 65 (1-2), 55-63.

159. Semmelhack, M. F.; Sarpong, R.; Bergman, J.; Ho, D. M., Evaluation of alkene isomerization as a trigger for enediyne activation. *Tetrahedron Letters* **2002**, 43 (4), 541-544.

160. Bouzide, A.; Sauve, G., Silver (I) oxide mediated highly selective monotosylation of symmetrical diols. Application to the synthesis of polysubstituted cyclic ethers. *Organic Letters* **2002**, 4 (14), 2329-2332.

161. Kappe, C. O.; Dallinger, D.; Murphree, S. S., *Practical Microwave Synthesis for Organic Chemists: Strategies, Instruments, and Protocols*. Wiley-VCH: Weinheim, 2009.

162. Munch, J.; Standker, L.; Adermann, K.; Schuz, A.; Schindler, M.; Chinnadurai, R.; Pohlmann, S.; Chaipan, C.; Biet, T.; Peters, T.; Meyer, B.; Wilhelm, D.; Lu, H.; Jing, W. G.; Jiang, S. B.; Forssmann, W. G.; Kirchhoff, F., Discovery and optimization of a natural HIV-1 entry inhibitor targeting the gp41 fusion peptide. *Cell* **2007**, 129 (2), 263-275.

163. Olsen, J. S.; Brown, C.; Capule, C. C.; Rubinshtein, M.; Doran, T. M.; Srivastava, R. K.; Feng, C. Y.; Nilsson, B. L.; Yang, J.; Dewhurst, S., Amyloid-binding Small Molecules Efficiently Block SEVI (Semen-derived Enhancer of Virus Infection)- and Semen-mediated Enhancement of HIV-1 Infection. *Journal of Biological Chemistry* **2010**, 285 (46), 35488-35496.

164. Nanga, R. P. R.; Brender, J. R.; Xu, J. D.; Hartman, K.; Subramanian, V.; Ramamoorthy, A., Three-Dimensional Structure and Orientation of Rat Islet Amyloid

Polypeptide Protein in a Membrane Environment by Solution NMR Spectroscopy. *Journal of the American Chemical Society* **2009**, *131* (23), 8252-8261.

165. Adapted from the website: uhavax.hartford.edu/bugl/hiv.htm.

166. Levine, H., Multiple ligand binding sites on A beta(1-40) fibrils. *Amyloid-Journal of Protein Folding Disorders* **2005**, *12* (1), 5-14.

167. Beer, B. E.; Doncel, G. F.; Krebs, F. C.; Shattock, R. J.; Fletcher, P. S.; Buckheit, R. W.; Watson, K.; Dezzutti, C. S.; Cummins, J. E.; Bromley, E.; Richardson-Harman, N.; Pallansch, L. A.; Lackman-Smith, C.; Osterling, C.; Mankowski, M.; Miller, S. R.; Catalone, B. J.; Welsh, P. A.; Howett, M. K.; Wigdahl, B.; Turpin, J. A.; Reichelderfer, P., In vitro preclinical testing of nonoxynol-9 as potential anti-human immunodeficiency virus microbicide: a retrospective analysis of results from five laboratories. *Antimicrobial Agents and Chemotherapy* **2006**, *50* (2), 713-723.

168. Fichorova, R. N.; Tucker, L. D.; Anderson, D. J., The molecular basis of nonoxynol-9-induced vaginal inflammation and its possible relevance to human immunodeficiency virus type 1 transmission. *Journal of Infectious Diseases* **2001**, *184* (4), 418-428.

169. Ayehunie, S.; Cannon, C.; Lamore, S.; Kubilus, J.; Anderson, D. J.; Pudney, J.; Klausner, M., Organotypic human vaginal-ectocervical tissue model for irritation studies of spermicides, microbicides, and feminine-care products. *Toxicology in Vitro* **2006**, *20* (5), 689-698.

170. Ashcroft, F. M., *Ion Channels and Disease*. Academic Press: San Diego, 2000.

171. Estes, D. J.; Memarsadeghi, S.; Lundy, S. K.; Marti, F.; Mikol, D. D.; Fox, D. A.; Mayer, M., High-throughput profiling of ion channel activity in primary human lymphocytes. *Analytical Chemistry* **2008**, *80* (10), 3728-3735.

172. Capone, R.; Blake, S.; Restrepo, M. R.; Yang, J.; Mayer, M., Designing nanosensors based on charged derivatives of gramicidin A. *Journal of the American Chemical Society* **2007**, *129* (31), 9737-9745.

173. Blake, S.; Capone, R.; Mayer, M.; Yang, J., Chemically reactive derivatives of gramicidin A for developing ion channel-based nanoprobe. *Bioconjugate Chemistry* **2008**, *19* (8), 1614-1624.

174. Koeppe, R. E.; Andersen, O. S., Engineering the gramicidin channel. *Annual Review of Biophysics and Biomolecular Structure* **1996**, *25*, 231-258.

175. Harold, F. M.; Baarda, J. R., Gramicidin Valinomycin and Cation Permeability of *Streptococcus Faecalis*. *Journal of Bacteriology* **1967**, *94* (1), 53-60.